Supplementary Information

Indazolin-3-ylidenes (Indy*): Easily Accessible, Sterically-Hindered Indazole-Derived *N*-Heterocyclic Carbenes and Application in Gold Catalysis

Jin Zhang,*[a] Ting Liu,[a] Gaopeng Zhang,[b] Jianglong Cai,[a] Yue Wang,[a] Jianbo Tong,*[a] Yangmin Ma,[a] Roman Szostak,[c] Michal Szostak*[d]

[a]*College of Chemistry and Chemical Engineering, Key Laboratory of Chemical Additives for China National Light Industry, Shaanxi University of Science and Technology, Xi'an 710021, China*

phone: (+ 86)-029-8161-8312 E-mail: zhangjin@sust.edu.cn; jianbotong@aliyun.com

[b]*Kaili Catalyst & New Materials CO., LTD, Shaanxi Key Laboratory of Catalytic Materials and Technology, Xi'an 710299, China*

[c]*Department of Chemistry, Wroclaw University, F. Joliot-Curie 14, Wroclaw 50-383, Poland*

[d]*Department of Chemistry, Rutgers University, 73 Warren Street, Newark, New Jersey 07102, United States* phone: (+ 1)-973-353-5329 E-mail: michal.szostak@rutgers.edu

Table of Contents

1. Additonal Information Referred to from the Main Manuscript

The %buried volume (%V_{bur}) and steric maps

Interestingly, the Indy* ligands are characterized by unsymmetrical quadrant distribution (**5a**: SE: 53.7%, NE: 36.9%, NW: 24.8%, SW, 34.8%; **5b**-mol1: SE: 49.3%, NE: 46.5%, NW: 24.6%, SW, 24.3%; **5b**-mol2: SE: 40.1%, NE: 47.8%, NW: 24.5%, SW, 25.2%) with 19.1-21.0% average difference between the SE/NE and NW/SW quadrants ($\Delta_{(SE+SE)/2-(NW+SW)/2}$). As expected, the N-2,6-bis(diphenylmethyl)aryl wingtip extends beyond the metal coordination sphere (**5a**: mean: C29–Au–C11, C17: 0.854 Å; C19: 0.938 Å; **5b**-mol1: mean: C43–Au1–C36, C55: 1.054 Å; C77: 0.898 Å; **5b**-mol2: mean: C79–Au2–C82, C17: 0.809 Å; C81: 0.998 Å). It is well-recognized that this structural arrangement is important in substrate approach and coordination of intermediates during the catalysis, while ligands with the extended and flexible sterics are privileged in various catalytic cycles and mechanisms.

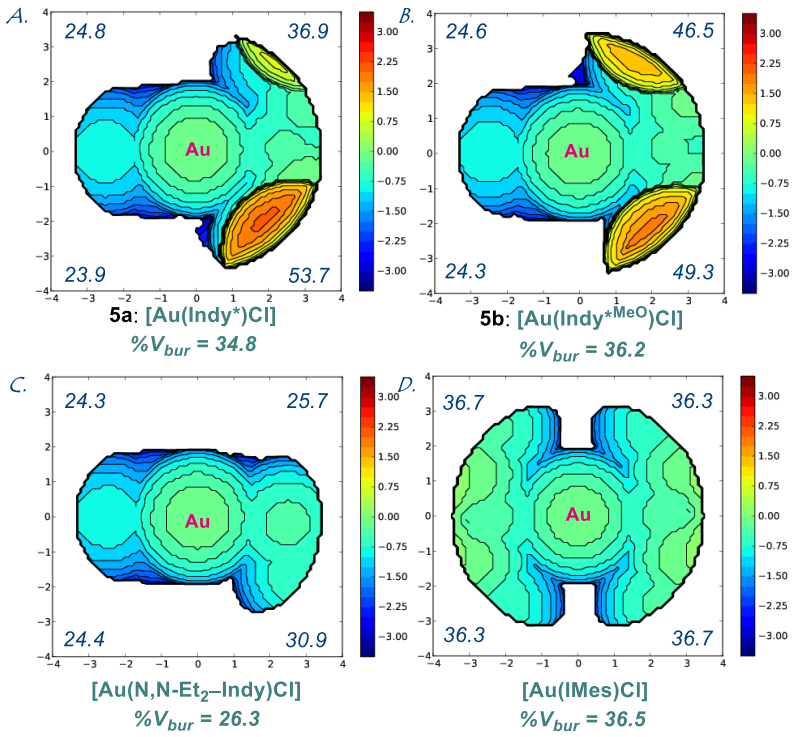

Chart S1. Topographical steric maps of Au(I) complexes **5a–5b**, Au[(N,N-Et_2–Indy)Cl] and [Au(IMes)Cl] showing %V_{bur} per quadrant.

Ion chromatography studies for the possibility of halogen scrambling

The identity of halogen anions of complexes **5a**-**5b** was ultrasonically extracted with deionized water, followed by a centrifugation procedure to ensure efficient separation. Subsequently, these species were ascertained via ion chromatography (model 940 Professional IC Vario, Metrohm) with column of MetrosepA Supp 5 (250 mmH×4.0 mm IC) and conductivity detector.

The peak corresponding to the chloride anion was conspicuously discernible in the ion chromatogram, while no such peak emerged for the iodide anion, indicating its absence within the analyzed sample (Chart S2-S5).

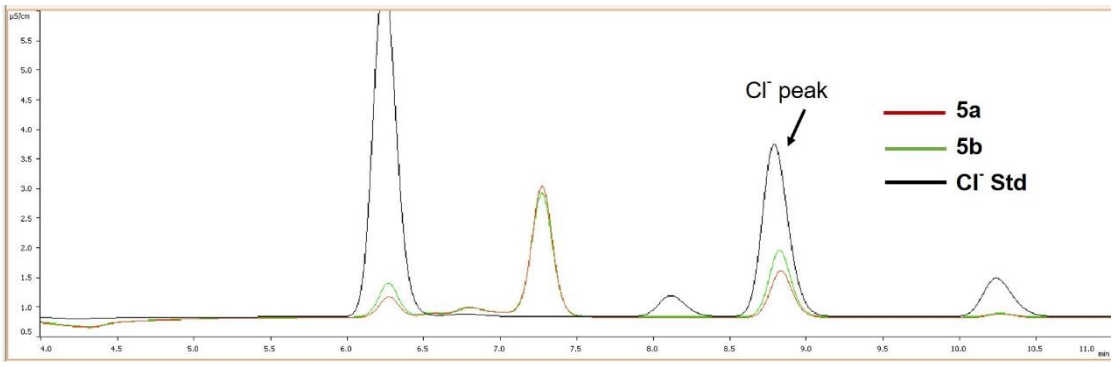

Chart S2. Ion chromatography of **5a**, **5b** and Cl^- standard.

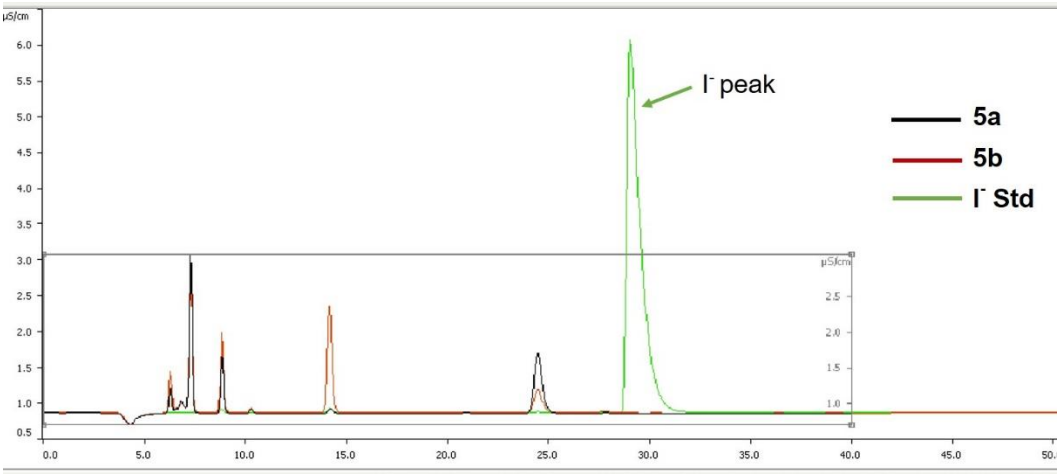

Chart S3. Ion chromatography of **5a**, **5b** and I^- standard.

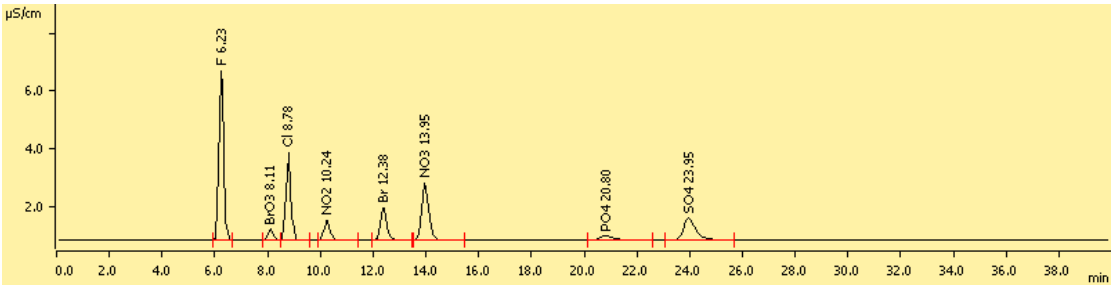

Chart S4. Ion chromatography of Cl^- standard.

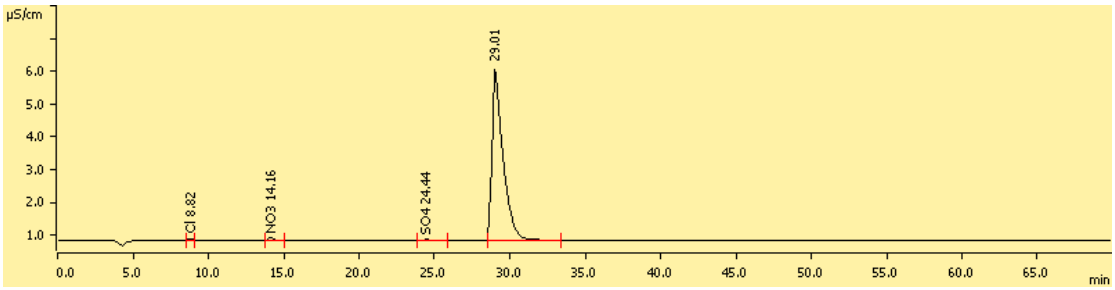

Chart S5. Ion chromatography of I^- standard.

2. General Information

All starting materials reported in the manuscript have been previously described in literature or prepared by the method reported previously. All experiments were performed using standard Schlenk techniques under nitrogen or argon unless stated otherwise. All solvents were purchased at the highest commercial grade and used as received or after purification by passing through activated alumina columns or distillation from sodium/benzophenone under nitrogen. All other chemicals were purchased at the highest commercial grade and used as received. All products were identified using ^{1}H NMR and ^{13}C NMR analysis and comparison with authentic samples. Reaction glassware was oven-dried at 140 °C for at least 24 h or flame-dried prior to use, allowed to cool under vacuum and purged with argon (three cycles). All yields refer to yields determined by ^{1}H NMR using an internal standard (optimization) unless stated otherwise. ^{1}H NMR and ^{13}C NMR spectra were recorded in $CDCl_3$ or DMSO-d_6 on a Bruker Ascend spectrometers at 400 (^{1}H NMR) and 100 MHz (^{13}C NMR) or 600 (^{1}H NMR) and 150 MHz (^{13}C NMR). All shifts are reported in parts per million (ppm) relative to residual $CHCl_3$ peak (7.26 and 77.16 ppm, ^{1}H NMR and ^{13}C NMR, respectively), DMSO-d_6 peak (2.50 and 39.52 ppm, ^{1}H NMR and ^{13}C NMR, respectively). All coupling constants (*J*) are reported in hertz (Hz). Abbreviations are: s = singlet, brs = broad singlet, d = doublet, t = triplet, q = quartet. Dibromomethane was used as an internal standard to determine NMR yields. Infrared spectra (IR) data were recorded on a Bruker INVENIO spectrometer and recorded in wavenumbers (cm'). High resolution mass spectra were acquired on a Q-Exactive Focus Hybrid Quadrupole-Orbitrap Mass Spectrometer (Thermo Fisher). Single crystal diffraction data were recorded on a Bruker APEX-II CCD diffractometer with Mo *K*a radiation. All flash chromatography was performed using silica gel, 60 Å, 300 mesh. TLC analysis was carried out on glass plates coated with silica gel 60 F254, 0.2 mm thickness. The plates were visualized using a 254 nm ultraviolet lamp. ^{1}H NMR, ^{13}C NMR and MS data are given for all compounds in the Supporting Experimental for characterization purposes.

3. Experimental Procedures and Characterization Data

3.1. General Procedure for Preparation of Indazolin-3-ylidene Precursors

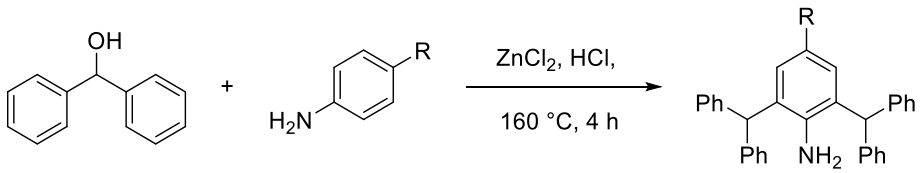

1

1a: R=Me
1b: R=OMe

2,6-Dibenzhydryl-4-methylaniline (1a)

A 250 mL round-bottom flask equipped with a magnetic stirring bar was charged with diphenylmethanol (18.42 g, 100 mmol, 4.0 equiv.) and *p*-toluidine (5.36 g, 50 mmol, 2.0 equiv.). The solid mixture was heated in an oil bath at 60 °C until a brown-black liquid was obtained. A colorless solution of anhydrous zinc chloride (3.41 g, 25 mmol, 1.0 equiv.) in concentrated hydrochloric acid (36% in H_2O, 4.3 mL, 50 mmol, 2.0 equiv.) was added dropwise to the eutectic melt. The temperature of the oil bath was then increased to 160 °C and the reaction mixture was stirred for an additional 3 h in the open vessel. After cooling to room temperature, the glassy solid was dissolved in dichloromethane and transferred into a separatory funnel. The organic solution was washed with water and dried over anhydrous K_2CO_3. Silica gel was added and the resulting suspension was filtered by gravity. The filtrate was concentrated using a rotary evaporator and washed with ether to obtain product **1a** that was of sufficient purity for the next step. (21.26 g, 97%).

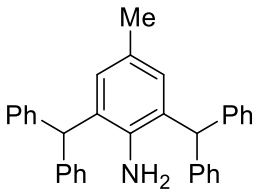

1a

^{1}H NMR (400 MHz, $CDCl_3$)) δ 7.27 (t, *J* = 7.3 Hz, 8H), 7.21 (t, *J* = 7.2 Hz, 4H), 7.09 (d, *J* = 7.1 Hz, 8H), 6.38 (s, 2H), 5.45 (s, 2H), 2.02 (s, 3H). ^{13}C NMR (101 MHz, $CDCl_3$)) δ 143.0, 139.8, 129.7, 129.5, 129.2, 128.6, 126.9, 126.7, 52.6, 21.1. The spectroscopic data were consistent with the data reported in previous report.[1]

2,6-Dibenzhydryl-4-methoxyaniline (1b)

A 250 mL round-bottom flask equipped with a magnetic stirring bar was charged with diphenylmethanol (18.42 g, 100 mmol, 4 equiv.) and 4-methoxyaniline (6.16 g, 50 mmol, 2 equiv.). The solid mixture was heated in an oil bath at 60 °C until a brown-black liquid was obtained. A colorless solution of anhydrous zinc chloride (3.41 g, 25 mmol, 1equiv.) in concentrated hydrochloric acid (36% in H_2O, 4.3 mL, 50 mmol, 2equiv.) was added dropwise

to the eutectic melt. The temperature of the oil bath was then increased to 160 °C and the reaction mixture was stirred for an additional 3 h in the open vessel. After cooling to room temperature, the glassy solid was dissolved in dichloromethane and transferred into a separatory funnel. The organic solution was washed with water and dried over anhydrous K_2CO_3. Silica gel was added and the resulting suspension was filtered by gravity. The filtrate was concentrated using a rotary evaporator and washed with ether to obtain product **1b** that was of sufficient for the next step. (21.63 g, 95%).

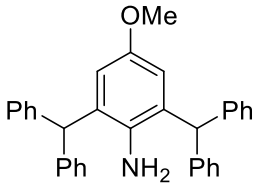

1b

^{1}H NMR (400 MHz, $CDCl_3$)) δ 7.30 - 7.25 (m, 8H), 7.21 (t, *J* = 7.1 Hz, 4H), 7.09 (d, *J* = 7.6 Hz, 8H), 6.20 (s, 2H), 5.48 (s, 2H), 3.42 (s, 3H). ^{13}C NMR (101 MHz, $CDCl_3$)) δ 151.9, 142.6, 135.9, 131.0, 129.6, 128.7, 126.8, 114.5, 55.2, 52.6. The spectroscopic data were consistent with the data reported in previous report.[1]

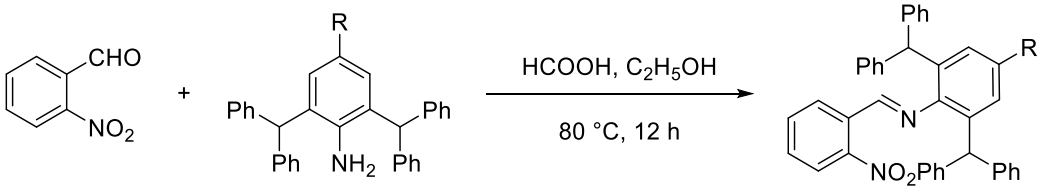

1 **2**

2a: R=Me
2b: R=OMe

(*E*)-*N*-(2,6-Dibenzhydryl-4-methylphenyl)-1-(2-nitrophenyl)methanimine (2a)

A mixture of *o*-nitrobenzaldehyde (6.04 g, 40 mmol, 1equiv.) and **1a** (21.10 g, 48 mmol, 1.2 equiv.) was stirred in anhydrous ethanol (80 mL) with dozens of drops of formic acid at 80 ℃ overnight. The resulting precipitate was filtered and washed with anhydrous ethanol to obtain product **2a**. (21.64 g, 94%)

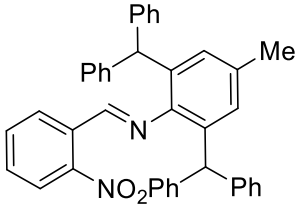

2a

^{1}H NMR (400 MHz, $CDCl_3$)) δ 8.03 (s, 1H), 7.85 (s, 1H), 7.63 (s, 1H), 7.59 (s, 1H), 7.54 (s, 1H), 7.22 - 7.17 (m, 8H), 7.16 (d, *J* = 6.7 Hz, 4H), 7.02 (s, 8H), 6.65 (s, 2H), 5.46 (s, 2H), 2.16 (s, 3H). ^{13}C NMR (101 MHz, $CDCl_3$) δ 159.9, 149.2, 148.1, 143.8, 133.1, 133.0, 132.9,

131.3, 129.8, 129.3, 129.0, 128.6, 128.3, 126.4, 124.4, 52.1, 21.5. HRMS (ESI) m/z: $[M+H]^+$ calcd for $C_{40}H_{33}N_2O_2^+$: 573.2537; found : 573.2517.

(*E*)-*N*-(2,6-Dibenzhydryl-4-methoxyphenyl)-1-(2-nitrophenyl)methanimine (2b)

A mixture of *o*-nitrobenzaldehyde (6.04 g, 40 mmol, 1equiv.) and **1b** (21.87 g, 48 mmol, 1.2 equiv.) was stirred in anhydrous ethanol (80 mL) with dozens of drops of formic acid at 80 ℃ overnight. The resulting precipitate was filtered and washed with anhydrous ethanol to obtain product **2b**. (22.43 g, 95%)

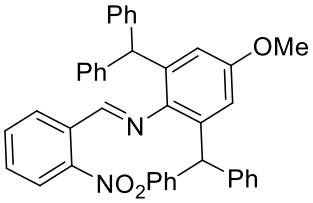

2b

^{1}H NMR (400 MHz, $CDCl_3$)) δ 8.00 (s, 1H), 7.85 (s, 1H), 7.66 (s, 1H), 7.59 (s, 1H), 7.53 (s, 1H), 7.24 - 7.17 (m, 8H), 7.16 (d, *J* = 6.8 Hz, 4H), 7.03 (d, *J* = 6.7 Hz, 8H), 6.42 (s, 2H), 5.49 (s, 2H), 3.54 (s, 3H). ^{13}C NMR (101 MHz, $CDCl_3$)) δ 160.4, 156.0, 149.2, 144.1, 143.5, 134.7, 132.9, 131.3, 129.7, 129.3, 128.7, 128.4, 126.5, 124.4, 114.2, 55.3, 52.2. HRMS (ESI) m/z: $[M+H]^+$ calcd for $C_{40}H_{33}N_2O_3^+$: 589.2486; found: 589.2466.

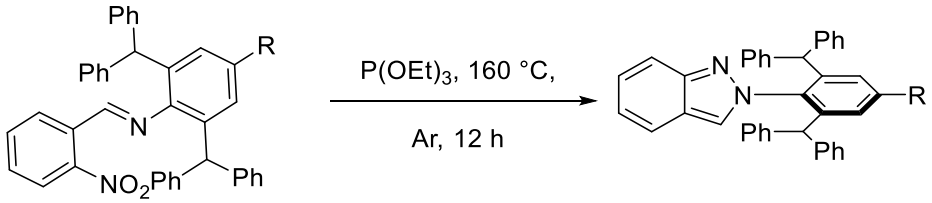

2 **3**

3a: R=Me
3b: R=OMe

2-(2,6-Dibenzhydryl-4-methylphenyl)-2*H*-indazole (3a)

Compound **2a** (17.18 g, 30 mmol, 1 equiv.) and triethyl phosphite (24.92 g, 150 mmol, 5 equiv.) were loaded into a sealed tube and stirred at 160 °C under argon for 12 h. The solvent was then removed under reduced pressure. The residue was purified by column chromatography to afford the product **3a**. (14.71 g, 91%)

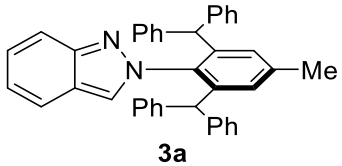

3a

^{1}H NMR (400 MHz, $CDCl_3$)) δ 7.85 - 7.80 (m, 1H), 7.33 (t, *J* = 8.5 Hz, 2H), 7.23 (t, *J* = 7.2 Hz, 4H), 7.18 (d, *J* = 7.1 Hz, 2H), 7.16 – 7.12 (m, 6H), 7.05 – 7.01 (m, 5H), 6.85 (s, 2H), 6.82 – 6.77 (m, 4H), 6.69 (s, 1H), 4.97 (s, 2H), 2.27 (s, 3H). ^{13}C NMR (101 MHz, $CDCl_3$)) δ 149.4, 143.3, 143.0, 141.7, 139.3, 137.1, 129.6, 129.5, 129.1, 128.3, 127.8, 126.5, 126.4,

121.6, 121.1, 120.7, 117.9, 51.1, 22.0. HRMS (ESI) m/z: $[M+H]^+$ calcd for $C_{40}H_{33}N_2^+$: 541.2638; found: 541.2629.

2-(2,6-Dibenzhydryl-4-methoxyphenyl)-2*H*-indazole (3b)

Compound **2b** (17.66 g, 30 mmol, 1 equiv.) and triethyl phosphite (24.92 g, 150 mmol, 5 equiv.) were loaded into a sealed tube and stirred at 160 °C under argon for 12 h. The solvent was then removed under reduced pressure. The residue was purified by column chromatography to afford the product **3b**. (14.92 g, 89%)

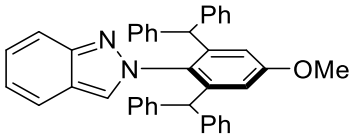

3b

^{1}H NMR (400 MHz, $CDCl_3$)) δ 7.90 - 7.85 (m, 1H), 7.39 - 7.34 (m, 2H), 7.31 - 7.25 (m, 4H), 7.23 - 7.17 (m, 8H), 7.09 (d, *J* = 6.9 Hz, 4H), 7.05 (d, *J* = 7.0 Hz, 1H), 6.86 (dd, *J* = 6.5, 2.9 Hz, 4H), 6.68 (d, *J* = 0.9 Hz, 1H), 6.61 (s, 2H), 5.05 (s, 2H), 3.66 (s, 3H). ^{13}C NMR (101 MHz, $CDCl_3$)) δ 159.6, 149.4, 143.6, 143.0, 142.8, 132.8, 129.6, 129.0, 128.3, 128.3, 128.0, 126.5, 126.4, 121.6, 121.1, 120.7, 117.8, 55.3, 51.3. HRMS (ESI) m/z: $[M+H]^+$ calcd for $C_{40}H_{33}N_2O^+$: 557.2587; found: 557.2571.

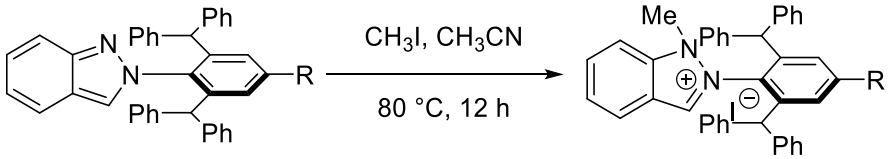

3 **4**

4a: R=Me
4b: R=OMe

2-(2,6-Dibenzhydryl-4-methylphenyl)-1-methyl-1*H*-indazol-2-ium iodide (4a)

An excess of CH_3I (7.10 g, 50 mmol, 5 equiv.) was added to a solution of compound **3a** (5.41 g, 10 mmol, 1 equiv.) in CH_3CN (15 mL) and the reaction mixture was stirred at 80 °C overnight. The solvent was then removed under reduced pressure. The residue was subsequently washed with diethyl ether to give the product **4a**. (5.43 g, 80%)

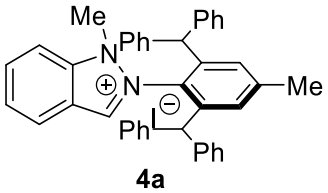

4a

^{1}H NMR (600 MHz, DMSO-*d*$_6$) δ 8.86 (s, 1H), 7.97 (t, *J* = 7.9 Hz, 2H), 7.84 (d, *J* = 8.9 Hz, 1H), 7.62 - 7.56 (m, 1H), 7.26 (d, *J* = 6.1 Hz, 12H), 6.97 (s, 2H), 6.95 (d, *J* = 7.5 Hz, 4H), 6.92 - 6.87 (m, 4H), 5.04 (s, 2H), 3.11 (s, 3H), 2.30 (s, 3H). ^{13}C NMR (151 MHz, DMSO-*d*$_6$) δ 143.6, 143.4, 141.4, 140.5, 136.2, 130.6, 129.6, 129.4, 129.1, 129.0, 128.3, 127.7, 127.5,

123.6, 119.7, 112.4, 51.1, 33.1, 22.1. HRMS (ESI) m/z: $[M\text{-}I]^+$ Calcd for $C_{41}H_{35}N_2^+$:555.2795; Found: 555.2784.

2-(2,6-Dibenzhydryl-4-methoxyphenyl)-1-methyl-1*H*-indazol-2-ium iodide (4b)

An excess of CH_3I (7.10 g, 50 mmol, 5 equiv.) was added to a solution of compound **3b** (5.57 g, 10 mmol, 1 equiv.) in CH_3CN (15 mL) and the reaction mixture was stirred at 80 °C overnight. The solvent was then removed under reduced pressure. The residue was subsequently washed with diethyl ether to give the product **4b**. (5.51 g, 79%)

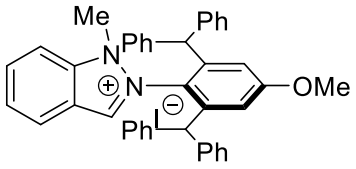

4b

^{1}H NMR (600 MHz, $CDCl_3$)) δ 8.74 (s, 1H), 8.02 (d, *J* = 8.4 Hz, 1H), 7.89 - 7.84 (m, 1H), 7.74 (d, *J* = 8.8 Hz, 1H), 7.51 - 7.45 (m, 1H), 7.22 (d, *J* = 7.1 Hz, 12H), 6.98 (d, *J* = 6.0 Hz, 4H), 6.90 - 6.84 (m, 4H), 6.60 (s, 2H), 4.97 (s, 2H), 3.64 (s, 3H), 3.10 (s, 3H). ^{13}C NMR (151 MHz, $CDCl_3$)) δ 162.4, 145.6, 140.3, 140.0, 139.2, 136.1, 135.2, 129.3, 129.1, 129.0, 128.8, 127.8, 127.5, 126.2, 123.8, 122.5, 119.4, 115.7, 111.5, 55.6, 52.1, 33.6. HRMS (ESI) m/z : $[M\text{-}I]^+$ Calcd for $C_{41}H_{35}N_2O^+$:571.2744; Found : 571.2736.

3.2. General Procedure for the Synthesis of NHC-Gold(I) Complexes

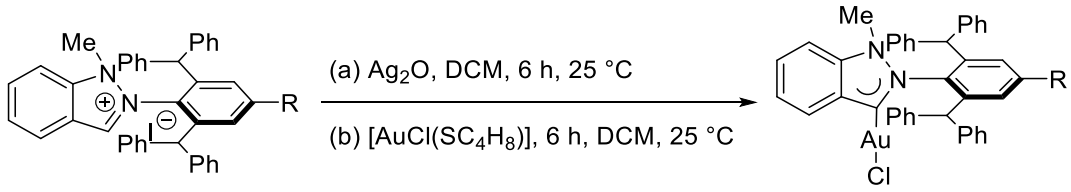

4 **5**

5a: R=Me
5b: R=OMe

(2-(2,6-Dibenzhydryl-4-methylphenyl)-1-methyl-2,3-dihydro-1*H*-indazol-3-yl)gold(I) chloride (5a)

Ag_2O (139 mg, 0.60 mmol, 1.2 equiv.) was added to a solution of salt **4a** (341 mg, 0.50 mmol, 1equiv.) in CH_2Cl_2 (2 mL). The resulting suspension was stirred for 6 h at ambient temperature, shielded from light. The reaction mixture was then filtered through Celite directly into a solution of $[AuCl(SC_4H_8)]$ (160 mg, 0.5 mmol, 1equiv.) in CH_2Cl_2 (2 mL) and the resulting mixture was stirred for 6 h at ambient temperature. The suspension was filtered through Celite and the solvent of the filtrate was removed under vacuum. The resulting residue was washed with diethyl ether and dried under vacuum, affording the product **5a**. (342 mg, 87%)

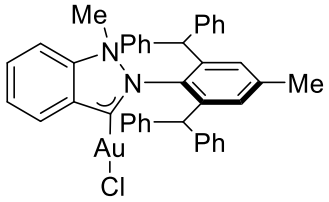

5a

^{1}H NMR (600 MHz, $CDCl_3$) δ 8.24 (d, *J* = 8.2 Hz, 1H), 7.66 (t, *J* = 7.6 Hz, 1H), 7.38 (t, *J* = 7.5 Hz, 1H), 7.26 (d, *J* = 4.7 Hz, 4H), 7.15 (dd, *J* = 22.6, 7.4 Hz, 12H), 6.90 (s, 2H), 6.85 (d, *J* = 8.5 Hz, 1H), 6.76 (d, *J* = 6.5 Hz, 4H), 5.26 (s, 2H), 2.30 (s, 3H), 1.71 (s, 3H). ^{13}C NMR (151 MHz, $CDCl_3$) δ 171.8, 143.1, 141.8, 141.7, 139.9, 138.6, 133.0, 132.7, 130.4, 129.9, 129.6, 129.3, 128.6, 128.5, 128.5, 127.1, 126.8, 122.9, 108.5, 51.1, 31.2, 22.0. HRMS (ESI) m/z : $[M\text{-}Cl]^+$ Calcd for $C_{41}H_{34}AuN_2^+$: 751.2382; Found : 751.2310. Elemental analysis: Calcd for $C_{41}H_{34}AuN_2Cl$: C 62.56%, H 4.354%, N 3.56%; Found: C 63.86%, H 4.363%, N 3.61%.

(2-(2,6-Dibenzhydryl-4-methoxyphenyl)-1-methyl-2,3-dihydro-1*H*-indazol-3-yl)gold(I) chloride (5b)

Ag_2O (139 mg, 0.60 mmol, 1.2 equiv.) was added to a solution of salt **4b** (349 mg, 0.50 mmol, 1equiv.) in CH_2Cl_2 (2 mL). The resulting suspension was stirred for 6 h at ambient temperature, shielded from light. The reaction mixture was then filtered through Celite directly into a solution of $[AuCl(SC_4H_8)]$ (160 mg, 0.5 mmol, 1equiv.) in CH_2Cl_2 (2 mL) and the resulting mixture was stirred for 6 h at ambient temperature. The suspension was filtered through Celite and the solvent of the filtrate was removed under vacuum. The resulting residue was washed with diethyl ether and dried under vacuum, affording the product **5b**. (353 mg, 88%)

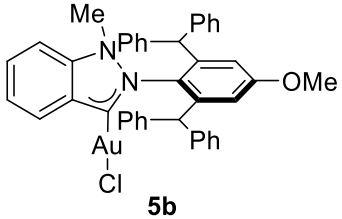

5b

^{1}H NMR (600 MHz, $CDCl_3$) δ 8.25 (d, *J* = 8.2 Hz, 1H), 7.66 (t, *J* = 7.7 Hz, 1H), 7.38 (t, *J* = 7.6 Hz, 1H), 7.26 (t, *J* = 3.8 Hz, 4H), 7.20 – 7.12 (m, 12H), 6.84 (d, *J* = 8.5 Hz, 1H), 6.78 (d, *J* = 6.6 Hz, 4H), 6.58 (s, 2H), 5.28 (s, 2H), 3.64 (s, 3H), 1.72 (s, 3H). ^{13}C NMR (151 MHz, $CDCl_3$) δ 172.4, 161.1, 145.1, 141.4, 139.7, 138.6, 133.0, 129.8, 129.5, 129.3, 128.6, 128.6, 128.5, 127.9, 127.1, 126.9, 122.8, 115.2, 108.5, 55.4, 51.4, 31.0. HRMS (ESI) m/z : $[M\text{-}Cl]^+$ Calcd for $C_{41}H_{34}AuN_2O^+$: 767.2331; Found : 767.2329. Elemental analysis: Calcd for $C_{41}H_{34}AuN_2OCl$: C 61.31%, H 4.267%, N 3.49%; Found: C 62.58%, H 4.335%, N 3.51%.

3.3. General Procedure for the Synthesis of [(NHC)RhCl(CO)$_2$] Complexes

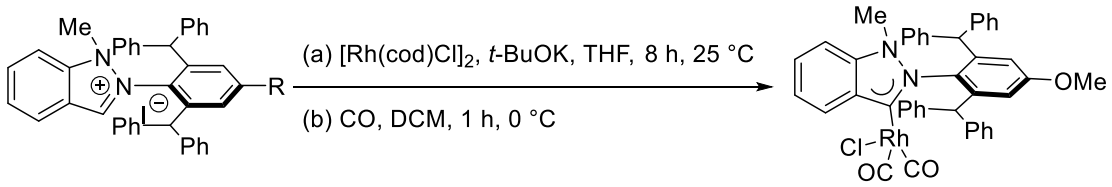

4 **6**

6a: R=Me
6b: R=OMe

[(NHC)Rh(CO)$_2$Cl] (6a). A 25 mL round-bottomed flask was equipped with a septum and a stir bar and flame-dried under a stream of argon. The flask was charged with *t*-BuOK (45 mg, 0.4 mmol, 2.0 equiv.) and THF (2 mL) and cooled with an ice bath. [Rh(COD)Cl]$_2$ (99 mg, 0.2 mmol, 1.0 equiv.) was introduced, and the resulting orange solution was stirred for 15 min in the ice bath and then for 45 min at room temperature. The salt **4a** (246 mg, 0.36 mmol, 1.8 equiv.) was added, and the reaction mixture evolved progressively from orange to yellow. After 8 h, the homogeneous solution was filtered through Celite with DCM as eluent and concentrated under reduced pressure to afford a yellow solid. Then the yellow solid was dissolved in DCM (5 mL). The solution was cooled to 0 °C and exposed to an atmosphere of CO (flask was equipped with a CO balloon connected via a syringe and a septum). After bubbling CO through the solution for 1 h the solvent was removed and the pure product **6a** as a yellowish-brown solid was obtained by column chromatography. (240 mg, 89%)

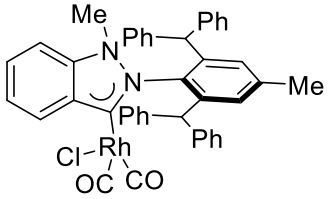

6a

^{1}H NMR (600 MHz, $CDCl_3$) δ 8.55 (d, *J* = 8.2 Hz, 1H), 7.60 (t, *J* = 7.7 Hz, 1H), 7.35 (t, *J* = 7.5 Hz, 1H), 7.24 (d, *J* = 7.2 Hz, 8H), 7.18 (s, 2H), 7.09 (d, *J* = 6.7 Hz, 6H), 7.06 (s, 2H), 6.80 (d, *J* = 7.6 Hz, 4H), 6.66 (d, *J* = 8.5 Hz, 1H), 5.67 (s, 2H), 2.35 (s, 3H), 1.24 (s, 3H). ^{13}C NMR (151 MHz, $CDCl_3$) δ 186.0, 185.7, 184.0, 183.6, 183.5, 183.3, 143.6, 142.1, 141.2, 140.8, 139.0, 133.6, 132.6, 131.6, 130.7, 130.5, 130.0, 129.9, 128.5, 128.0, 127.0, 126.6, 122.5, 51.2, 31.5, 22.1. FT-IR (CH_2Cl_2): ν~ (CO_{sym}) 2070 cm^{-1} (s) and ν~ (CO_{asym}) 1990 cm^{-1} (s).

[(NHC)Rh(CO)$_2$Cl] (6b). A 25 mL round-bottomed flask was equipped with a septum and a stir bar and flame-dried under a stream of argon. The flask was charged with *t*-BuOK (45 mg, 0.4 mmol, 2.0 equiv.) and THF (2 mL) and cooled with an ice bath. [Rh(COD)Cl]$_2$ (99 mg, 0.2 mmol, 1.0 equiv.) was introduced, and the resulting orange solution was stirred for 15 min in the ice bath and then for 45 min at room temperature. The salt **4b** (252 mg, 0.36 mmol, 1.8 equiv.) was added, and the reaction mixture evolved progressively from orange to yellow. After 8 h, the homogeneous solution was filtered through Celite with DCM as eluent

and concentrated under reduced pressure to afford a yellow solid. Then the yellow solid was dissolved in DCM (5 mL). The solution was cooled to 0 °C and exposed to an atmosphere of CO (flask was equipped with a CO balloon connected via a syringe and a septum). After bubbling CO through the solution for 1 h the solvent was removed and the pure product **6b** as a yellowish-brown solid was obtained by column chromatography. (242 mg, 88%)

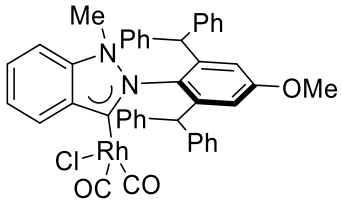

6b

^{1}H NMR (600 MHz, $CDCl_3$) δ 8.54 (d, *J* = 8.2 Hz, 1H), 7.59 (t, *J* = 7.7 Hz, 1H), 7.37 – 7.33 (m, 1H), 7.24 (d, *J* = 4.6 Hz, 8H), 7.20 – 7.16 (m, 2H), 7.09 (q, *J* = 5.7 Hz, 6H), 6.82 (d, *J* = 7.2 Hz, 4H), 6.74 (s, 2H), 6.64 (d, *J* = 8.5 Hz, 1H), 5.68 (s, 2H), 3.67 (s, 3H), 1.23 (s, 3H). ^{13}C NMR (151 MHz, $CDCl_3$) δ 186.0, 185.7, 184.0, 184.0, 183.8, 183.5, 160.8, 145.6, 141.9, 140.6, 138.9, 132.6, 131.6, 130.7, 130.0, 129.9, 128.9, 128.5, 128.1, 127.0, 126.7, 122.5, 115.3, 108.8, 55.5, 51.5, 31.4. FT-IR (CH_2Cl_2): ν~ (CO_{sym}) 2070 cm^{-1} (s) and ν~ (CO_{asym}) 1989 cm^{-1} (s).

3.4. General Procedure for the Synthesis of NHC – Selenium Complexes

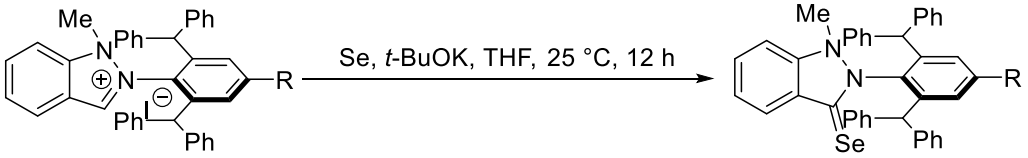

4 **7**

7a: R=Me
7b: R=OMe

2-(2,6-Dibenzhydryl-4-methylphenyl)-1-methyl-1,2-dihydro-3*H*-indazole-3-selenone (7a)

An oven-dried vial equipped with a stir bar was charged with salt **4a** (341 mg, 0.5 mmol, 1.0 equiv.), Se (59 mg, 0.75 mmol, 1.5 equiv.) and *t*-BuOK (67 mg, 0.6 mmol, 1.2 equiv.). The reaction mixture was placed under argon and subjected to three evacuation/backfilling cycles under vacuum. Dry THF was added and the reaction mixture was stirred at room temperature overnight. The suspension was filtered through Celite and the solvent of the filtrate was removed under vacuum. The product **7a** was obtained by column chromatography. (269 mg, 85%).

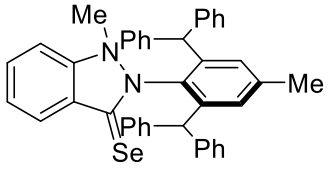

7a

^{1}H NMR (600 MHz, $CDCl_3$) δ 8.29 (d, *J* = 8.0 Hz, 1H), 7.59 (t, J = 7.5 Hz, 1H), 7.31 (d, J = 7.2 Hz, 4H), 7.28 (d, J = 7.4 Hz, 1H), 7.21 (t, J = 6.7 Hz, 4H), 7.17 - 7.07 (m, 8H), 6.91 (s, 2H), 6.88 - 6.79 (m, 4H), 6.68 (d, J = 8.4 Hz, 1H), 5.22 (s, 2H), 2.29 (s, 3H), 1.36 (s, 3H). ^{13}C NMR (151 MHz, $CDCl_3$) δ 163.1, 144.3, 142.6, 140.9, 140.8, 140.3, 132.6, 130.5, 129.7, 128.4, 128.1, 126.9, 126.7, 126.4, 122.0, 108.4, 52.0, 31.3, 22.0. ^{77}Se NMR (114 MHz, Chloroform-*d*) δ 153.40. HRMS (ESI) m/z: $[M+H]^+$ Calcd for $C_{41}H_{35}N_2Se^+$:635.1960; Found: 635.1951.

2-(2,6-Dibenzhydryl-4-methoxyphenyl)-1-methyl-1,2-dihydro-3*H*-indazole-3-selenone (7b)

An oven-dried vial equipped with a stir bar was charged with salt **4b** (349 mg, 0.5 mmol, 1.0 equiv.), Se (59 mg, 0.75 mmol, 1.5 equiv.) and *t*-BuOK (67 mg, 0.6 mmol, 1.2 equiv.). The reaction mixture was placed under argon and subjected to three evacuation/backfilling cycles under vacuum. Dry THF was added and the reaction mixture was stirred at room temperature overnight. The suspension was filtered through Celite and the solvent of the filtrate was removed under vacuum. The product **7b** was obtained by column chromatography. (279 mg, 86%).

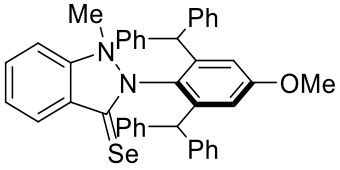

7b

^{1}H NMR (600 MHz, Chloroform-*d*) δ 8.29 (d, *J* = 8.1 Hz, 1H), 7.58 (t, *J* = 7.7 Hz, 1H), 7.32 (d, *J* = 7.7 Hz, 4H), 7.28 (t, *J* = 7.5 Hz, 1H), 7.20 (t, *J* = 7.6 Hz, 4H), 7.13 (dd, *J* = 10.3, 5.3 Hz, 8H), 6.88 - 6.83 (m, 4H), 6.67 (d, *J* = 8.4 Hz, 1H), 6.61 (s, 2H), 5.23 (s, 2H), 3.62 (s, 3H), 1.37 (s, 3H). ^{13}C NMR (151 MHz, $CDCl_3$)) δ 163.4, 160.9, 146.4, 142.5, 140.6, 140.3, 132.7, 129.7, 129.7, 128.5, 128.4, 128.3, 127.0, 126.9, 126.6, 125.7, 122.1, 115.4, 108.5, 55.4, 52.3, 31.3. ^{77}Se NMR (114 MHz, Chloroform-*d*) δ 152.88. HRMS (ESI) m/z : $[M+H]^+$ Calcd for $C_{41}H_{35}N_2OSe^+$: 651.1909; Found : 651.1902.

3.5 General Procedure for the Cyclisation of Propargylic Amides.

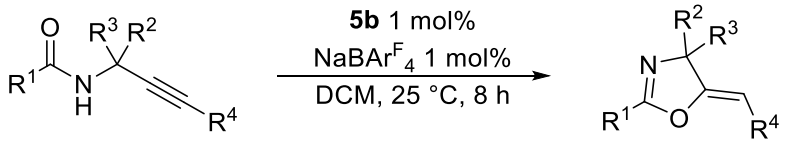

8 **9**

An oven-dried vial equipped with a stir bar was charged with propargylic amides (0.2 mmol, 1.0 equiv.), Au catalyst **5b** (1.0 mol%), $NaBAr^F_4$ (1.0 mol%) in 0.5 M DCM. The reaction mixture was stirred at 25 ˚C for 8 h. The volatiles were removed in vacuo and the products were purified by column chromatography.

5-Methylene-2-phenyl-4,5-dihydrooxazole (9a)

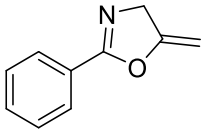

After purification (Silica Gel, n-hexane/ethyl acetate 10:1) **9a** was isolated as a colorless oil in 97% yield (30.9 mg). ^{1}H NMR (600 MHz, $CDCl_3$) δ 7.98 (d, *J* = 7.4 Hz, 2H), 7.52 (t, *J* = 7.4 Hz, 1H), 7.44 (t, *J* = 7.7 Hz, 2H), 4.82 (q, *J* = 3.0 Hz, 1H), 4.66 (t, *J* = 2.7 Hz, 2H), 4.37 (q, *J* = 2.6 Hz, 1H). ^{13}C NMR (151 MHz, $CDCl_3$) δ 164.0, 158.9, 132.0, 128.6, 128.2, 126.8, 84.0, 57.8. The spectroscopic data were consistent with the data reported in previous report.[2]

5-Methylene-2-(*o*-tolyl)-4,5-dihydrooxazole (9b)

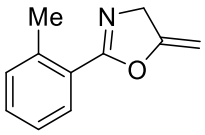

After purification (Silica Gel, n-hexane/ethyl acetate 10:1) **9b** was isolated as a yellow oil in 94% yield (32.5 mg).^{1}H NMR (600 MHz, $CDCl_3$) δ 7.84 (d, *J* = 7.9 Hz, 1H), 7.37 (t, *J* = 7.5 Hz, 1H), 7.29 – 7.22 (m, 2H), 4.81 – 4.76 (m, 1H), 4.69 (t, *J* = 2.8 Hz, 2H), 4.34 (q, *J* = 2.6 Hz, 1H), 2.61 (s, 3H).^{13}C NMR (151 MHz, $CDCl_3$) δ 164.1, 158.5, 139.3, 131.5, 131.1, 129.9, 126.1, 125.8, 83.4, 22.0. The spectroscopic data were consistent with the data reported in previous report.[3]

5-Methylene-2-(*m*-tolyl)-4,5-dihydrooxazole (9c)

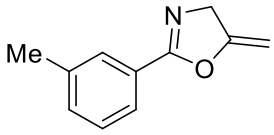

After purification (Silica Gel, n-hexane/ethyl acetate 10:1) **9c** was isolated as a yellow oil in 94% yield (32.5 mg). ^{1}H NMR (600 MHz, $CDCl_3$) δ 7.81 (s, 1H), 7.79 – 7.74 (m, 1H), 7.33 (d, *J* = 5.0 Hz, 2H), 4.82 (q, *J* = 3.0 Hz, 1H), 4.65 (t, *J* = 2.8 Hz, 2H), 4.36 (q, *J* = 2.6 Hz, 1H), 2.40 (s, 3H). ^{13}C NMR (151 MHz, $CDCl_3$) δ 164.1, 159.0, 138.4, 132.8, 128.7, 128.6, 126.7, 125.3, 83.9, 57.8, 21.4. The spectroscopic data were consistent with the data reported in previous report.[4]

5-Methylene-2-(*p*-tolyl)-4,5-dihydrooxazole (9d)

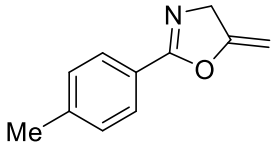

After purification (Silica Gel, n-hexane/ethyl acetate 10:1) **9d** was isolated as a yellow solid in 95% yield (32.9 mg). ^{1}H NMR (600 MHz, $CDCl_3$) δ 7.86 (d, *J* = 8.2 Hz, 2H), 7.24 (d, *J* = 8.0 Hz, 2H), 4.80 (q, *J* = 3.0 Hz, 1H), 4.63 (t, *J* = 2.8 Hz, 2H), 4.35 (q, *J* = 2.7 Hz, 1H), 2.40 (s, 3H). ^{13}C NMR (151 MHz, $CDCl_3$) ^{13}C NMR (151 MHz, $CDCl_3$) δ 164.0, 159.1, 142.4, 129.4, 128.1, 124.1, 83.7, 57.9, 21.8. The spectroscopic data were consistent with the data reported in previous report.[5]

2-(4-(tert-butyl)phenyl)-5-methylene-4,5-dihydrooxazole **(9e)**

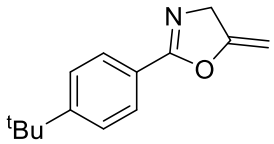

After purification (Silica Gel, n-hexane/ethyl acetate 10:1) **9e** was isolated as a yellow solid in 71% yield (30.5 mg). ^{1}H NMR (600 MHz, $CDCl_3$) δ 7.90 (d, *J* = 8.5 Hz, 2H), 7.46 (d, *J* = 8.5 Hz, 2H), 4.81 (q, *J* = 3.0 Hz, 1H), 4.64 (t, *J* = 2.8 Hz, 2H), 4.35 (q, *J* = 2.6 Hz, 1H), 1.34 (s, 9H). ^{13}C NMR (151 MHz, $CDCl_3$) δ 163.9, 159.1, 155.5, 128.0, 125.6, 124.1, 83.7, 57.9, 35.2, 31.3.

2-(4-Methoxyphenyl)-5-methylene-4,5-dihydrooxazole (9f)

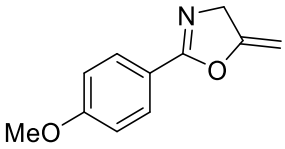

After purification (Silica Gel, n-hexane/ethyl acetate 10:1) **9f** was isolated as a white solid in 96% yield (34.0 mg). ^{1}H NMR (600 MHz, $CDCl_3$) δ 7.92 (d, *J* = 8.9 Hz, 2H), 6.94 (d, *J* = 8.9 Hz, 2H), 4.79 (q, *J* = 3.0 Hz, 1H), 4.62 (t, *J* = 2.8 Hz, 2H), 4.34 (q, *J* = 2.6 Hz, 1H), 3.86 (s, 3H). ^{13}C NMR (151 MHz, $CDCl_3$) δ 163.6, 162.6, 159.1, 129.9, 119.3, 114.0, 83.6, 57.8, 55.5. The spectroscopic data were consistent with the data reported in previous report.[6]

5-Methylene-2-(3,4,5-trimethoxyphenyl)-4,5-dihydrooxazole (9g)

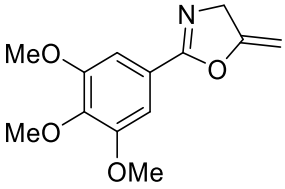

After purification (Silica Gel, n-hexane/ethyl acetate 10:1) **9g** was isolated as a white solid in 70% yield (34.9 mg). ^{1}H NMR (600 MHz, $CDCl_3$) δ 7.22 (s, 2H), 4.83 (q, *J* = 3.0 Hz, 1H), 4.65 (t, *J* = 2.8 Hz, 2H), 4.37 (q, *J* = 2.7 Hz, 1H), 3.92 (s, 6H), 3.91 (s, 3H). ^{13}C NMR

(151 MHz, $CDCl_3$) δ 163.7, 153.3, 141.3, 122.0, 84.0, 61.1, 57.9, 56.4. The spectroscopic data were consistent with the data reported in previous report.[4]

4-(5-Methylene-4,5-dihydrooxazol-2-yl)benzonitrile (9h)

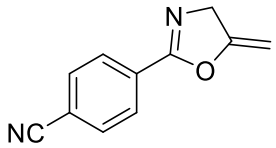

After purification (Silica Gel, n-hexane/ethyl acetate 10:1) **9h** was isolated as a white solid in 54% yield (19.9 mg). ^{1}H NMR (600 MHz, $CDCl_3$) δ 8.09 (d, *J* = 8.4 Hz, 2H), 7.75 (d, *J* = 8.5 Hz, 2H), 4.86 (q, *J* = 3.1 Hz, 1H), 4.69 (t, *J* = 2.9 Hz, 2H), 4.43 (q, *J* = 2.7 Hz, 1H). ^{13}C NMR (151 MHz, $CDCl_3$) δ 162.4, 158.4, 132.4, 130.9, 128.7, 118.2, 115.4, 84.9, 58.1. The spectroscopic data were consistent with the data reported in previous report.[7]

5-Methylene-2-(4-(trifluoromethyl)phenyl)-4,5-dihydrooxazole (9i)

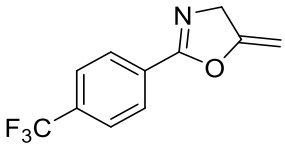

After purification (Silica Gel, n-hexane/ethyl acetate 10:1) **9i** was isolated as a white solid in 80% yield (36.3 mg). ^{1}H NMR (600 MHz, $CDCl_3$) δ 8.10 (d, *J* = 8.2 Hz, 2H), 7.71 (d, *J* = 8.2 Hz, 2H), 4.85 (q, *J* = 3.0 Hz, 1H), 4.69 (t, *J* = 2.8 Hz, 2H), 4.41 (q, *J* = 2.7 Hz, 1H). ^{13}C NMR (151 MHz, $CDCl_3$) δ 162.8, 158.6, 133.4 (q, *J*= 19.7 Hz), 128.5 (q, *J* = 272.6 Hz), 125.7 (q, *J*= 3.8 Hz), 124.7, 123.0, 84.6, 58.0. ^{19}F NMR (565 MHz, $CDCl_3$) *δ* -63.03. The spectroscopic data were consistent with the data reported in previous report.[2]

2-(4-Chlorophenyl)-5-methylene-4,5-dihydrooxazole (9j)

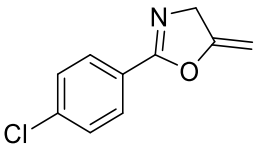

After purification (Silica Gel, n-hexane/ethyl acetate 10:1) **9l** was isolated as a yellow solid in 89% yield (34,4 mg). ^{1}H NMR (600 MHz, $CDCl_3$) δ 7.91 (d, *J* = 8.5 Hz, 2H), 7.42 (d, *J* = 8.5 Hz, 2H), 4.82 (q, *J* = 2.9 Hz, 1H), 4.64 (t, *J* = 2.7 Hz, 2H), 4.38 (q, *J* = 2.5 Hz, 1H). ^{13}C NMR (151 MHz, $CDCl_3$) δ 163.0, 158.8, 138.2, 129.5, 129.0, 125.4, 84.2, 57.9. The spectroscopic data were consistent with the data reported in previous report.[5]

2-(4-bromophenyl)-5-methylene-4,5-dihydrooxazole(9k)

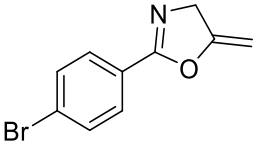

After purification (Silica Gel, n-hexane/ethyl acetate 10:1) **9k** was isolated as a white solid in 98% yield (46.4 mg). ^{1}H NMR (600 MHz, $CDCl_3$) δ 7.84 (d, *J* = 8.6 Hz, 2H), 7.58 (d, *J* = 8.6 Hz, 2H), 4.82 (q, *J* = 3.0 Hz, 1H), 4.63 (t, *J* = 2.8 Hz, 2H), 4.38 (q, *J* = 2.7 Hz, 1H). ^{13}C NMR (151 MHz, $CDCl_3$ δ 163.1, 158.8, 132.0, 129.6, 126.7, 125.8, 84.3, 57.9. The spectroscopic data were consistent with the data reported in previous report.[8]

2-(4-iodophenyl)-5-methylene-4,5-dihydrooxazole (9l)

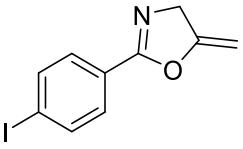

After purification (Silica Gel, n-hexane/ethyl acetate 10:1) **9l** was isolated as a white solid in 66% yield (37.6 mg). ^{1}H NMR (600 MHz, $CDCl_3$) δ 7.79 (d, *J* = 8.4 Hz, 2H), 7.69 (d, *J* = 8.4 Hz, 2H), 4.81 (q, *J* = 3.0 Hz, 1H), 4.63 (t, *J* = 2.8 Hz, 2H), 4.37 (q, *J* = 2.7 Hz, 1H). ^{13}C NMR (151 MHz, $CDCl_3$) δ 163.3, 158.8, 137.9, 129.6, 126.4, 99.1, 84.3, 57.93.

5-Methylene-2-(naphthalen-2-yl)-4,5-dihydrooxazole (9m)

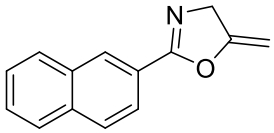

After purification (Silica Gel, n-hexane/ethyl acetate 10:1) **9m** was isolated as a colorless oil in 80% yield (33.5 mg) ^{1}H NMR (600 MHz, $CDCl_3$) δ 8.47 (s, 1H), 8.05 (d, *J* = 10.0 Hz, 1H), 7.93 (d, *J* = 7.9 Hz, 1H), 7.87 (dd, *J* = 13.3, 8.3 Hz, 2H), 7.62 – 7.51 (m, 2H), 4.87 (q, *J* = 3.0 Hz, 1H), 4.71 (t, *J* = 2.8 Hz, 2H), 4.40 (q, *J* = 2.7 Hz, 1H). ^{13}C NMR (151 MHz, $CDCl_3$) δ 164.0, 159.0, 135.1, 132.8, 129.1, 129.0, 128.5, 128.0, 126.8, 124.4, 124.1, 84.0, 58.0. The spectroscopic data were consistent with the data reported in previous report.[4]

5-Methylene-2-(thiophen-2-yl)-4,5-dihydrooxazole (9n)

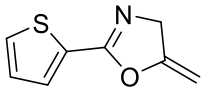

After purification (Silica Gel, n-hexane/ethyl acetate 10:1) **9n** was isolated as a yellow oil in 89% yield (29.4 mg). ^{1}H NMR (600 MHz, $CDCl_3$) δ 7.66 (d, *J* = 3.4 Hz, 1H), 7.50 (d, *J* = 4.9 Hz, 1H), 7.16 – 7.05 (m, 1H), 4.81 (q, *J* = 2.9 Hz, 1H), 4.63 (t, *J* = 2.6 Hz, 2H), 4.36 (q, *J* = 2.5 Hz, 1H). ^{13}C NMR (151 MHz, $CDCl_3$) δ 159.7, 158.8, 130.9, 130.5, 129.4, 127.9, 84.2, 57.8. The spectroscopic data were consistent with the data reported in previous report.[9].

2-(furan-2-yl)-5-methylene-4,5-dihydrooxazole (9o)

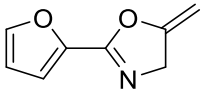

After purification (Silica Gel, n-hexane/ethyl acetate 10:1) **9o** was isolated as a colourless liquid in 78% yield (23.2 mg). ^{1}H NMR (600 MHz, $CDCl_3$) δ 7.58 (s, 1H), 7.03 (d, *J* = 3.4

Hz, 1H), 6.53 (dd, *J* = 3.4, 1.7 Hz, 1H), 4.83 – 4.80 (m, 1H), 4.64 (t, *J* = 2.8 Hz, 2H), 4.38 (q, *J* = 2.7 Hz, 1H). ^{13}C NMR (151 MHz, $CDCl_3$) δ 163.3, 158.8, 137.9, 129.6, 126.4, 99.1, 84.3, 57.9. The spectroscopic data were consistent with the data reported in previous report.[10]

2-Cyclohexyl-4,4-dimethyl-5-methylene-4,5-dihydrooxazole (9p)

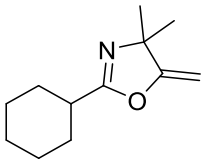

After purification (Silica Gel, n-hexane/ethyl acetate 10:1) **9p** was isolated as a colorless liquid in 80% yield (30.9 mg). ^{1}H NMR (600 MHz, $CDCl_3$) δ 4.56 (d, *J* = 2.7 Hz, 1H), 4.11 (d, *J* = 2.7 Hz, 1H), 2.35 (tt, *J* = 11.5, 3.5 Hz, 1H), 2.00 – 1.92 (m, 2H), 1.83 – 1.75 (m, 2H), 1.68 (d, *J* = 11.5 Hz, 2H), 1.49 – 1.45 (m, 2H), 1.33 (s, 6H), 1.27 (s, 2H). ^{13}C NMR (151 MHz, $CDCl_3$) δ 168.4, 166.9, 81.4, 68.3, 37.4, 29.8, 29.6, 25.9, 25.7. The spectroscopic data were consistent with the data reported in previous report.[7]

4,4-Dimethyl-5-methylene-2-(4-nitrophenyl)-4,5-dihydrooxazole (9q)

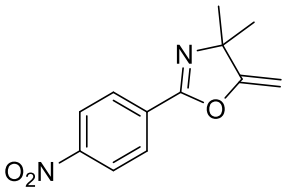

After purification (Silica Gel, n-hexane/ethyl acetate 10:1) **9q** was isolated as a white solid in 92% yield (42.7 mg). ^{1}H NMR (600 MHz, $CDCl_3$) δ 8.30 (d, *J* = 8.9 Hz, 2H), 8.17 (d, *J* = 9.0 Hz, 2H), 4.80 (d, *J* = 3.1 Hz, 1H), 4.32 (d, *J* = 3.1 Hz, 1H), 1.48 (s, 6H). ^{13}C NMR (151 MHz, $CDCl_3$) δ 167.5, 158.3, 149.8, 132.9, 129.3, 123.8, 83.6, 69.8, 29.8. The spectroscopic data were consistent with the data reported in previous report.[12]

(*Z*)-5-Benzylidene-4,4-dimethyl-2-(*p*-tolyl)-4,5-dihydrooxazole (9r)

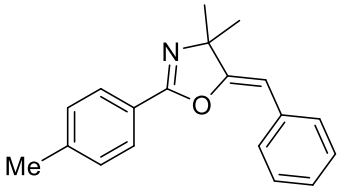

After purification (Silica Gel, n-hexane/ethyl acetate 10:1) **9r** was isolated as a white solid in 95% yield (52.7 mg). ^{1}H NMR (600 MHz, $CDCl_3$) δ 7.97 (d, *J* = 8.1 Hz, 2H), 7.64 (d, *J* = 7.6 Hz, 2H), 7.39 (t, *J* = 7.7 Hz, 2H), 7.29 (d, *J* = 7.9 Hz, 2H), 7.21 (t, *J* = 7.4 Hz, 1H), 5.53 (s, 1H), 2.42 (s, 3H), 1.53 (s, 6H). ^{13}C NMR (151 MHz, $CDCl_3$) δ 160.9, 160.0, 142.5, 135.2, 129.4, 128.6, 128.3, 128.0, 126.2, 124.2, 99.3, 70.9, 29.8, 21.8. The spectroscopic data were consistent with the data reported in previous report.[7]

(*Z*)-5-Benzylidene-4,4-dimethyl-2-phenyl-4,5-dihydrooxazole (9s)

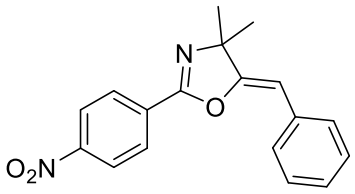

After purification (Silica Gel, n-hexane/ethyl acetate 10:1) **9s** was isolated as a yellow solid in 86% yield (53.0 mg). ^{1}H NMR (600 MHz, $CDCl_3$) δ 8.32 (d, *J* = 8.8 Hz, 2H), 8.24 (d, *J* = 8.9 Hz, 2H), 7.62 (d, *J* = 7.7 Hz, 2H), 7.41 (t, *J* = 7.7 Hz, 2H), 7.24 (t, *J* = 7.4 Hz, 1H), 5.59 (s, 1H), 1.56 (s, 6H). ^{13}C NMR (151 MHz, $CDCl_3$) δ 160.0, 158.2, 149.8, 134.6, 132.7, 129.3, 128.7, 128.0, 126.6, 123.8, 100.4, 71.5, 29.6. The spectroscopic data were consistent with the data reported in previous report.[11]

(*Z*)-5-Benzylidene-4,4-dimethyl-2-(thiophen-2-yl)-4,5-dihydrooxazole (9t)

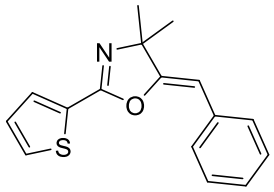

After purification (Silica Gel, n-hexane/ethyl acetate 10:1) **9t** was isolated as a white solid in 84% yield (45.2 mg). ^{1}H NMR (600 MHz, $CDCl_3$) δ 7.79 (dd, *J* = 3.7, 1.1 Hz, 1H), 7.62 (d, *J* = 7.3 Hz, 2H), 7.53 (dd, *J* = 5.0, 1.1 Hz, 1H), 7.38 (t, *J* = 7.8 Hz, 2H), 7.21 (t, *J* = 7.4 Hz, 1H), 7.15 (dd, *J* = 4.9, 3.7 Hz, 1H), 5.53 (s, 1H), 1.53 (s, 6H). ^{13}C NMR (151 MHz, $CDCl_3$) δ 160.5, 155.7, 135.0, 131.1, 130.6, 129.5, 128.6, 128.1, 127.9, 126.4, 99.6, 71.2, 29.8. The spectroscopic data were consistent with the data reported in previous report[7].

2-(benzo[d][1,3]dioxol-5-yl)-5-methylene-4,5-dihydrooxazole (9u)

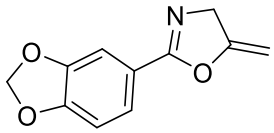

After purification (Silica Gel, n-hexane/ethyl acetate 10:1) **9u** was isolated as a white solid in 80% yield (32.5 mg). ^{1}H NMR (600 MHz, $CDCl_3$) δ 7.52 (d, *J* = 8.1 Hz, 1H), 7.42 (s, 1H), 6.83 (d, *J* = 8.2 Hz, 1H), 6.01 (s, 2H), 4.77 (q, *J* = 2.9 Hz, 1H), 4.60 (t, *J* = 2.7 Hz, 2H), 4.33 (q, *J* = 2.6 Hz, 1H). ^{13}C NMR (151 MHz, $CDCl_3$) δ 163.4, 159.1, 150.8, 148.0, 123.3, 120.9, 108.3, 101.8, 83.6, 57.8. The spectroscopic data were consistent with the data reported in previous report.[7]

4-(5-Methylene-4,5-dihydrooxazol-2-yl)-*N*,*N*-dipropylbenzenesulfonamide (9v)

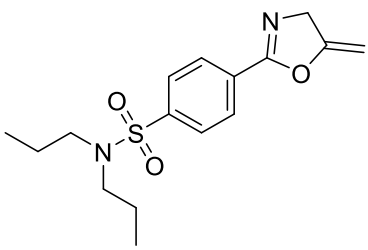

After purification (Silica Gel, n-hexane/ethyl acetate 10:1) **9v** was isolated as a white solid in 63% yield (40.6 mg). ^{1}H NMR (600 MHz, $CDCl_3$) δ 8.10 (d, *J* = 8.4 Hz, 2H), 7.87 (d, *J* = 8.5 Hz, 2H), 4.85 (q, *J* = 3.0 Hz, 1H), 4.68 (t, *J* = 2.8 Hz, 2H), 4.41 (q, *J* = 2.7 Hz, 1H), 3.14 – 3.07 (m, 4H), 1.54 (h, *J* = 7.4 Hz, 4H), 0.86 (t, *J* = 7.4 Hz, 6H). ^{13}C NMR (151 MHz, $CDCl_3$) δ 162.5, 158.5, 143.3, 130.0, 128.6, 127.1, 84.6, 57.9, 49.9, 21.9, 11.2. The spectroscopic data were consistent with the data reported in previous report.[7]

2.6. General Procedure for the Hydroamination and Hydrohydrazination of Alkynes

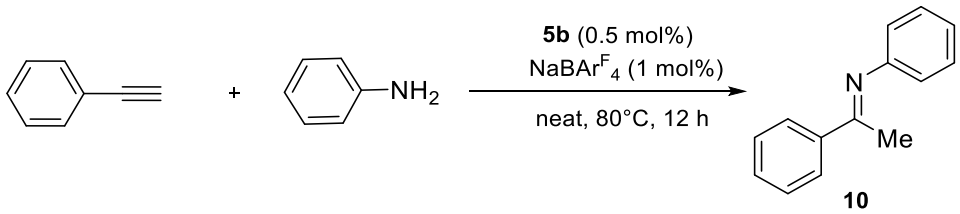

In air, a vial was charged with [NHC–Au] catalyst **5b** (0.5 mol%), NaBAr$^F_4$ (1 mol%) and the phenylacetylene (0.2 mmol, 1.0 equiv.). After stirring for five minutes, aniline (0.22 mmol, 1.1 equiv.) was added as a solution and the reaction mixture was stirred for 12 h at 80 °C.

(*E*)-*N*,1-Diphenylethan-1-imine (10)

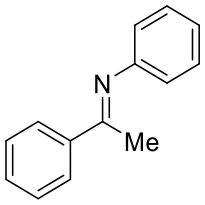

After purification using Florisil eluting with a gradient mixture of n-hexane/ethyl acetate 10:1. **10** was isolated as a yellow oil in 98% yield (38.2 mg).^{1}H NMR (600 MHz, $CDCl_3$) δ 8.00 – 7.94 (m, 2H), 7.49 – 7.42 (m, 3H), 7.35 (t, *J* = 7.8 Hz, 2H), 7.09 (t, *J* = 7.4 Hz, 1H), 6.83 – 6.74 (m, 2H), 2.23 (s, 3H). ^{13}C NMR (151 MHz, $CDCl_3$) δ 165.6, 151.8, 139.6, 130.6, 129.1, 128.5, 127.3, 123.4, 119, 17.5. The spectroscopic data were consistent with the data reported in previous report.[13]

Table S1. Catalyst Effect on Au–NHC-Catalyzed Amide Cycloisomerization[a]

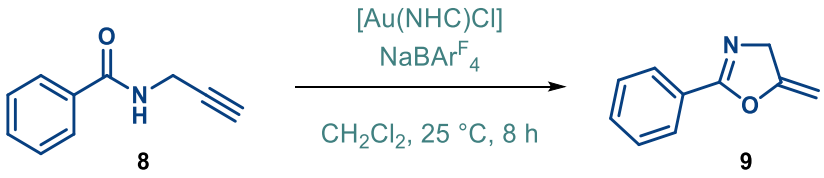

entry	catalyst	[Au–NHC] (mol%)	additive	yield (%)
1	[Au(**Indy***)Cl]	1.0	NaBAr$^F_4$	95
2	[Au(**Indy***^{MeO})Cl]	1.0	NaBAr$^F_4$	97
3	[Au(**IMes**)Cl]	1.0	NaBAr$^F_4$	52
4	[Au(**IPr**)Cl]	1.0	NaBAr$^F_4$	76

[a]Conditions: **8** (1.0 equiv), Au–NHC (1.0 mol%), NaBAr$^F_4$ (1.0 mol%), CH_2Cl_2, 25 °C, 8 h.

4. Crystallographic Studies

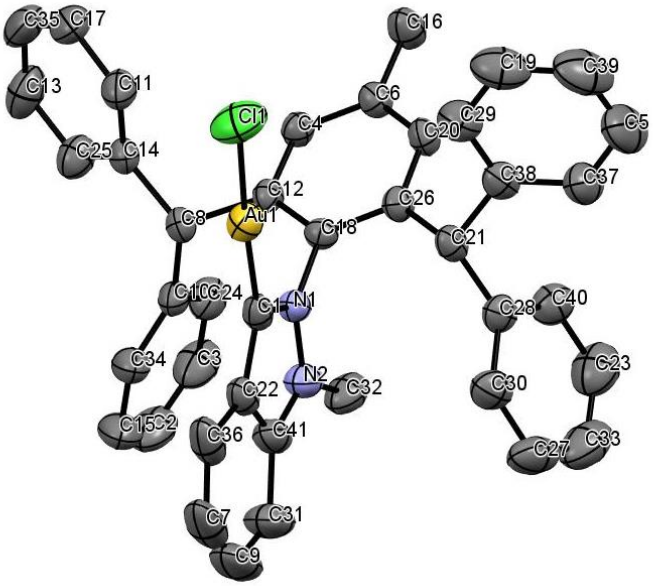

Figure S1. Crystal structure of **5a** *(50% ellipsoids)*. Hydrogen atoms and counterion have been omitted for clarity. Selected bond lengths [Å] and angles [°]: Au–C1, 1.981(3); Au–Cl, 2.284(1); N1–C1, 1.337(4); N1–C18, 1.444(4); C1–C22, 1.420(4);C1–Au–Cl, 175.42(9); C1–N1–C18, 128.2(3); N1–C1–C22, 105.0(3). (Crystallographic data has been deposited with the Cambridge Crystallographic Data Center as supplementary publication no. CCDC 2158126).

Table S2. *Crystal Data and Structure Refinement Summary for* ***5a.***

Crystal data

$C_{41}H_{34}AuClN_2$	$F(000)$ = 1560
M_r = 787.12	D_x = 1.547 Mg m^{-3}
Monoclinic, $P2_1/n$	Mo $K\alpha$ radiation, λ = 0.71073 Å
a = 9.6522 (15) Å	Cell parameters from 9967 reflections
b = 17.489 (3) Å	θ = 2.3–27.4°
c = 20.153 (3) Å	μ = 4.46 mm^{-1}
β = 96.606 (5)°	T = 273 K
V = 3379.4 (10) Å^3	Block, colourless
Z = 4	

Data collection

Bruker APEX-II CCD diffractometer	6468 reflections with $I > 2\sigma(I)$
ϕ and ω scans	$R_{int} = 0.051$
Absorption correction: multi-scan *SADABS2016*/2 (Bruker,2016/2) was used for absorption correction. wR2(int) was 0.1548 before and 0.0626 after correction. The Ratio of minimum to maximum transmission is 0.4749. The $\lambda/2$ correction factor is Not present.	$\theta_{max} = 27.5°$, $\theta_{min} = 2.3°$
$T_{min} = 0.354$, $T_{max} = 0.746$	$h = -12 \rightarrow 12$
118513 measured reflections	$k = -22 \rightarrow 22$
7768 independent reflections	$l = -26 \rightarrow 26$

Refinement

Refinement on F^2	Primary atom site location: dual
Least-squares matrix: full	Hydrogen site location: inferred from neighbouring sites
$R[F^2 > 2\sigma(F^2)] = 0.028$	H-atom parameters constrained
$wR(F^2) = 0.059$	$w = 1/[\sigma^2(F_o^2) + (0.0147P)^2 + 4.3527P]$ where $P = (F_o^2 + 2F_c^2)/3$
$S = 1.13$	$(\Delta/\sigma)_{max} = 0.001$
7768 reflections	$\Delta\rangle_{max} = 0.76$ e Å^{-3}
408 parameters	$\Delta\rangle_{min} = -1.23$ e Å^{-3}
0 restraints	

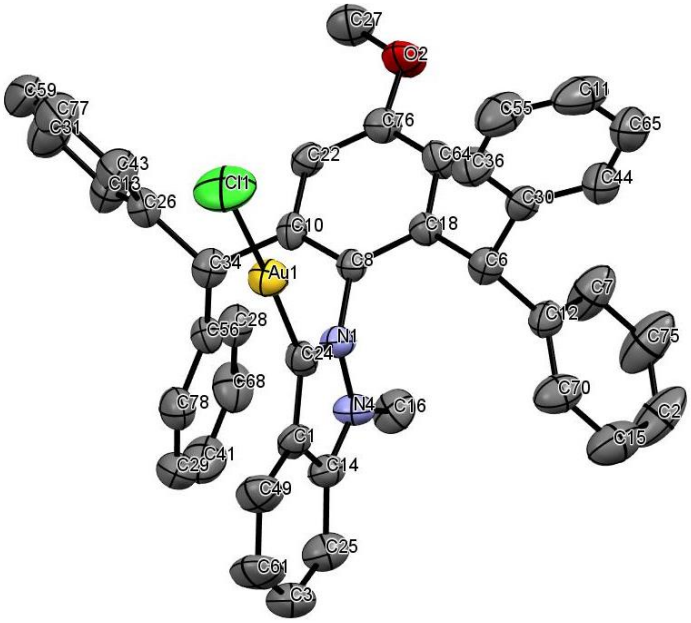

Figure S2. Crystal structure of **5b** *(50% ellipsoids)*. Hydrogen atoms and counterion have been omitted for clarity. Selected bond lengths [Å] and angles [°]: Au1–C24, 1.983(7); Au1–Cl, 2.296(2); N1-C24, 1.348(8); N1–C8, 1.444(4); C1–C24, 1.450(7); C24–Au1–Cl, 177.0(2); C24–N1–C8, 128.7(5); N1–C24–C1, 105.4(5). (Crystallographic data has been deposited with the Cambridge Crystallographic Data Center as supplementary publication no. CCDC 2158125.)

Table S3. *Crystal Data and Structure Refinement Summary for* ***5b.***

Crystal data

$2(C_{41}H_{34}AuClN_2O)$	$F(000)$ = 3184
M_r = 1606.23	D_x = 1.551 Mg m^{-3}
Monoclinic, $P2_1/c$	Mo $K\alpha$ radiation, λ = 0.71073 Å
a = 26.499 (4) Å	Cell parameters from 9915 reflections
b = 11.4792 (15) Å	θ = 2.4–27.3°
c = 22.902 (3) Å	μ = 4.39 mm^{-1}
β = 99.026 (4)°	T = 273 K
V = 6880.1 (15) Å^3	Block, colourless
Z = 4	

Data collection

Bruker APEX-II CCD diffractometer	7737 reflections with $I > 2\sigma(I)$
ϕ and ω scans	$R_{int} = 0.175$
Absorption correction: multi-scan *SADABS2016*/2 (Bruker,2016/2) was used for absorption correction. wR2(int) was 0.1103 before and 0.0871 after correction. The Ratio of minimum to maximum transmission is 0.8262. The $\lambda/2$ correction factor is Not present.	$\theta_{max} = 25.0°$, $\theta_{min} = 2.1°$
$T_{min} = 0.616$, $T_{max} = 0.746$	$h = -31 \rightarrow 31$
179149 measured reflections	$k = -13 \rightarrow 13$
12126 independent reflections	$l = -27 \rightarrow 27$

Refinement

Refinement on F^2	Primary atom site location: dual
Least-squares matrix: full	Hydrogen site location: inferred from neighbouring sites
$R[F^2 > 2\sigma(F^2)] = 0.042$	H-atom parameters constrained
$wR(F^2) = 0.088$	$w = 1/[\sigma^2(F_o^2) + (0.0183P)^2 + 13.3639P]$ where $P = (F_o^2 + 2F_c^2)/3$
$S = 1.04$	$(\Delta/\sigma)_{max} = 0.002$
12126 reflections	$\Delta\rangle_{max} = 0.87$ e Å^{-3}
833 parameters	$\Delta\rangle_{min} = -0.86$ e Å^{-3}
0 restraints	

5. Computational Details

Computational Methods. For frontier orbital calculations, all of the calculations were performed using Gaussian 09 suite of programs. All of the geometry optimizations were performed at the B3LYP level of theory in the gas phase and the 6-311++G(d,p) basis set. For geometry optimizations, we employed the X-ray structures of gold(I) chloride complexes of 2-(2,6-dibenzhydryl-4-methylphenyl)-1-methyl-1*H*-indazol-2-ium and 2-(2,6-dibenzhydryl-4-methoxyphenyl)-1-methyl-1*H*-indazol-2-ium as the starting geometry and performed full optimization. The absence of imaginary frequencies was used to characterize the structures as minima on the potential energy surface. All of the optimized geometries were verified as minima (no imaginary frequencies). Energetic parameters were calculated under standard conditions (298.15 K and 1 atm). Structural representations were generated using CYLview software (Legault, C. Y. CYLview version 1.0 BETA, University of Sherbrooke). All other representations were generated using GaussView (GaussView, version 5, Dennington, R.; Keith, T.; Millam, J. Semichem Inc., Shawnee Mission, KS, 2009) or ChemCraft software (Andrienko, G. L. ChemCraft version b562a, https://www.chemcraftprog.com).

Additional Discussion. It is now established that computation of HOMO and LUMO provides the most accurate estimation of nucleophilicity (higher HOMO) and electrophilicity (lower LUMO) of NHC ligands. The HOMO of Indy* (-5.68 eV) and Indy*^{MeO} (-5.64 eV) indicate significantly stronger σ-donation than IPr (-6.01 eV), which is a standard electronic model for σ-donating NHCs. Furthermore, the LUMO of Indy* (-1.24 eV) and Indy*^{MeO} (-1.20 eV) are also lower than the corresponding π-accepting orbital of IPr (-0.48 eV). Moreover, the HOMO–1 orbital (π-donor) of Indy* (-6.07 eV) and Indy*^{MeO} (-6.03 eV) can be compared with the corresponding orbital for IPr (-6.55 eV). Thus, it is evident that Indy* ligands combine the steric properties of 2,6-

bis(diphenylmethyl)aryl N-wingtip substitution with σ-donating and π-electronic character of non-classical N-heterocyclic carbenes.

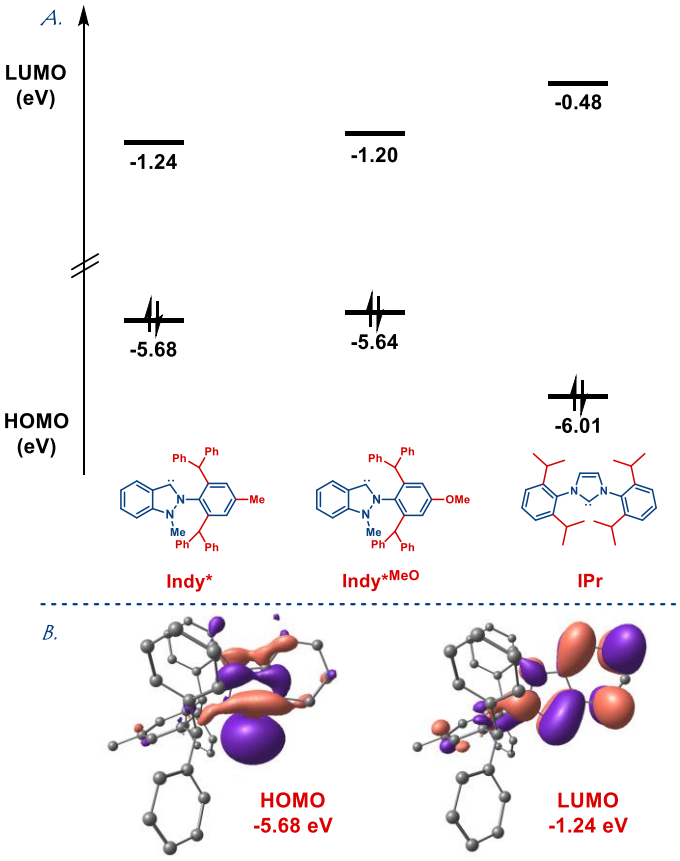

Chart S6. (A) Graphical representation of HOMO and LUMO energy levels (eV). B3LYP 6-311++g(d,p) level. (B) HOMO and LUMO of Indy*.

6. NMR Spectra

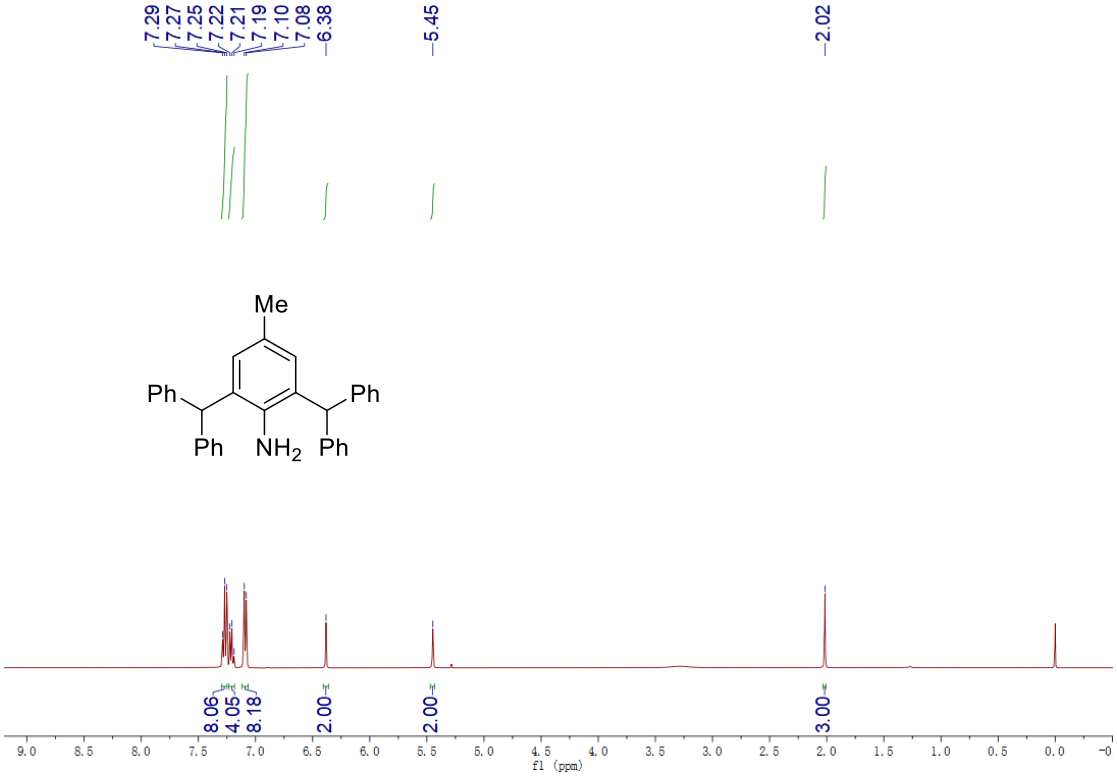

Figure S3. ^{1}H NMR (400 MHz, $CDCl_3$) Spectrum of Compound **1a**

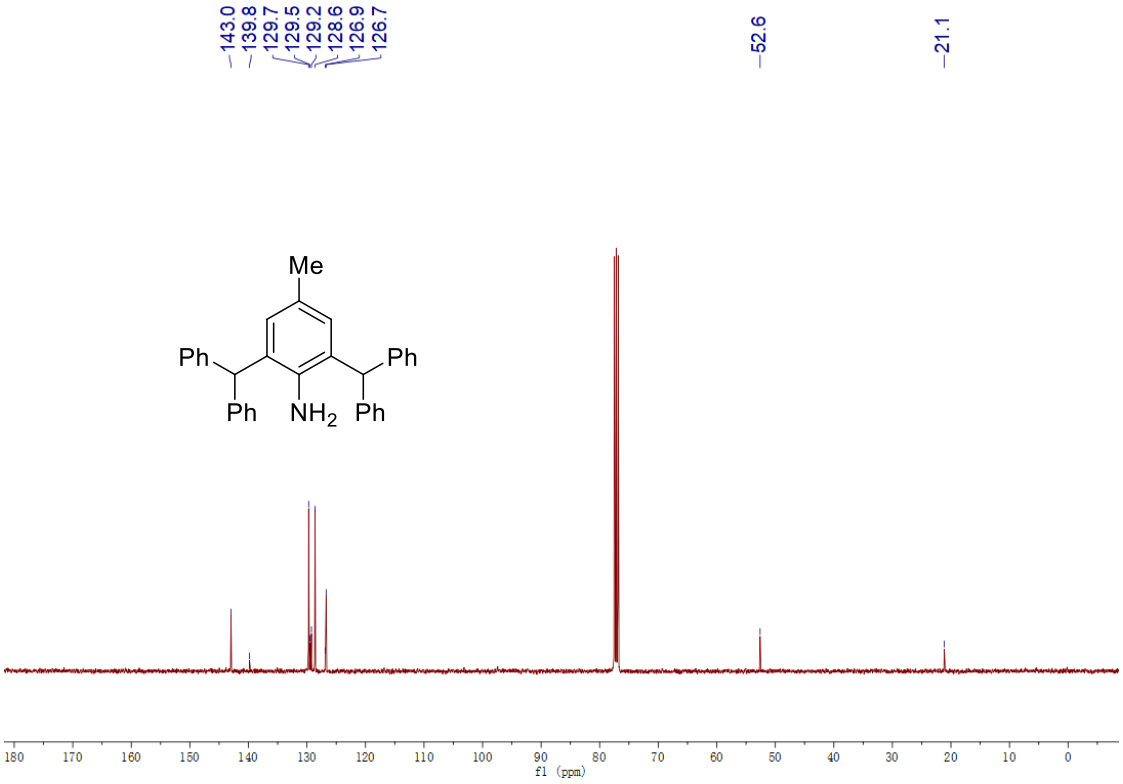

Figure S4. ^{13}C NMR (101 MHz, $CDCl_3$) Spectrum of Compound **1a**

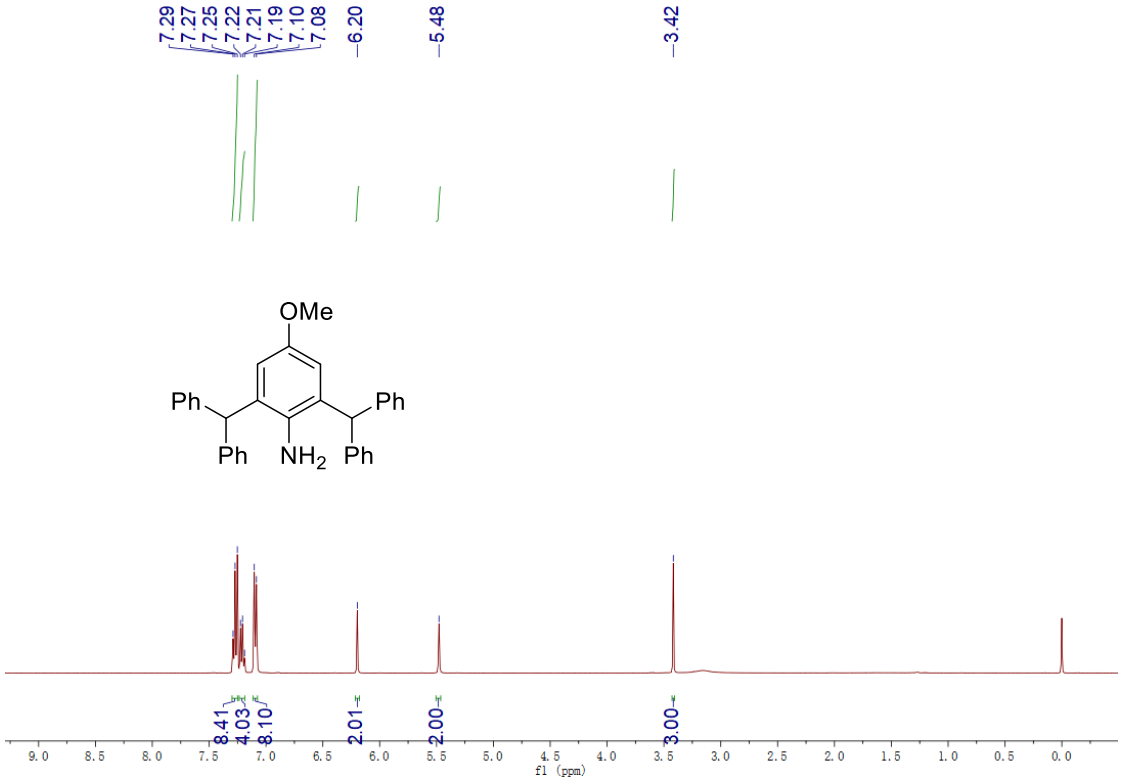

Figure S5. ^{1}H NMR (400 MHz, $CDCl_3$) Spectrum of Compound **1b**

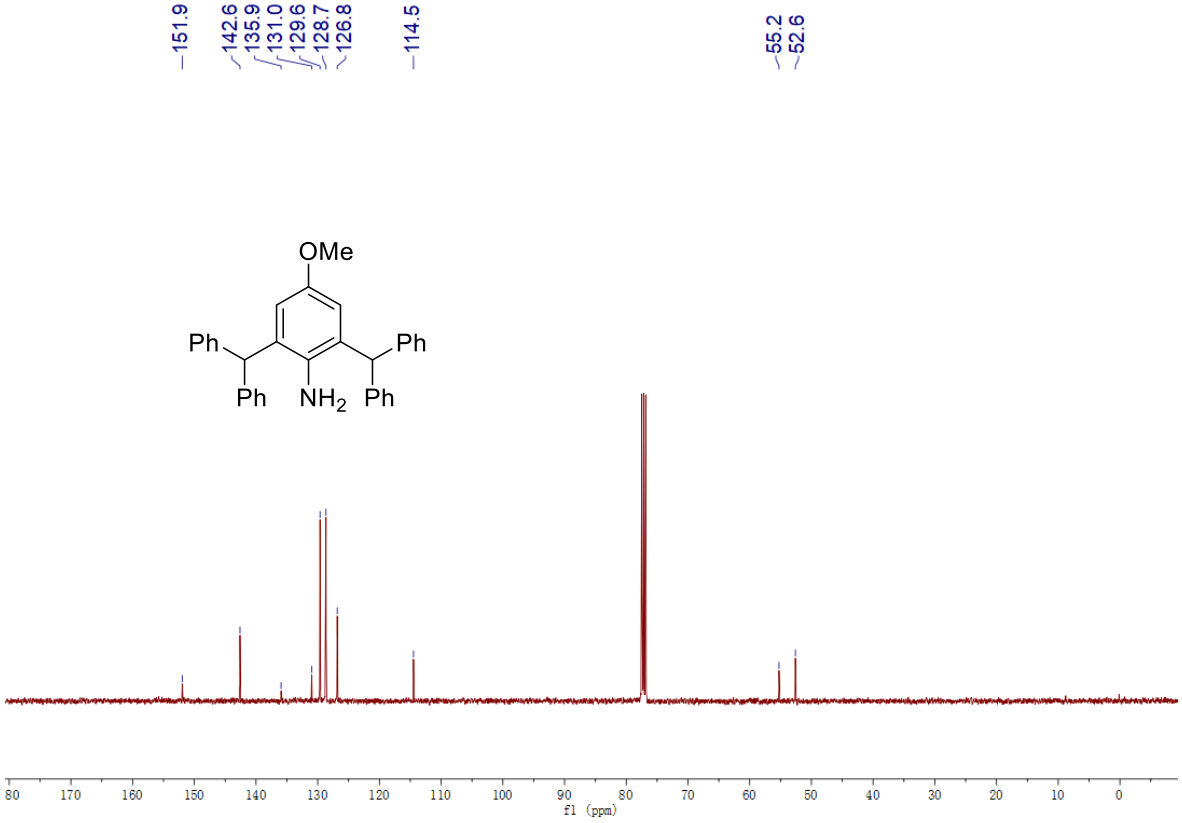

Figure S6. ^{13}C NMR (101 MHz, $CDCl_3$) Spectrum of Compound **1b**

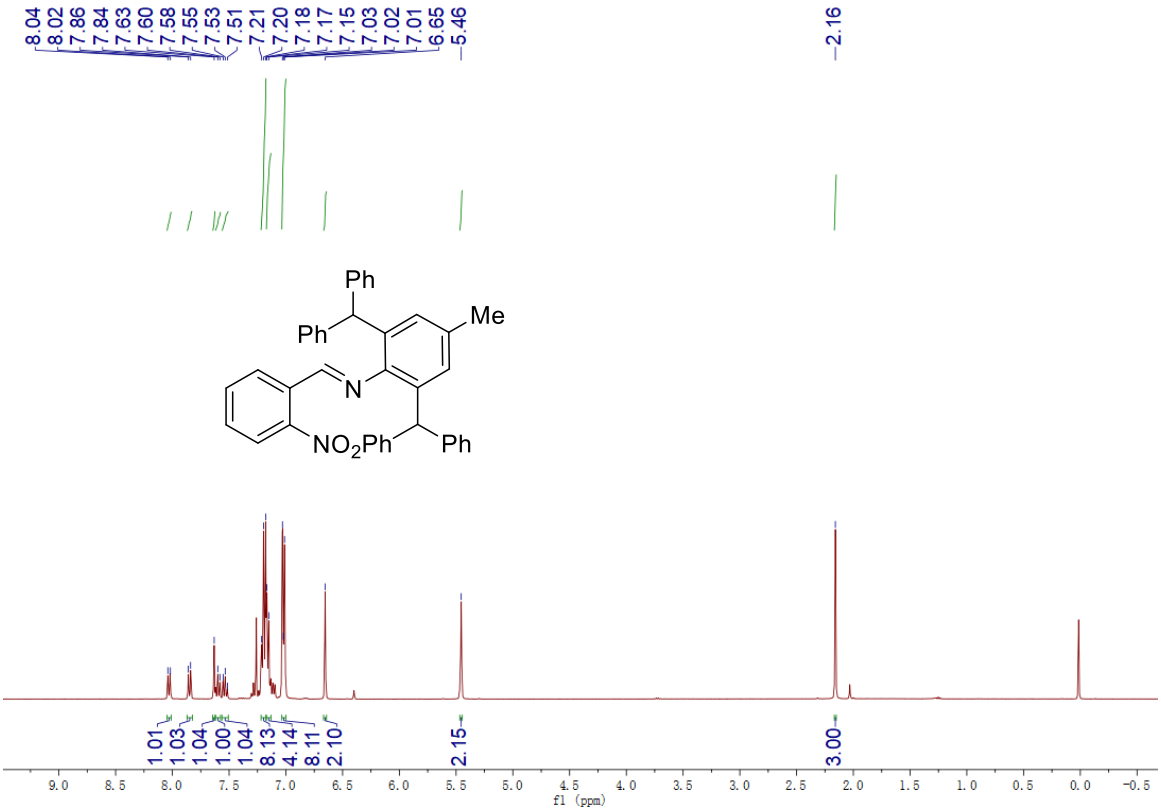

Figure S7. ^{1}H NMR (400 MHz, $CDCl_3$) Spectrum of Compound **2a**

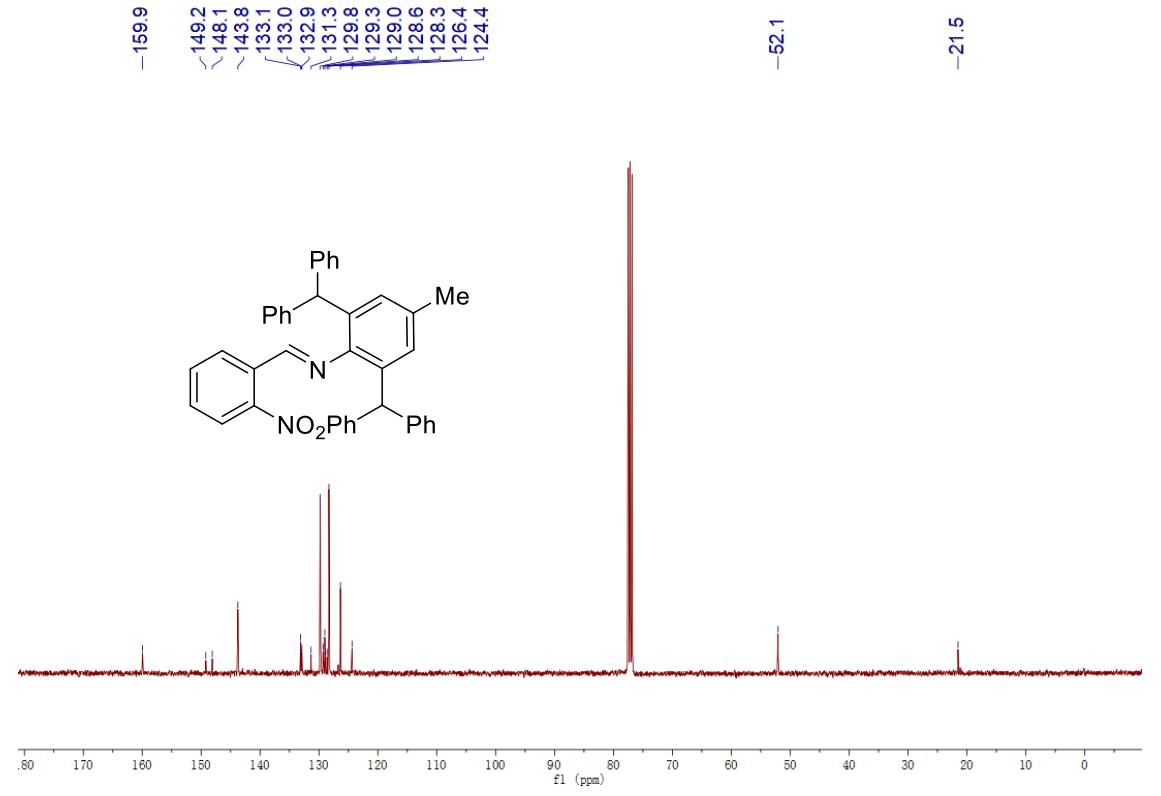

Figure S8. ^{13}C NMR (101 MHz, $CDCl_3$) Spectrum of Compound **2a**

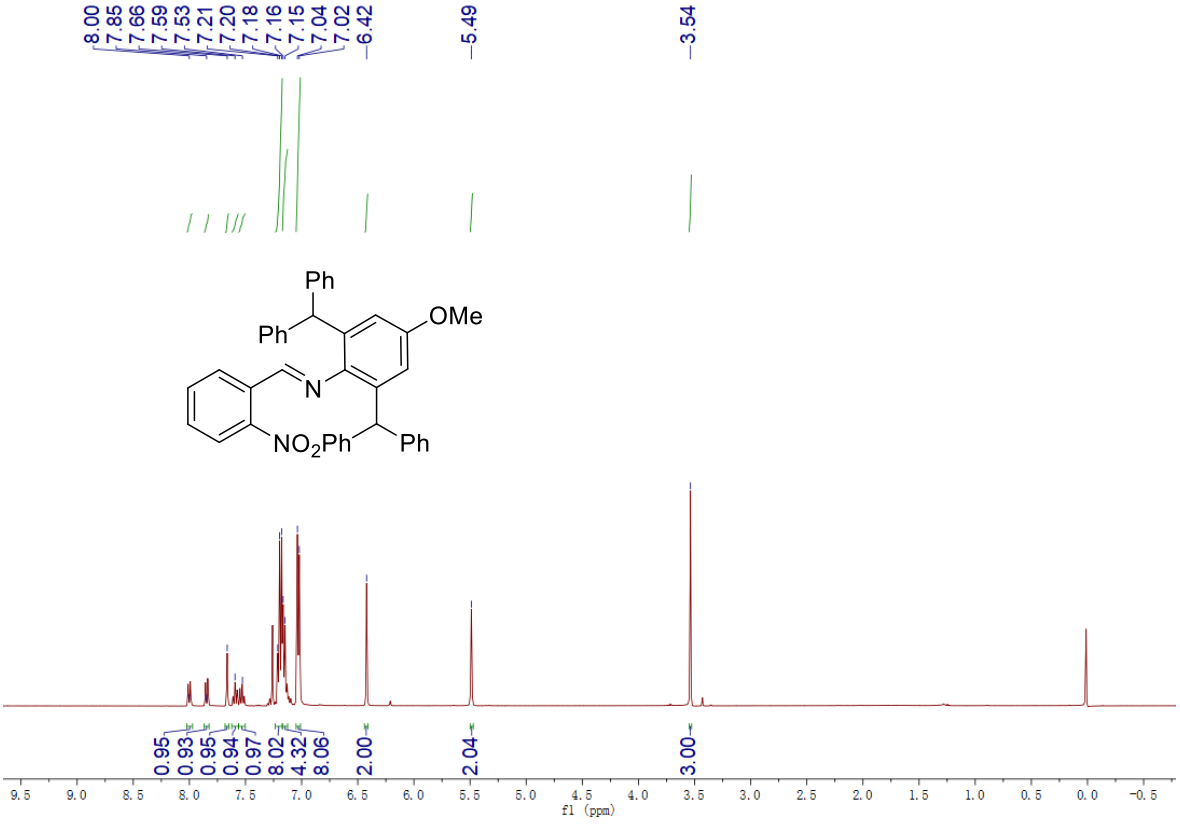

Figure S9. ^{1}H NMR (400 MHz, $CDCl_3$) Spectrum of Compound **2b**

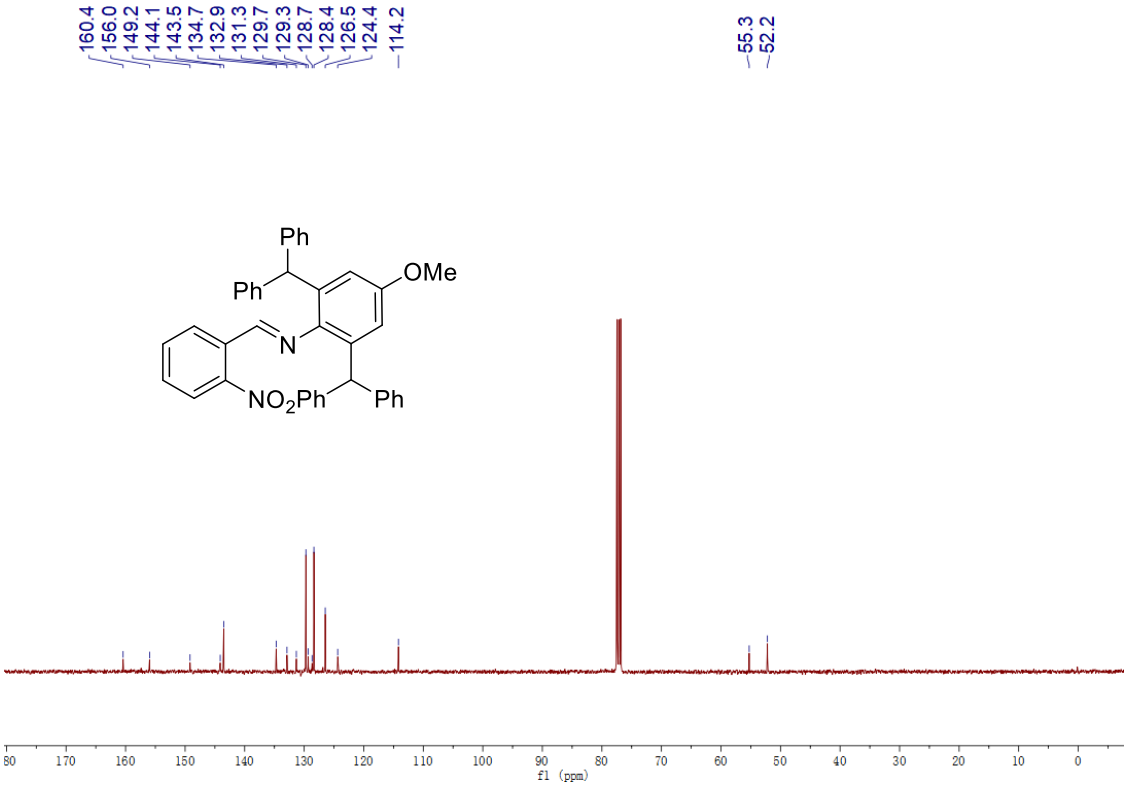

Figure S10. ^{13}C NMR (101 MHz, $CDCl_3$) Spectrum of Compound **2b**

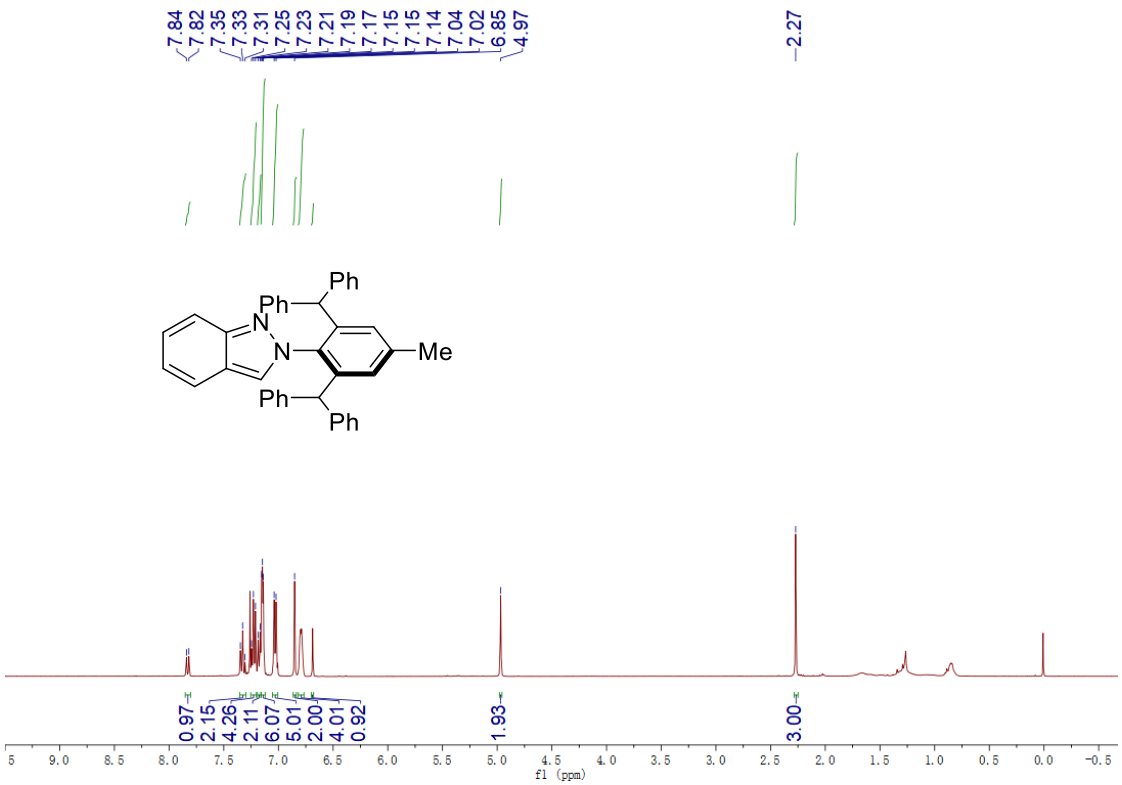

Figure S11. ^{1}H NMR (400 MHz, $CDCl_3$) Spectrum of Compound **3a**

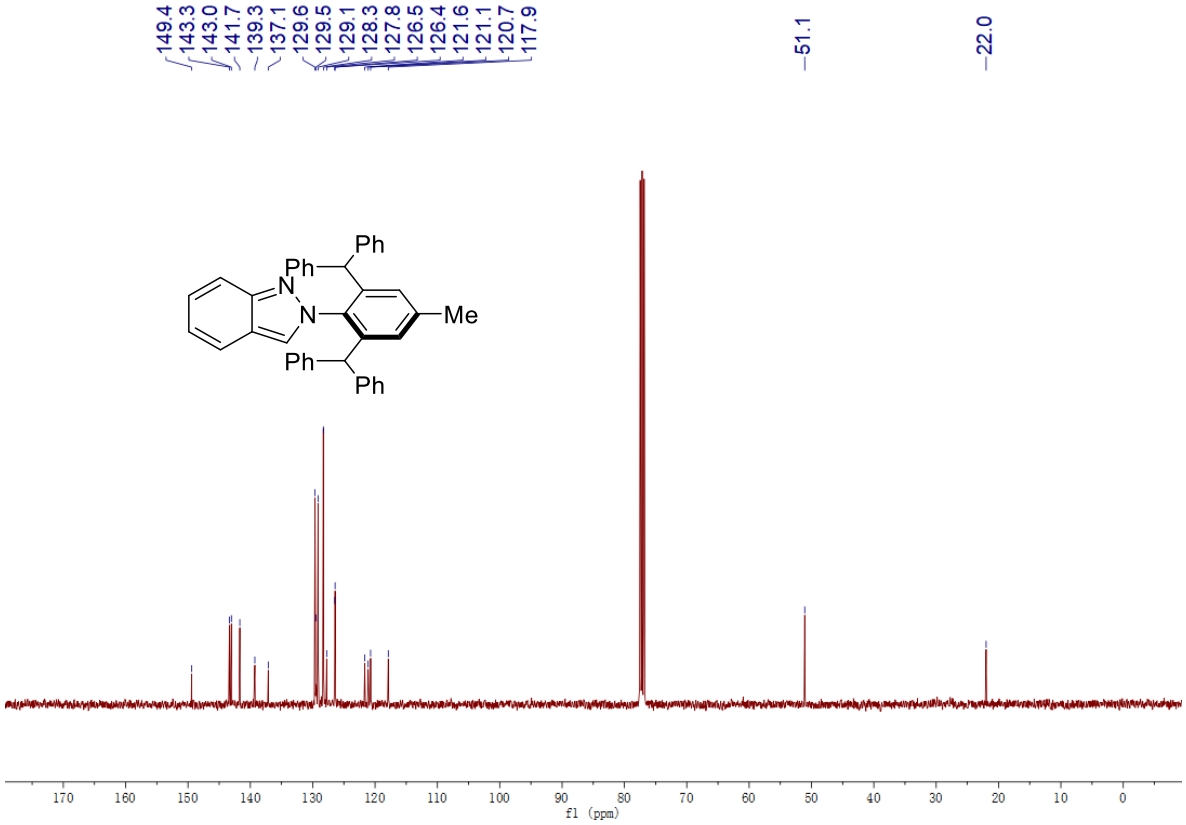

Figure S12. ^{13}C NMR (101 MHz, $CDCl_3$) Spectrum of Compound **3a**

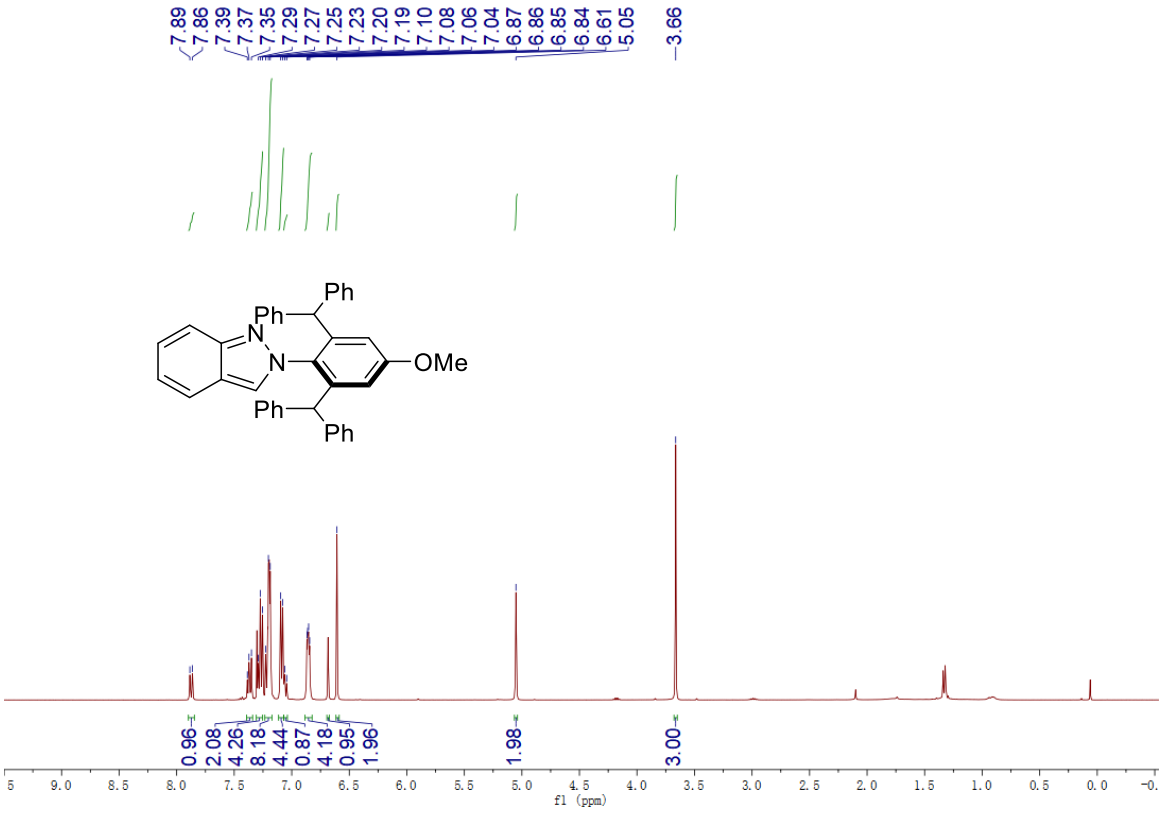

Figure S13. ^{1}H NMR (400 MHz, $CDCl_3$) Spectrum of Compound **3b**

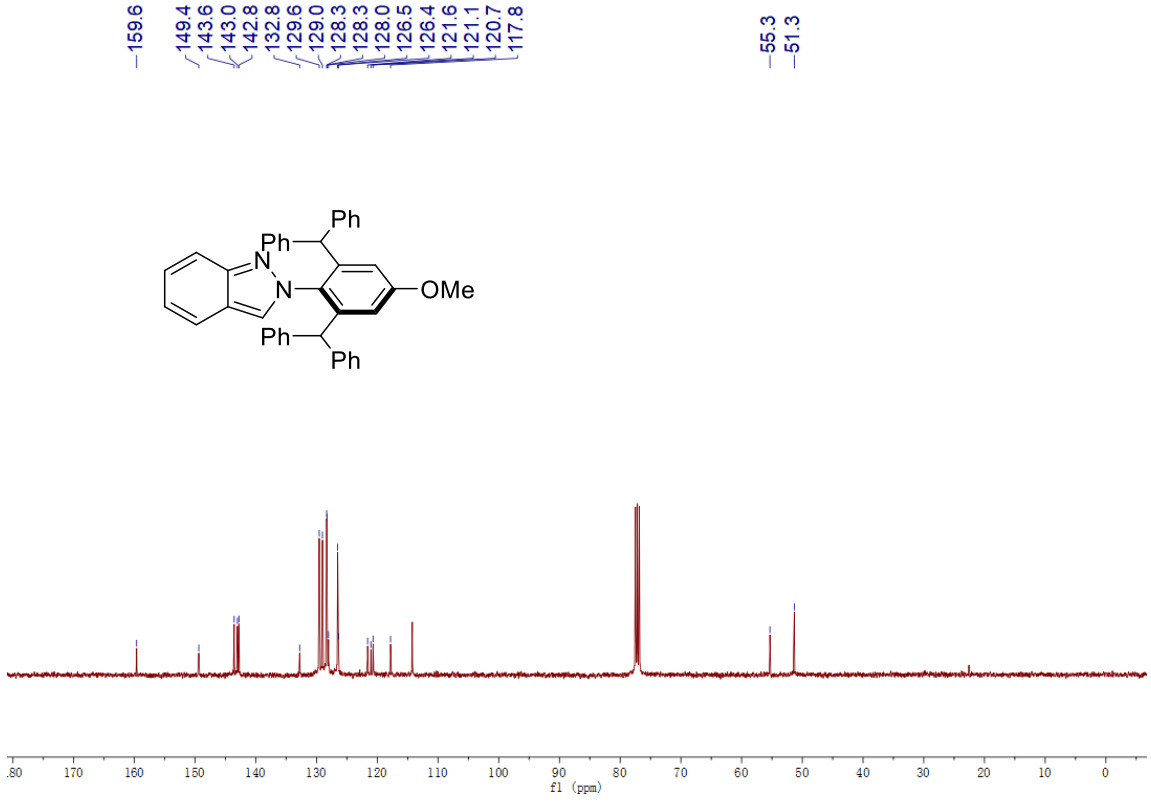

Figure S14. ^{13}C NMR (101 MHz, $CDCl_3$) Spectrum of Compound **3b**

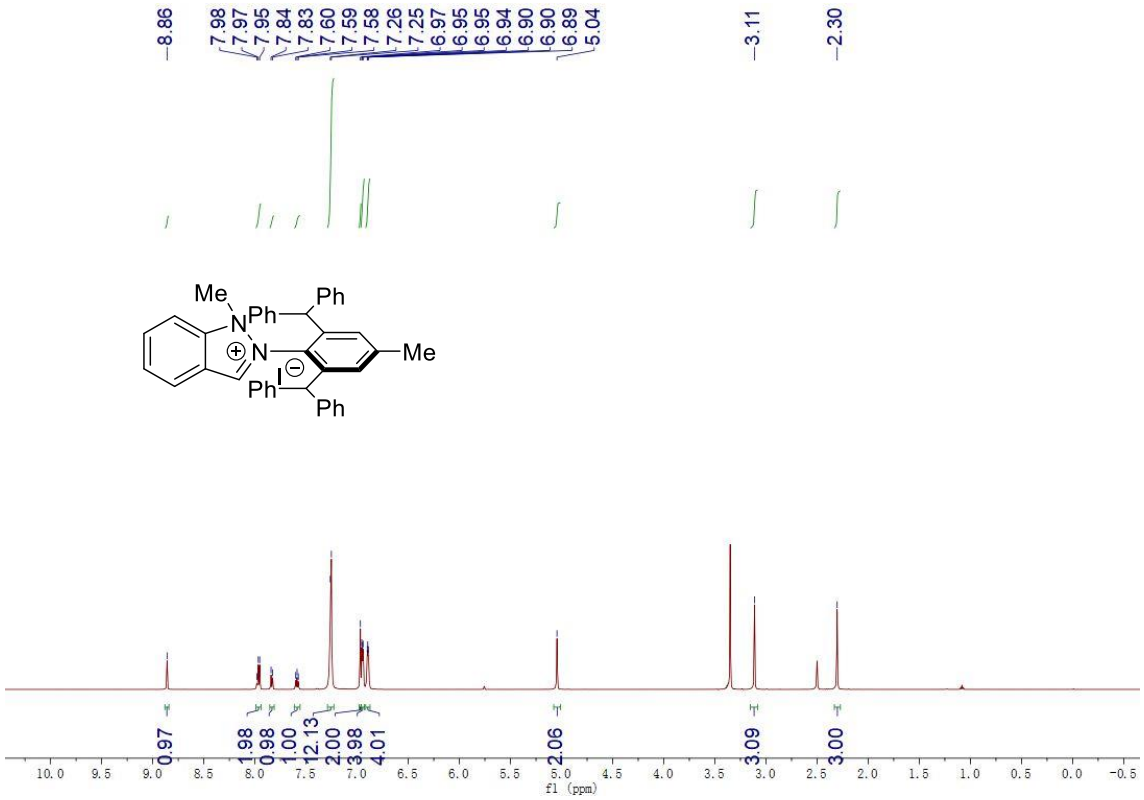

Figure S15. ^{1}H NMR (600 MHz, DMSO-d_6) Spectrum of Compound **4a**

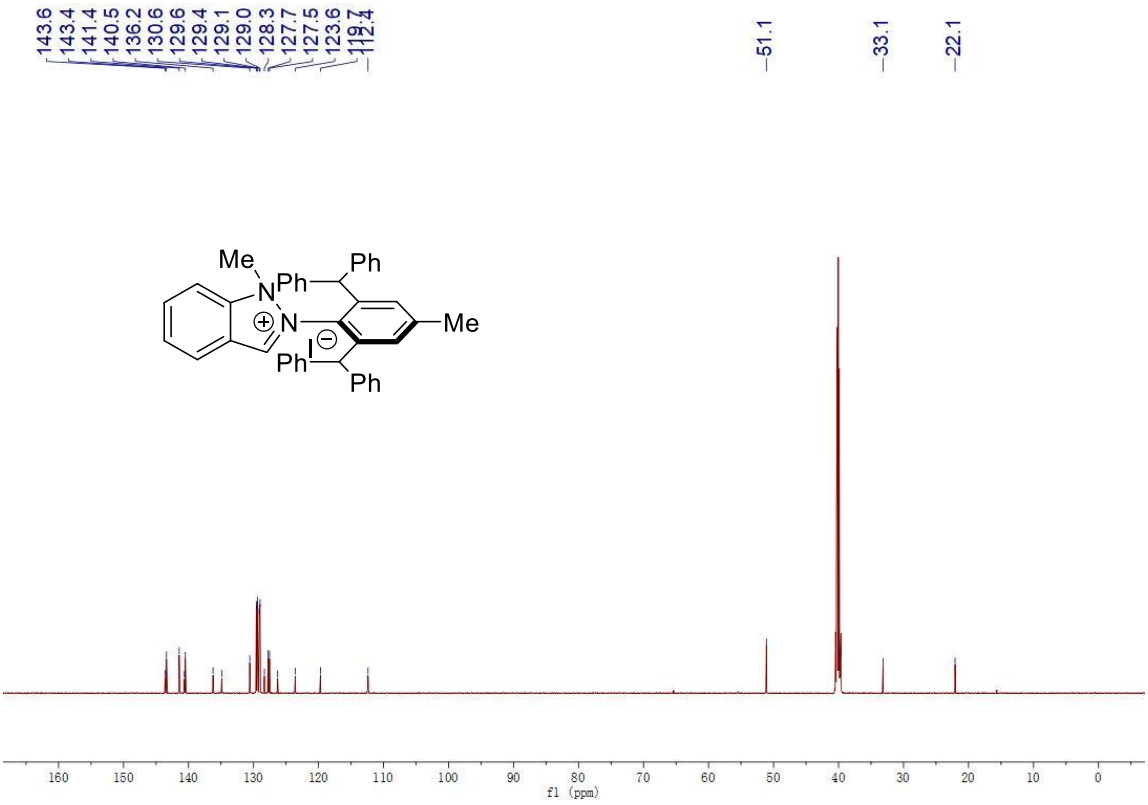

Figure S16. ^{13}C NMR (151 MHz, DMSO-d_6) Spectrum of Compound **4a**

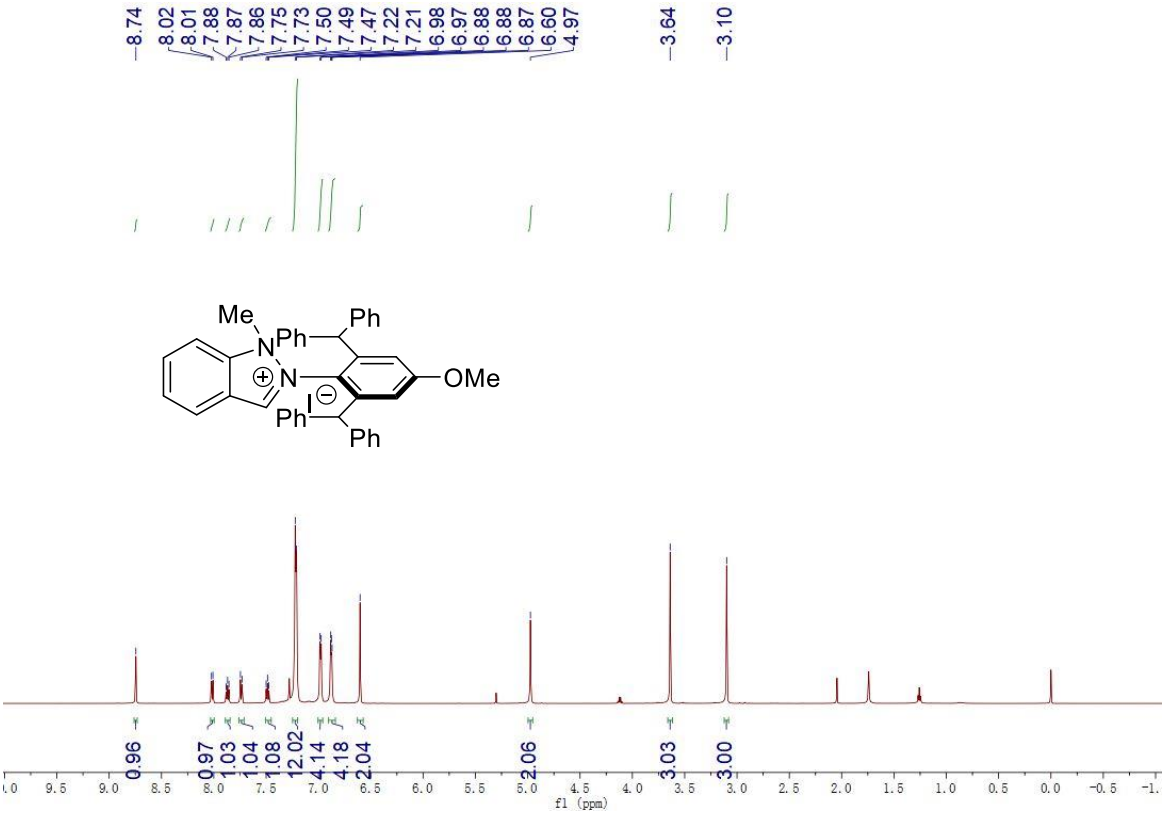

Figure S17. ^{1}H NMR (600 MHz, $CDCl_3$) Spectrum of Compound **4b**

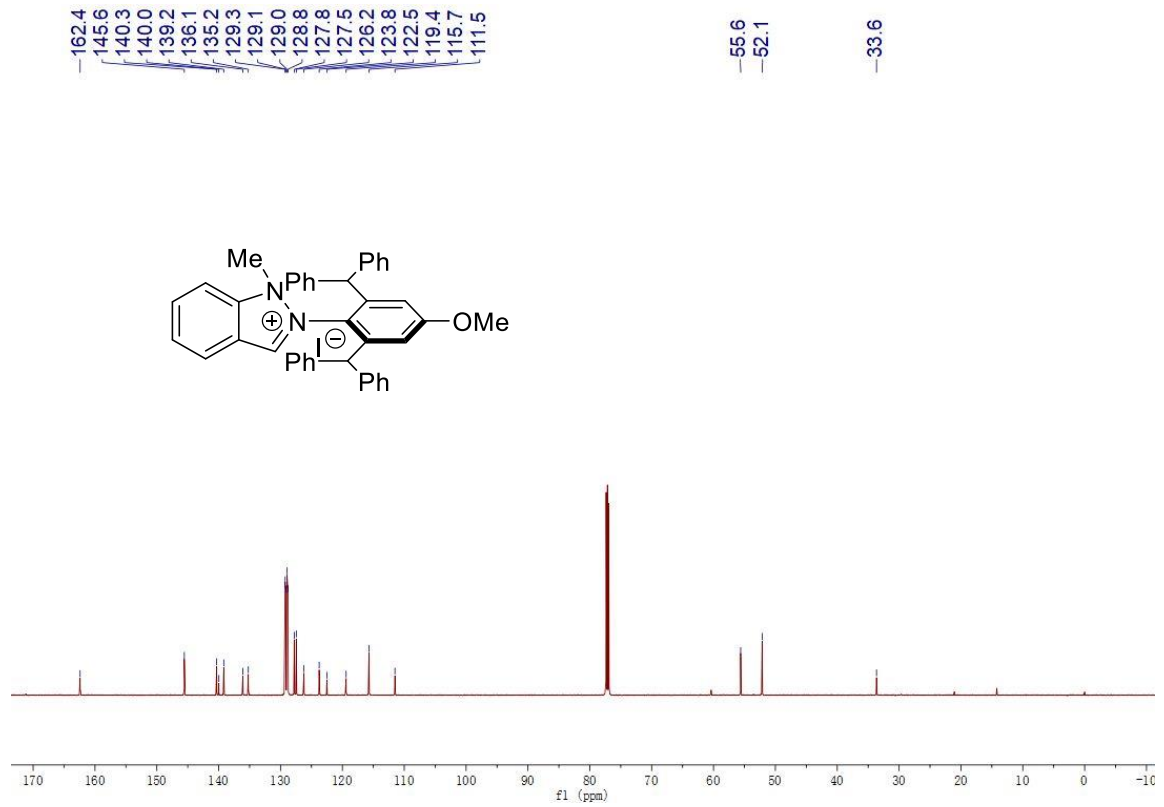

Figure S18. ^{13}C NMR (151 MHz, $CDCl_3$) Spectrum of Compound **4b**

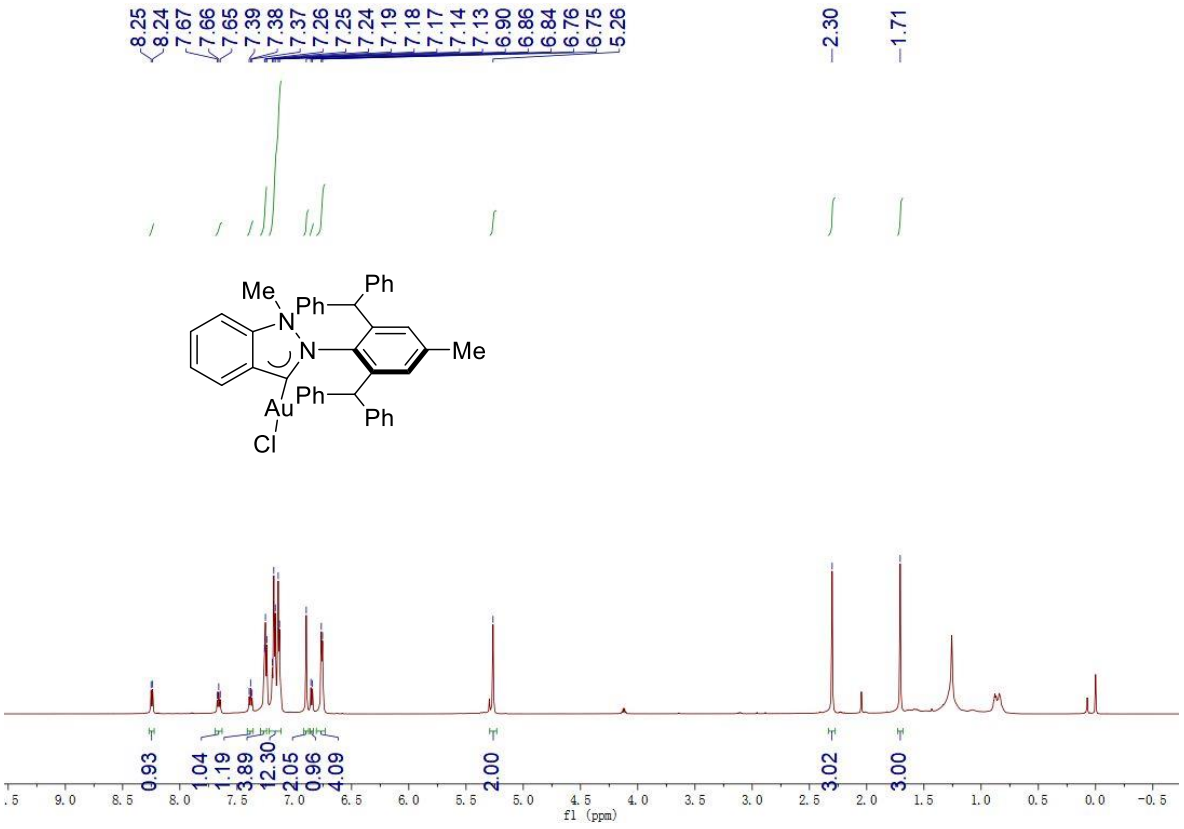

Figure S19. ^{1}H NMR (600 MHz, $CDCl_3$) Spectrum of Compound **5a**

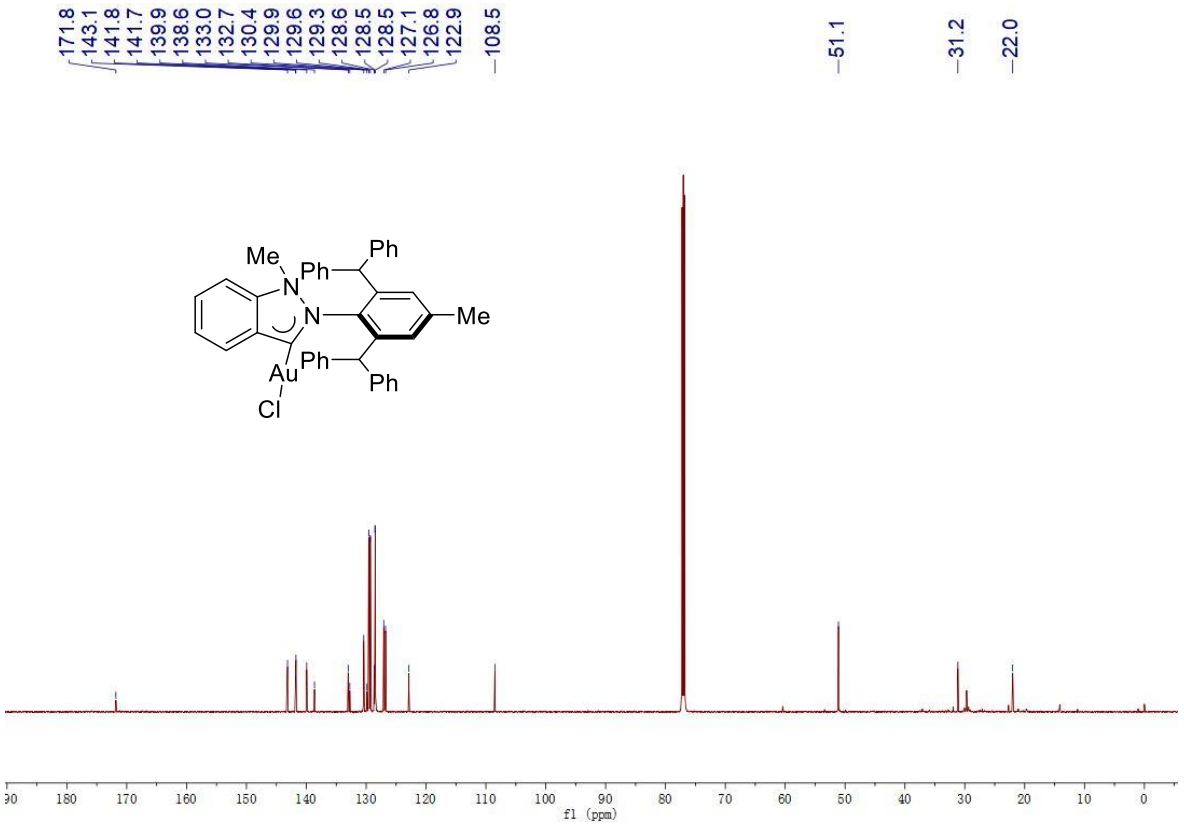

Figure S20. ^{13}C NMR (151 MHz, $CDCl_3$) Spectrum of Compound **5a**

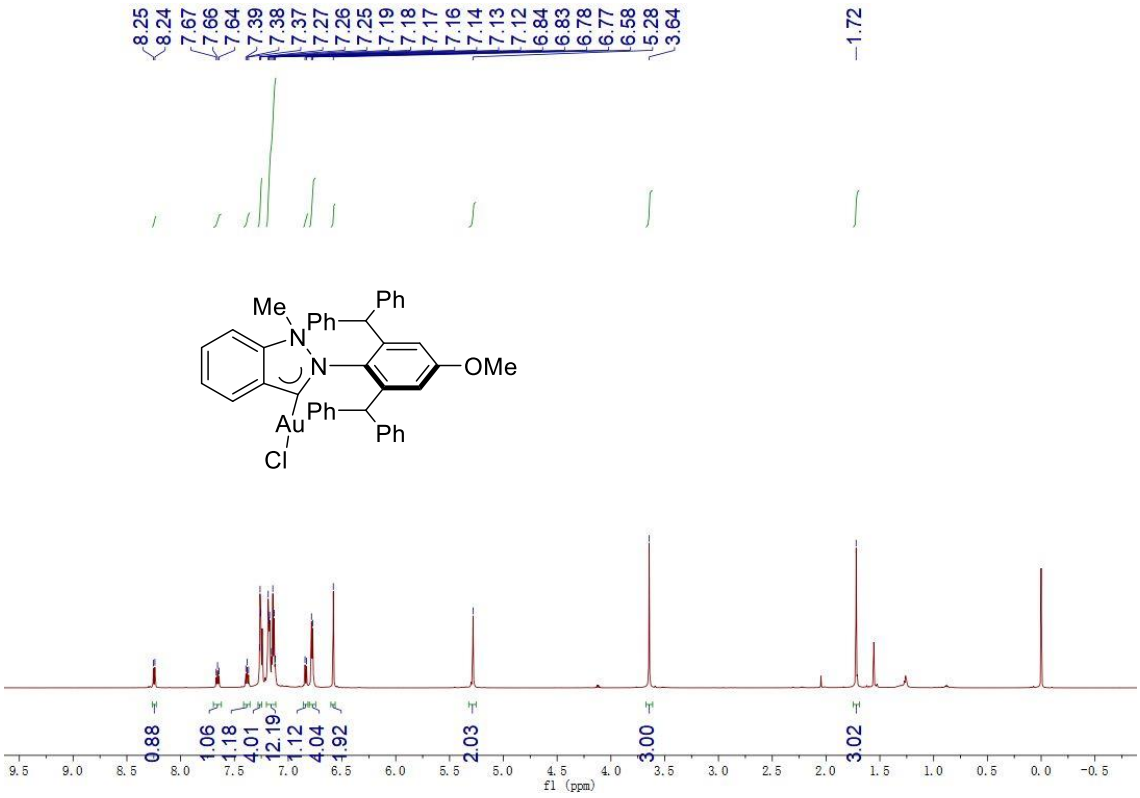

Figure S21. ^{1}H NMR (600 MHz, $CDCl_3$) Spectrum of Compound **5b**

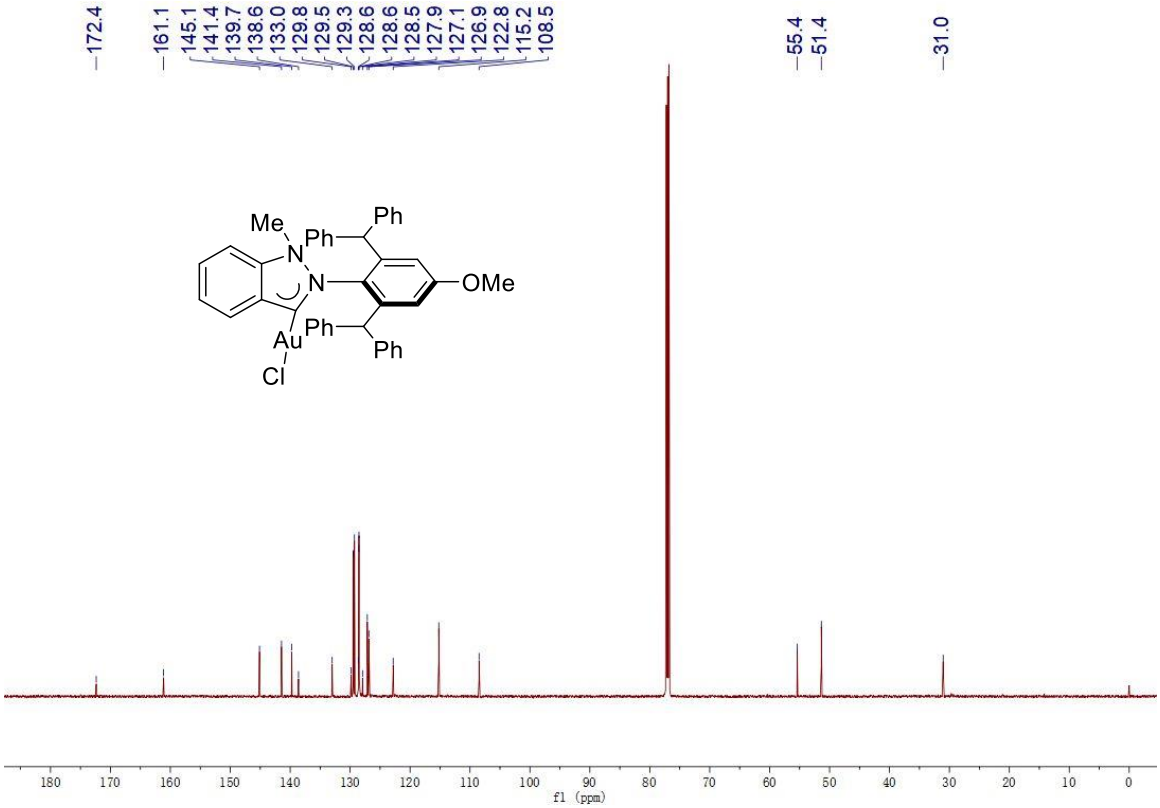

Figure S22. ^{13}C NMR (151 MHz, $CDCl_3$) Spectrum of Compound **5b**

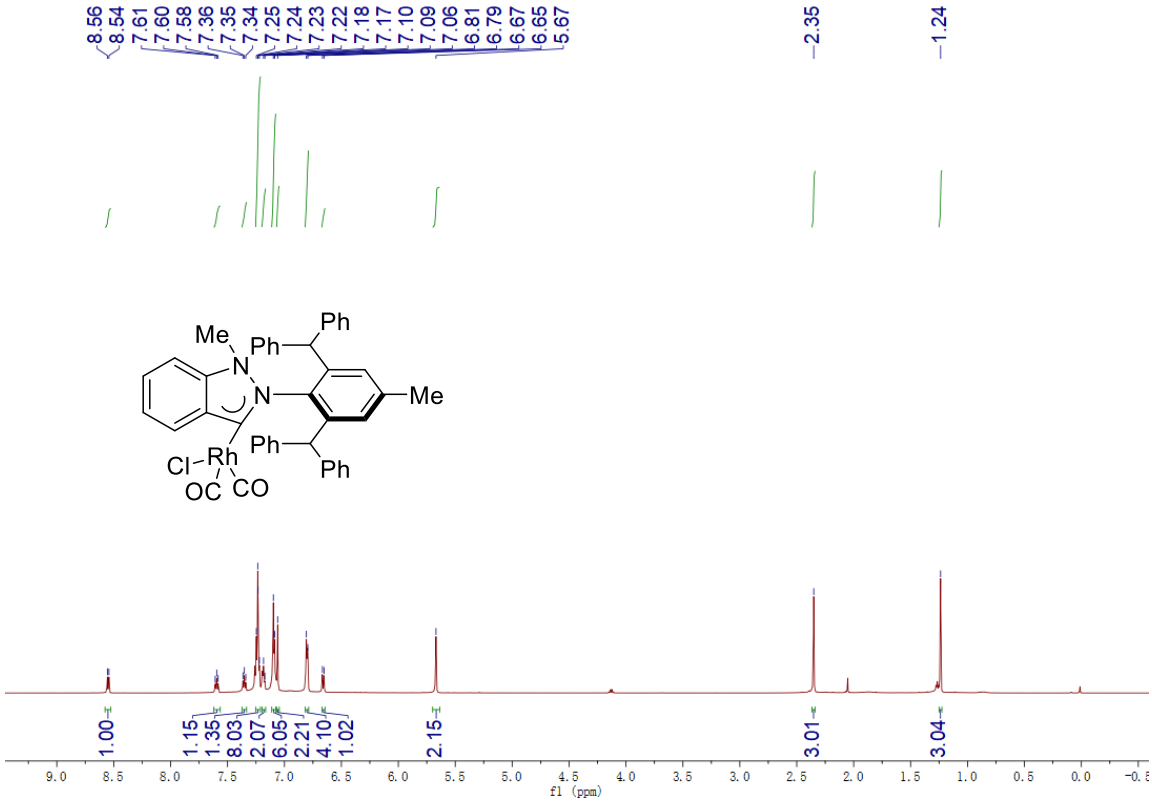

Figure S23. ^{1}H NMR (600 MHz, $CDCl_3$) Spectrum of Compound **6a**

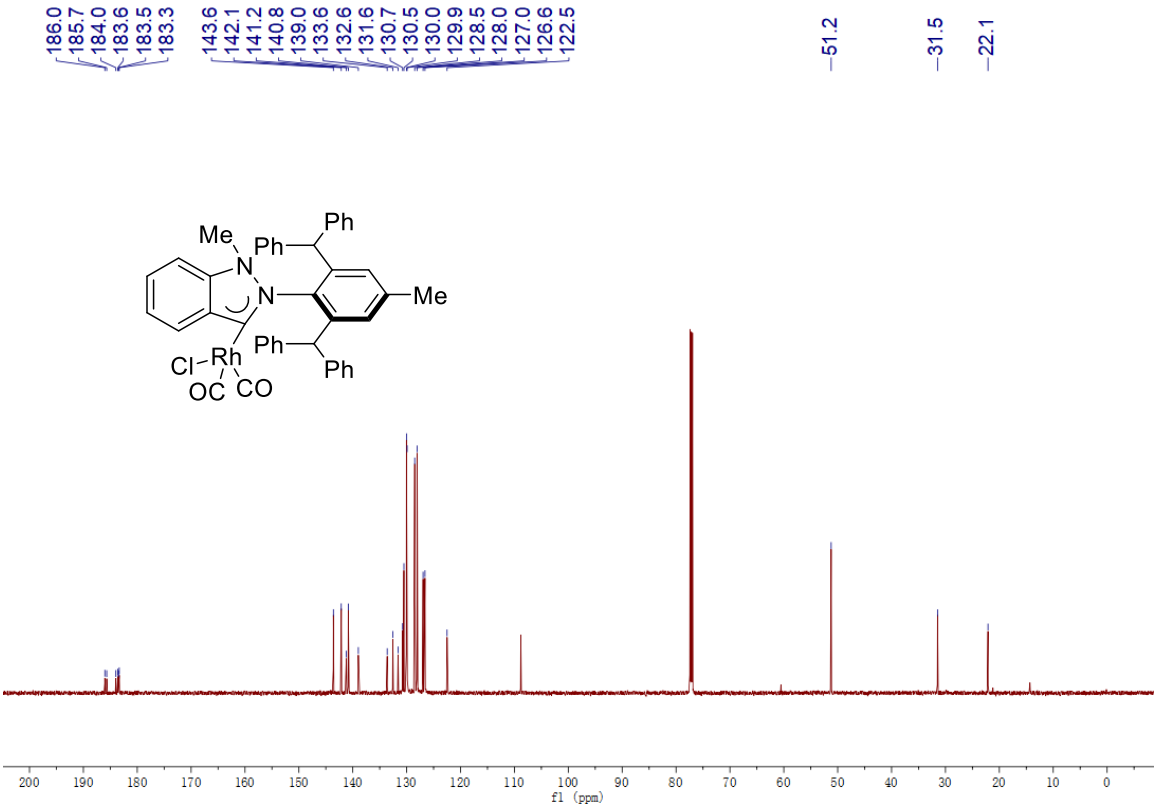

Figure S24. ^{13}C NMR (151 MHz, $CDCl_3$) Spectrum of Compound **6a**

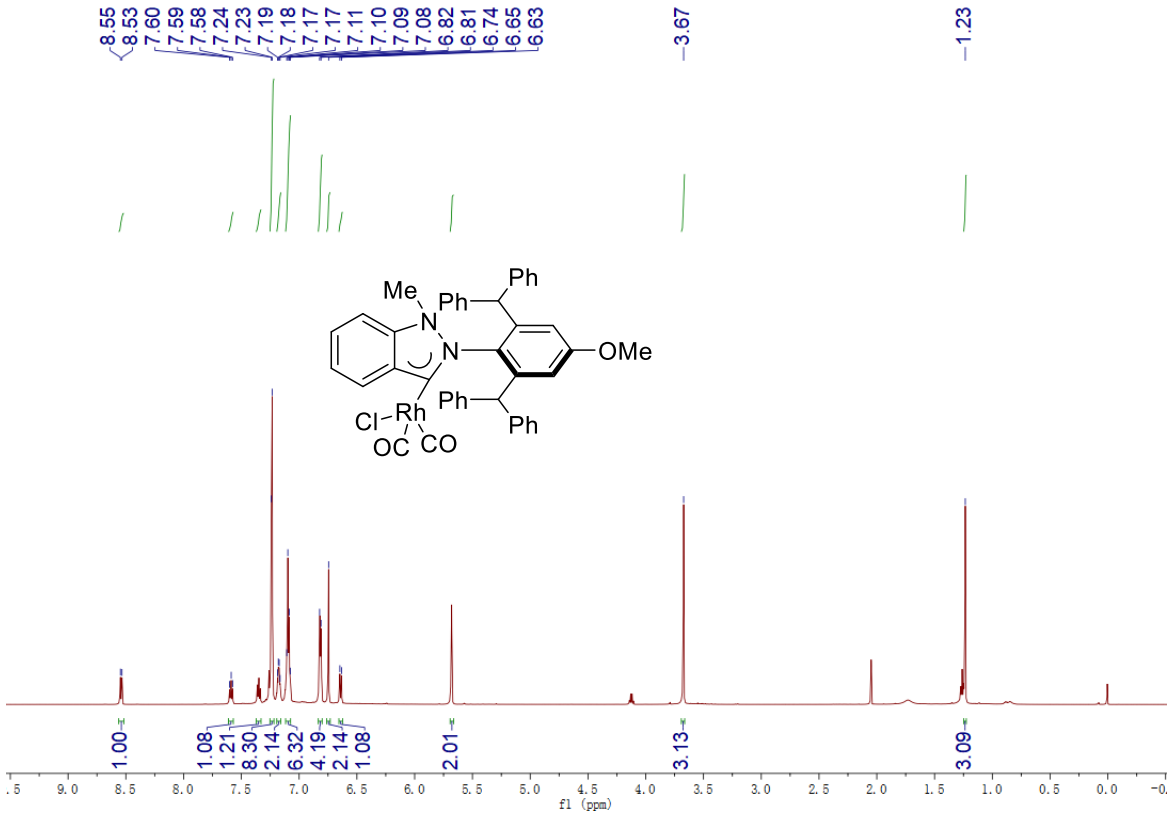

Figure S25. ^{1}H NMR (600 MHz, $CDCl_3$) Spectrum of Compound **6b**

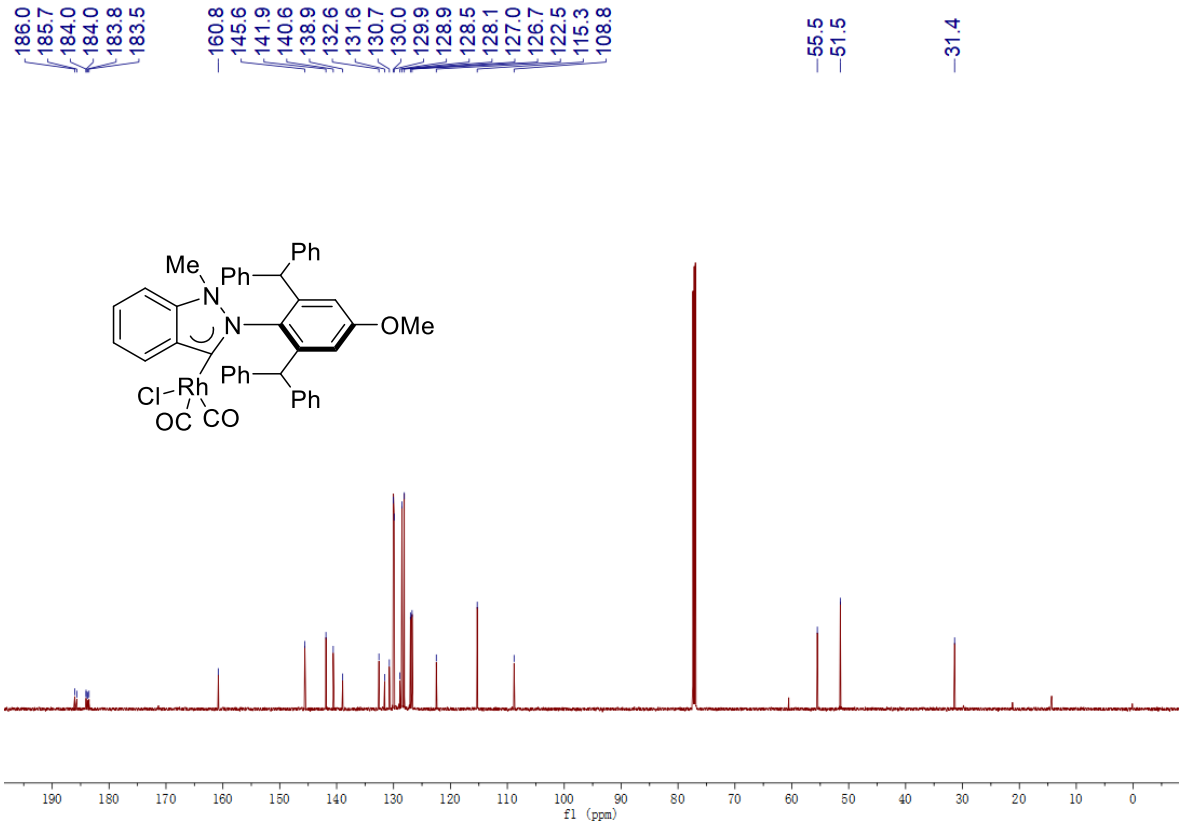

Figure S26. ^{13}C NMR (151 MHz, $CDCl_3$) Spectrum of Compound **6b**

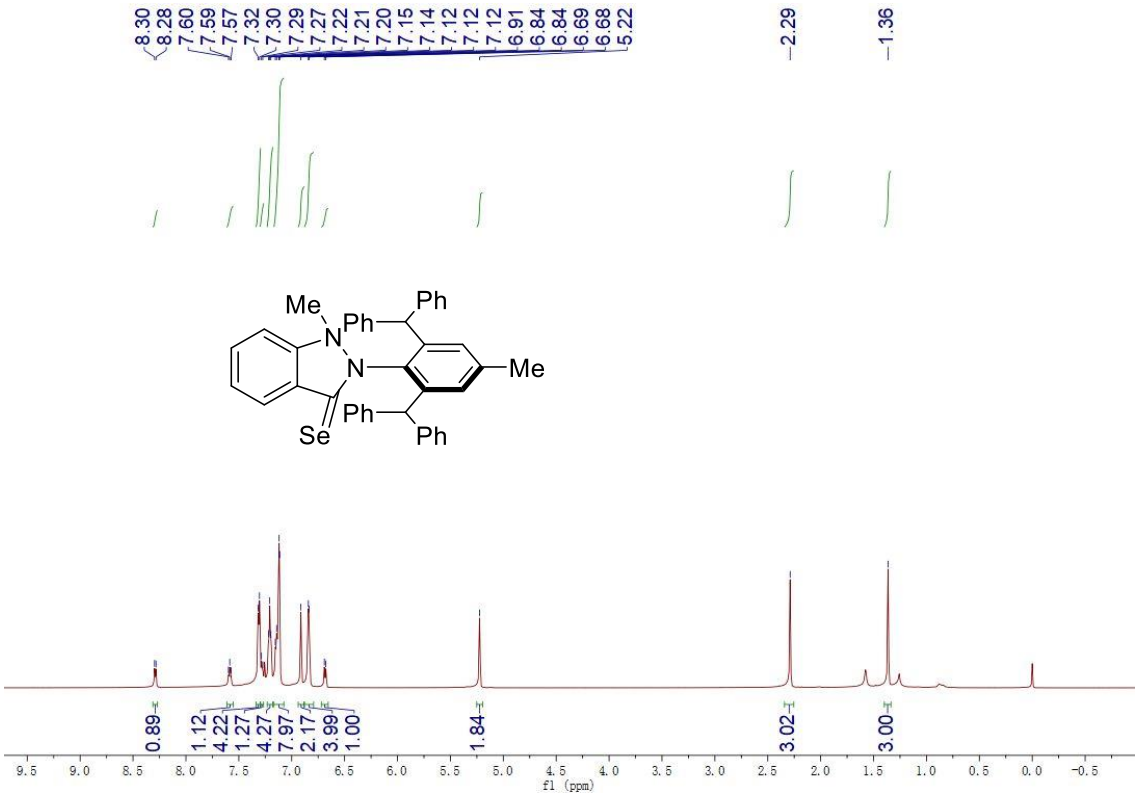

Figure S27. ^{1}H NMR (600 MHz, $CDCl_3$) Spectrum of Compound **7a**

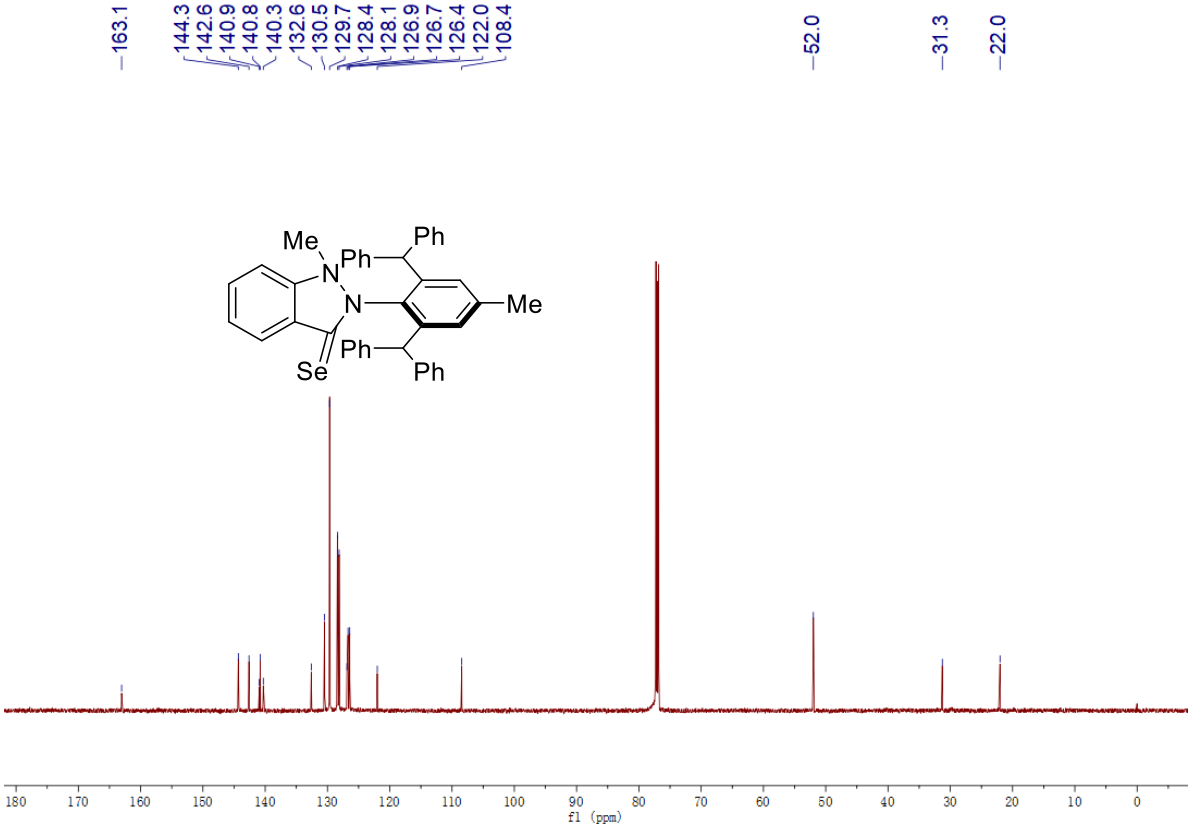

Figure S28. ^{13}C NMR (151 MHz, $CDCl_3$) Spectrum of Compound **7a**

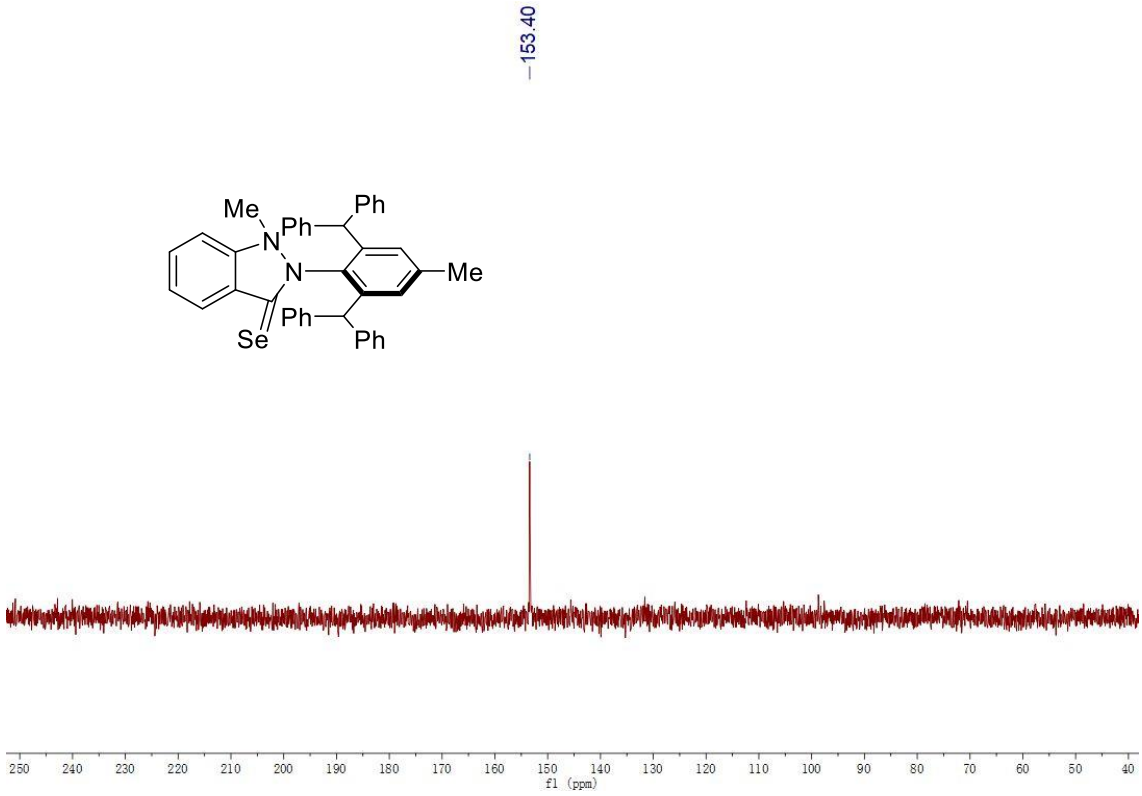

Figure S29. ^{77}Se NMR (114 MHz, $CDCl_3$) Spectrum of Compound **7a**

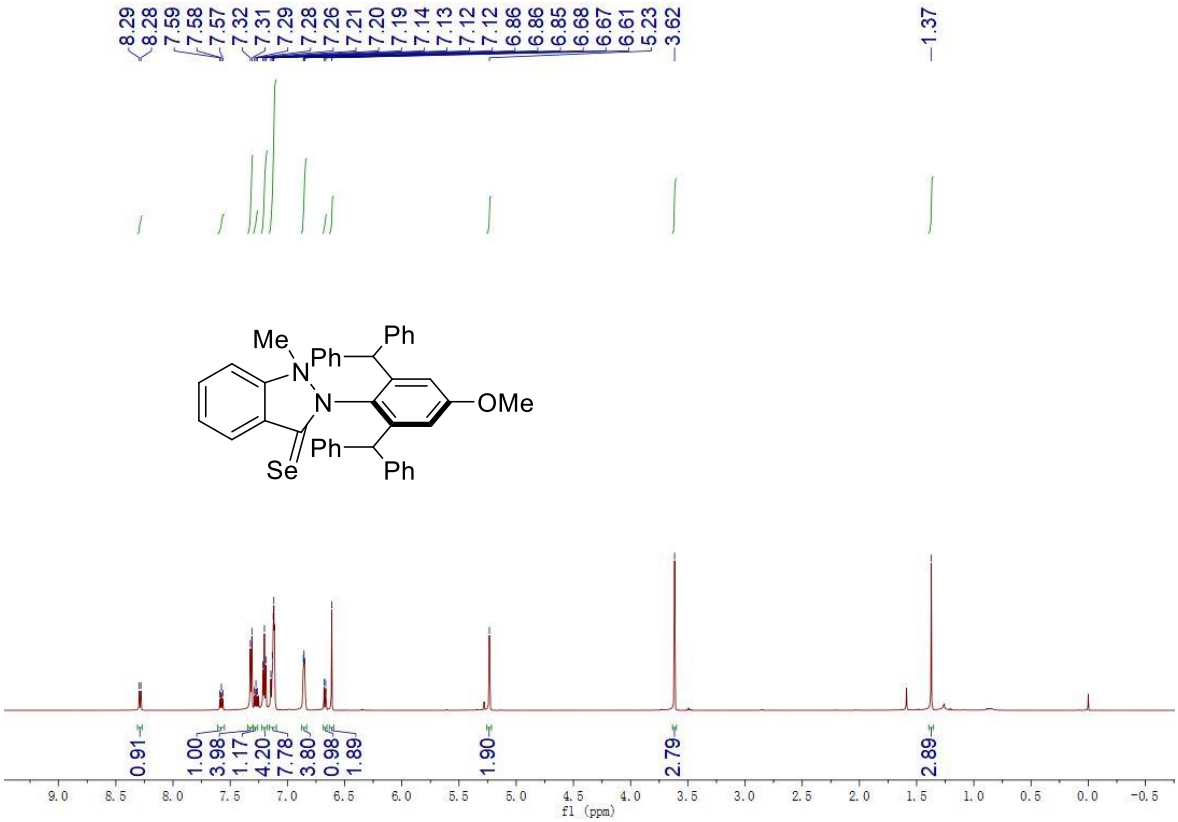

Figure S30. ^{1}H NMR (600 MHz, $CDCl_3$) Spectrum of Compound **7b**

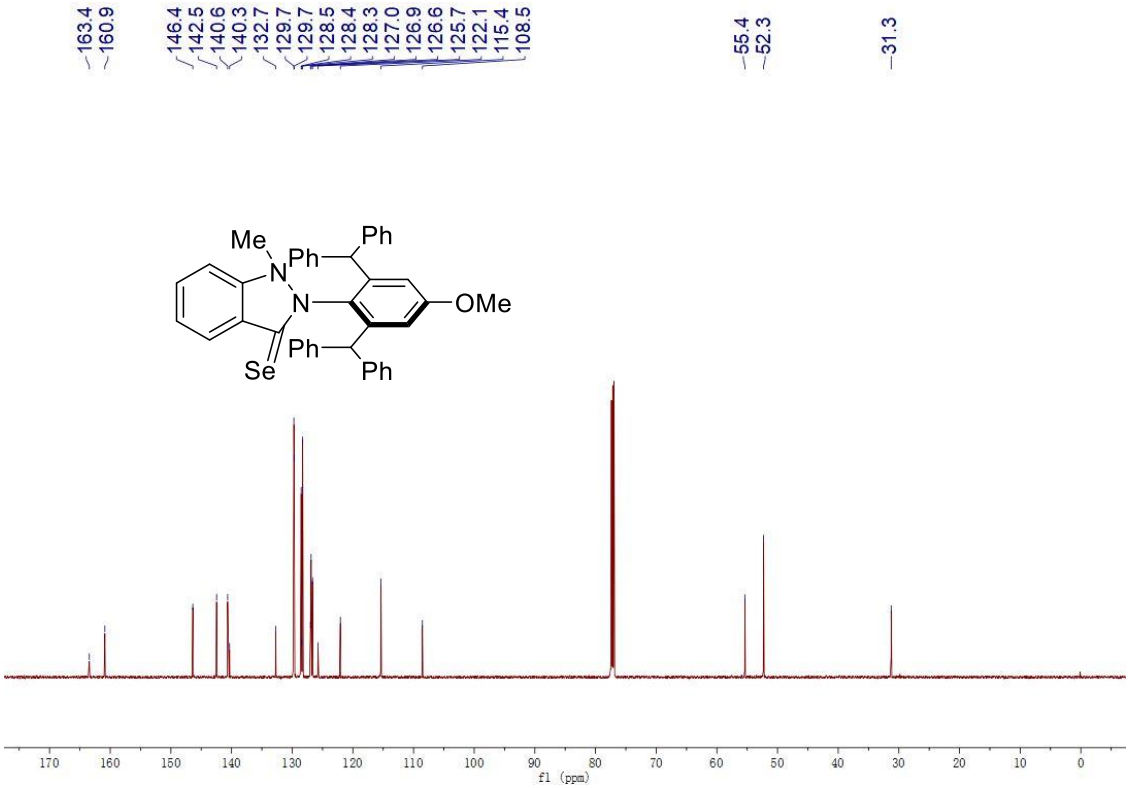

Figure S31. ^{13}C NMR (151 MHz, $CDCl_3$) Spectrum of Compound **7b**

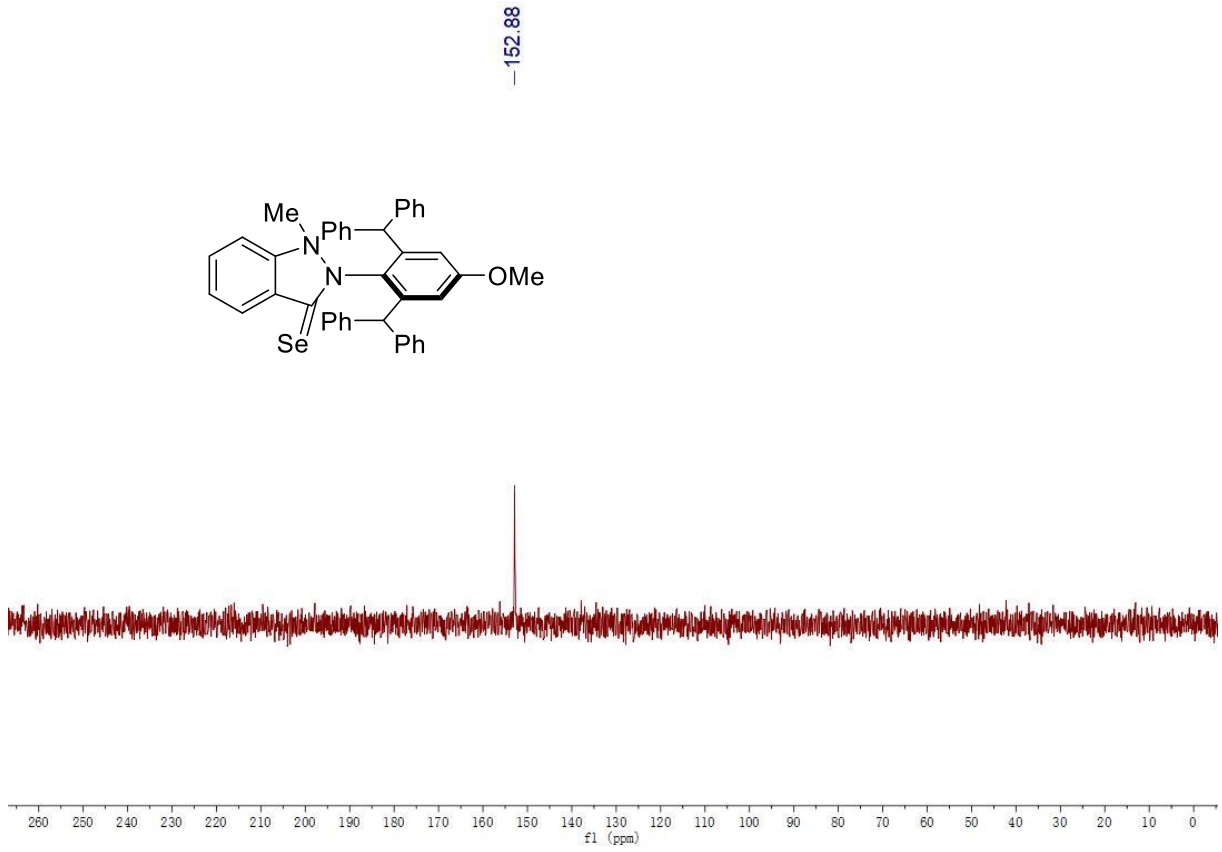

Figure S32. ^{77}Se NMR (114 MHz, $CDCl_3$) Spectrum of Compound **7b**

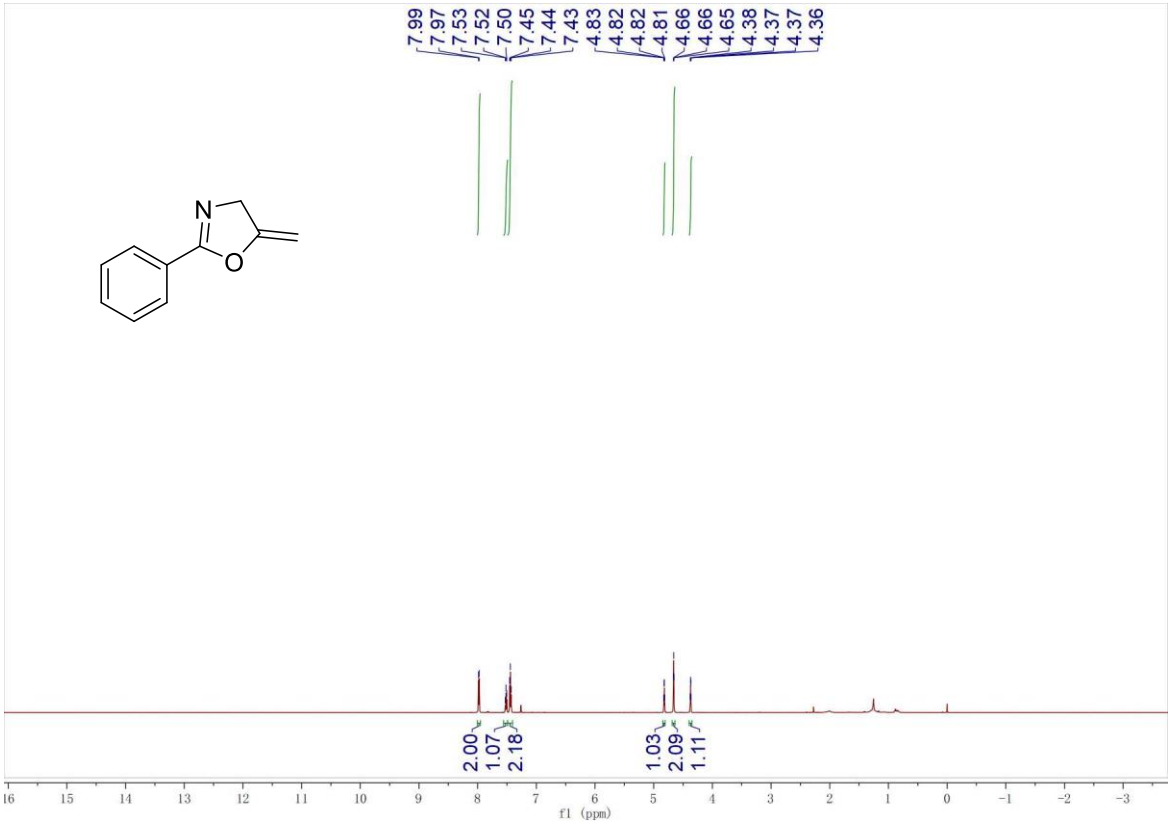

Figure S33. ^{1}H NMR (600 MHz, $CDCl_3$) Spectrum of Compound **9a**

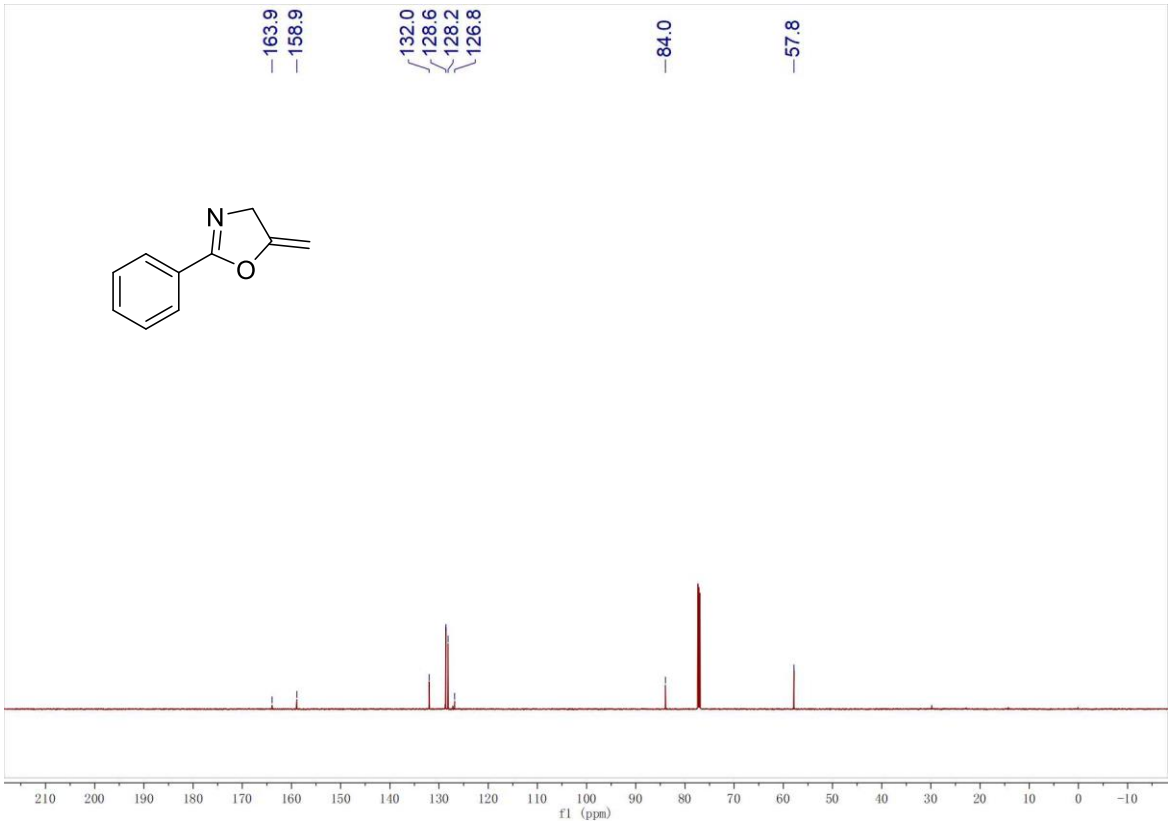

Figure S34. ^{13}C NMR (151 MHz, $CDCl_3$) Spectrum of Compound **9a**

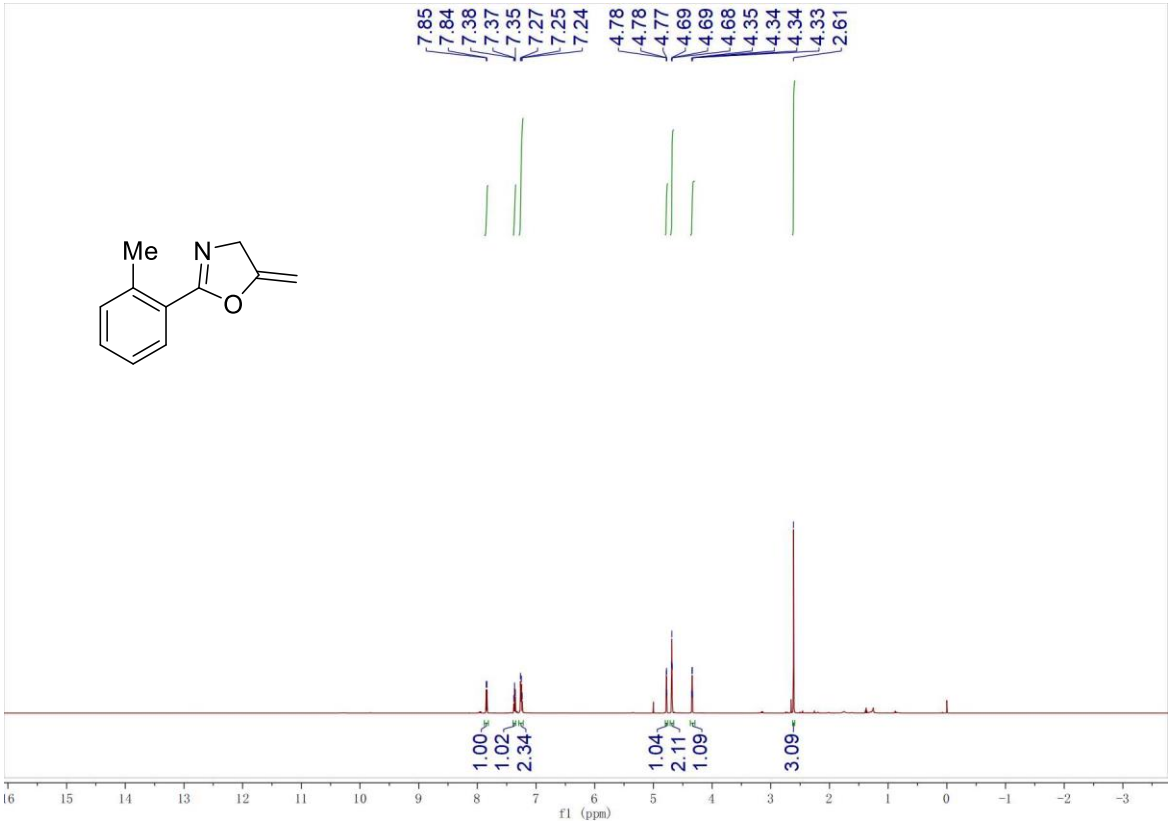

Figure S35. ^{1}H NMR (600 MHz, $CDCl_3$) Spectrum of Compound **9b**

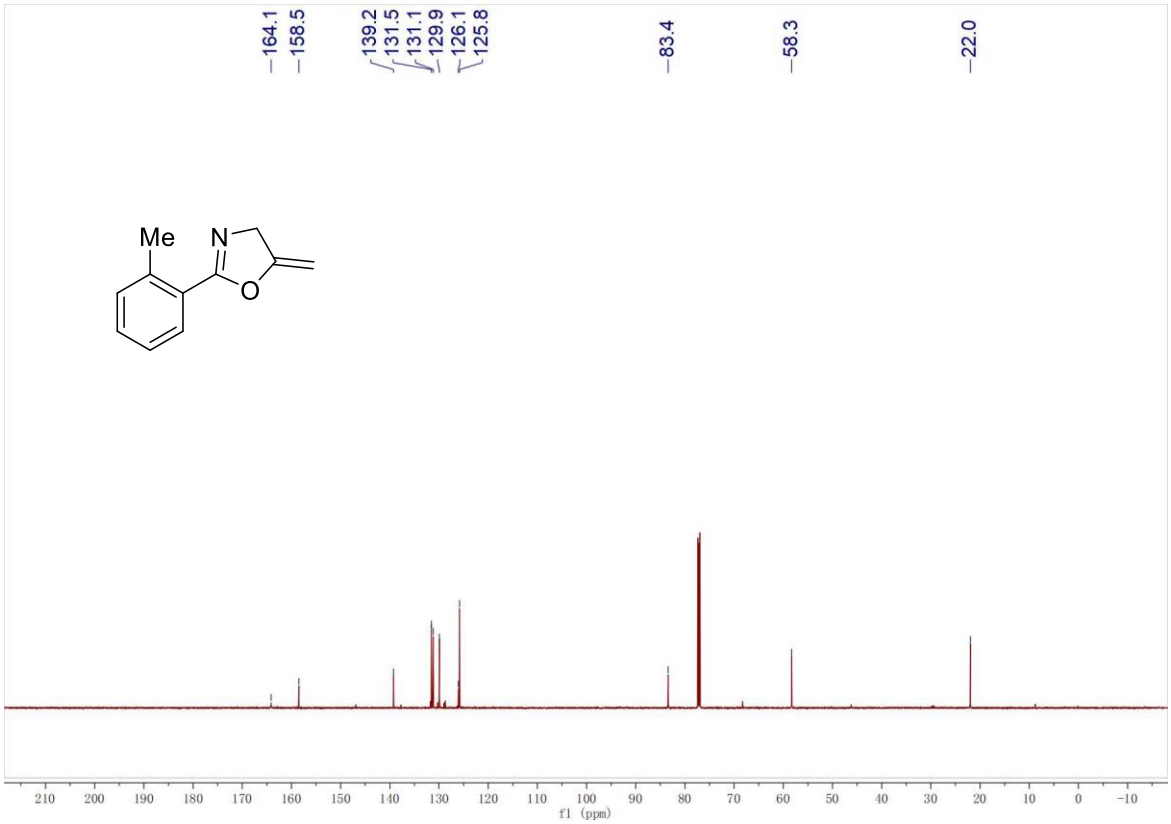

Figure S36. ^{13}C NMR (151 MHz, $CDCl_3$) Spectrum of Compound **9b**

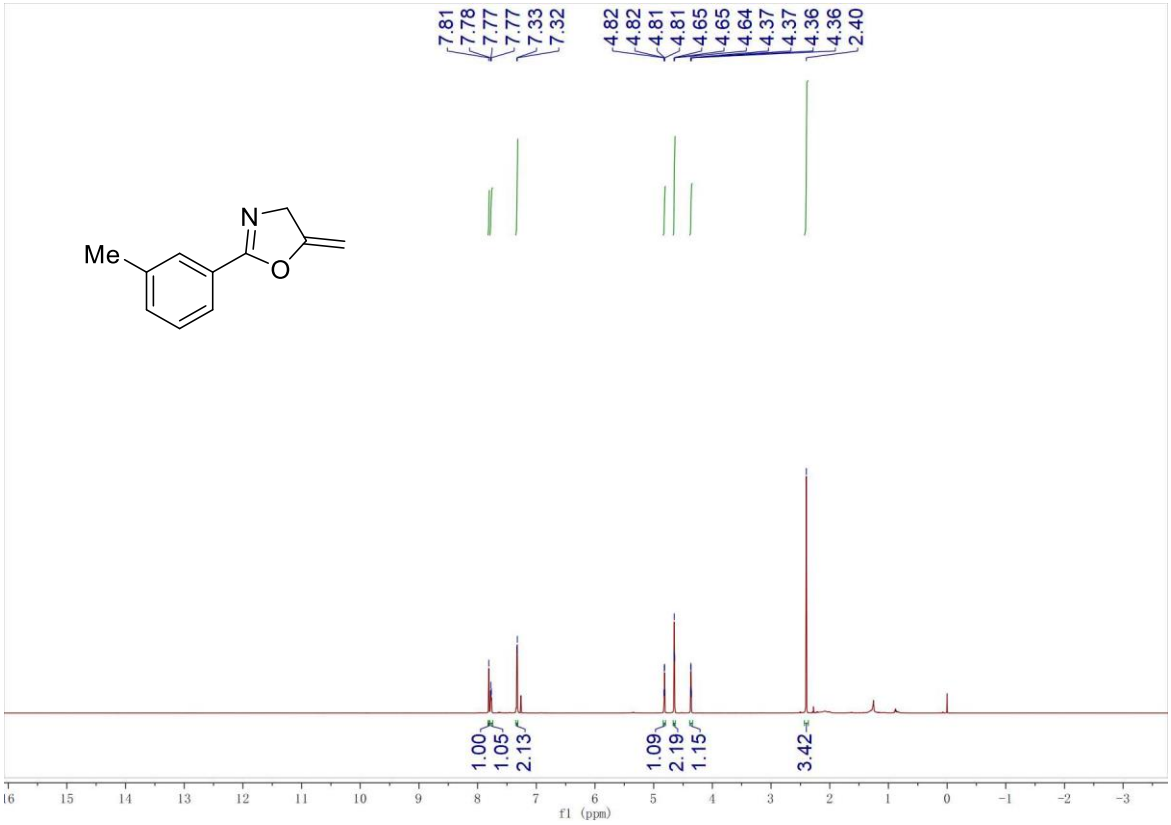

Figure S37. ^{1}H NMR (600 MHz, $CDCl_3$) Spectrum of Compound **9c**

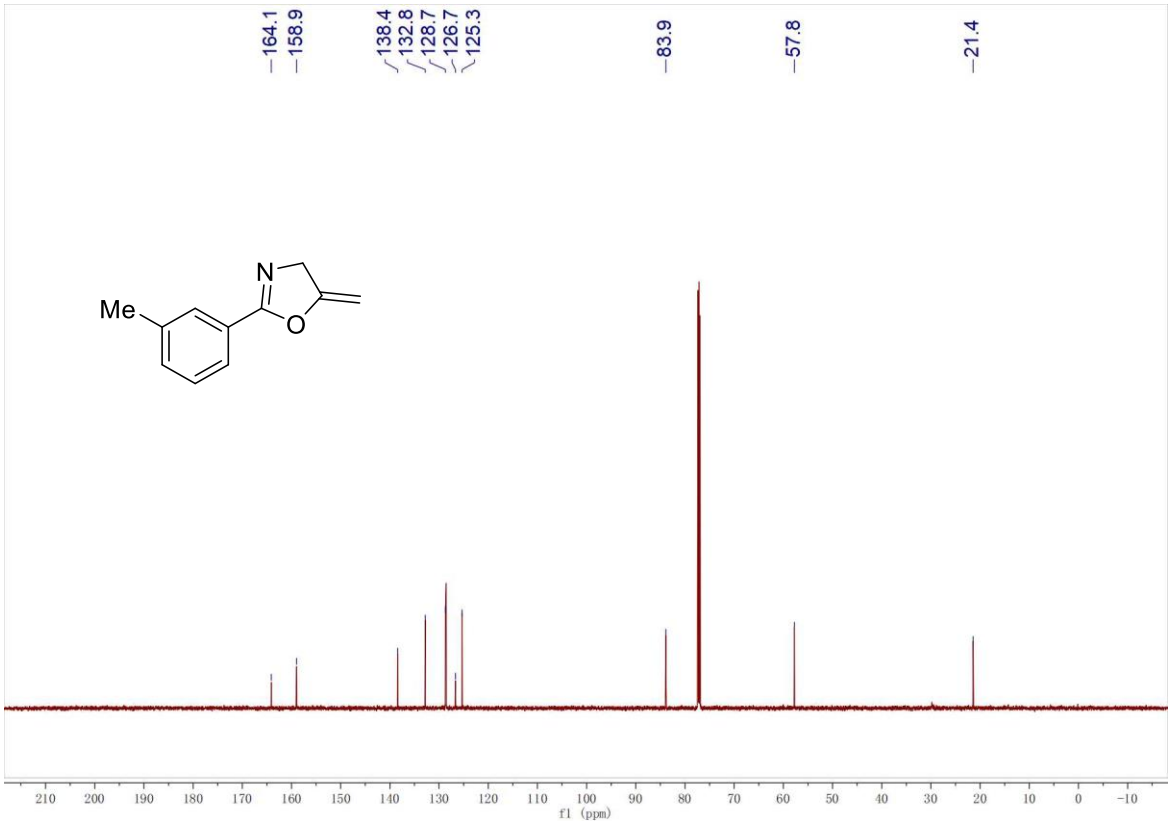

Figure S38. ^{13}C NMR (151 MHz, $CDCl_3$) Spectrum of Compound **9c**

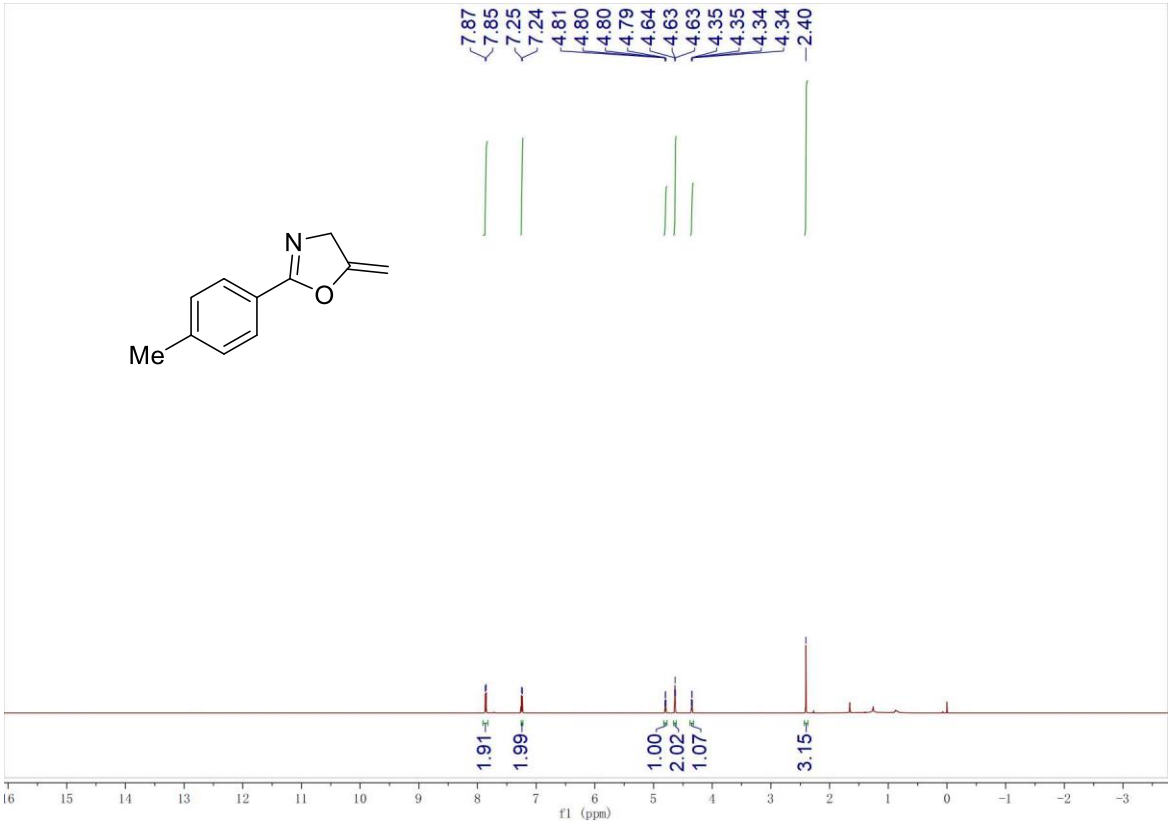

Figure S39. ^{1}H NMR (600 MHz, $CDCl_3$) Spectrum of Compound **9d**

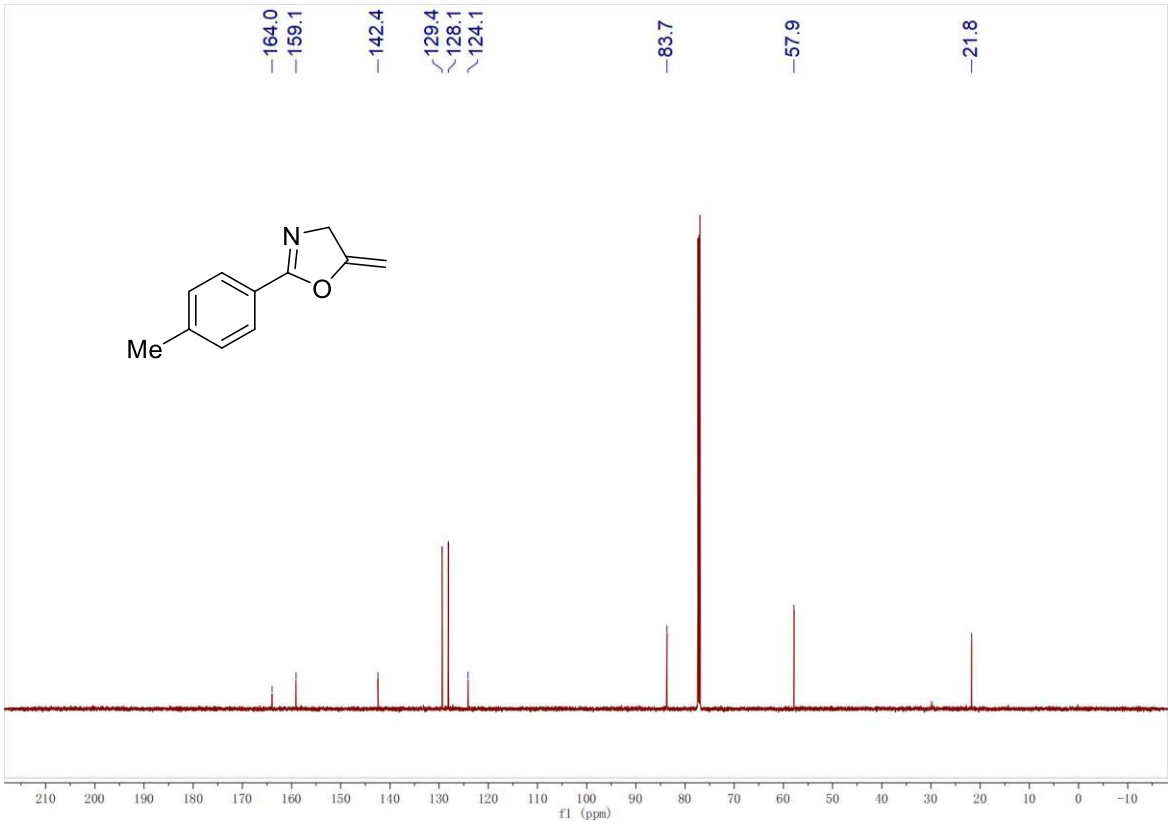

Figure S40. ^{13}C NMR (151 MHz, $CDCl_3$) Spectrum of Compound **9d**

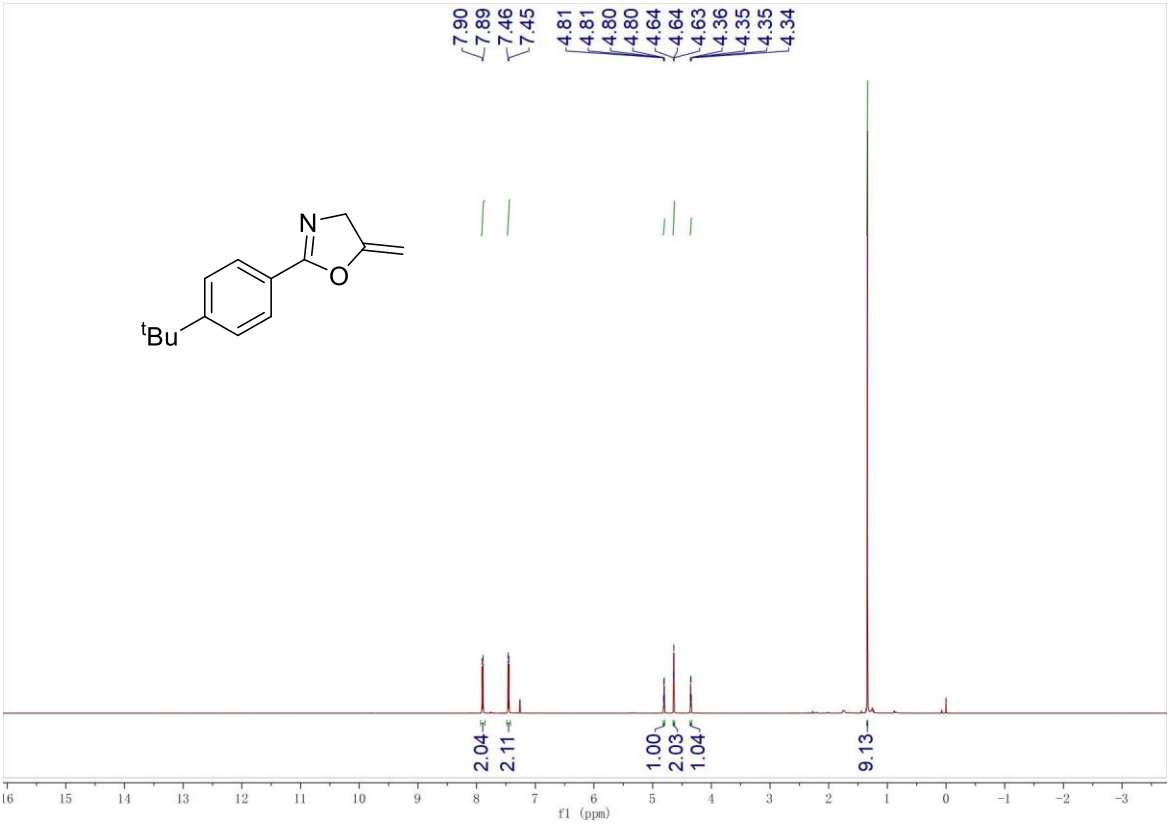

Figure S41. ^{1}H NMR (600 MHz, $CDCl_3$) Spectrum of Compound **9e**

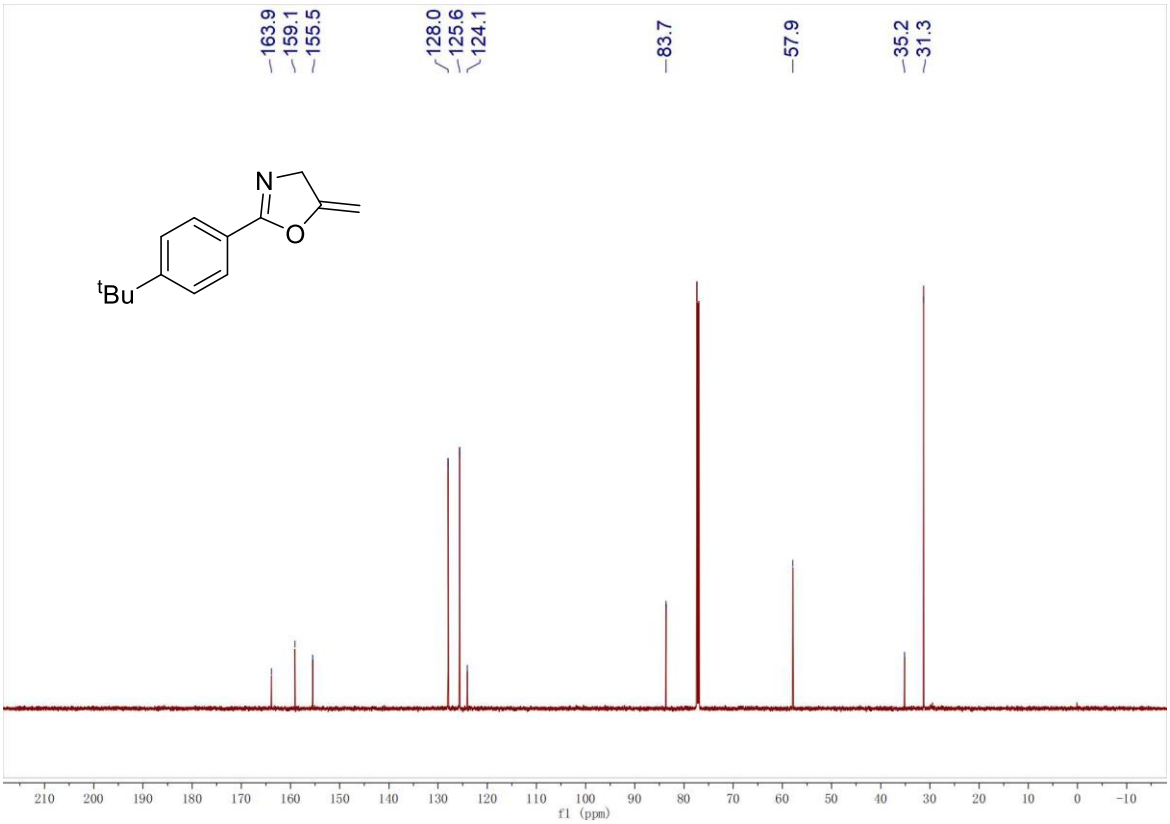

Figure S42. ^{13}C NMR (151 MHz, $CDCl_3$) Spectrum of Compound **9e**

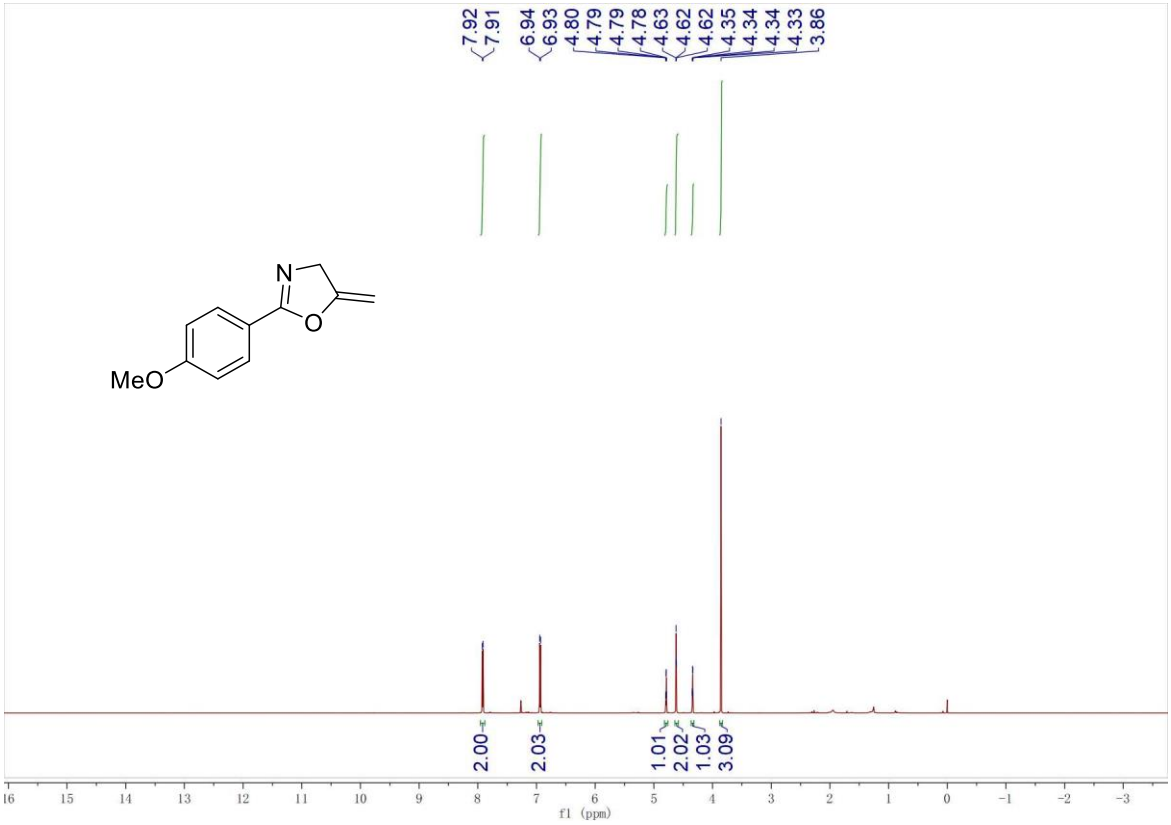

Figure S43. ^{1}H NMR (600 MHz, $CDCl_3$) Spectrum of Compound **9f**

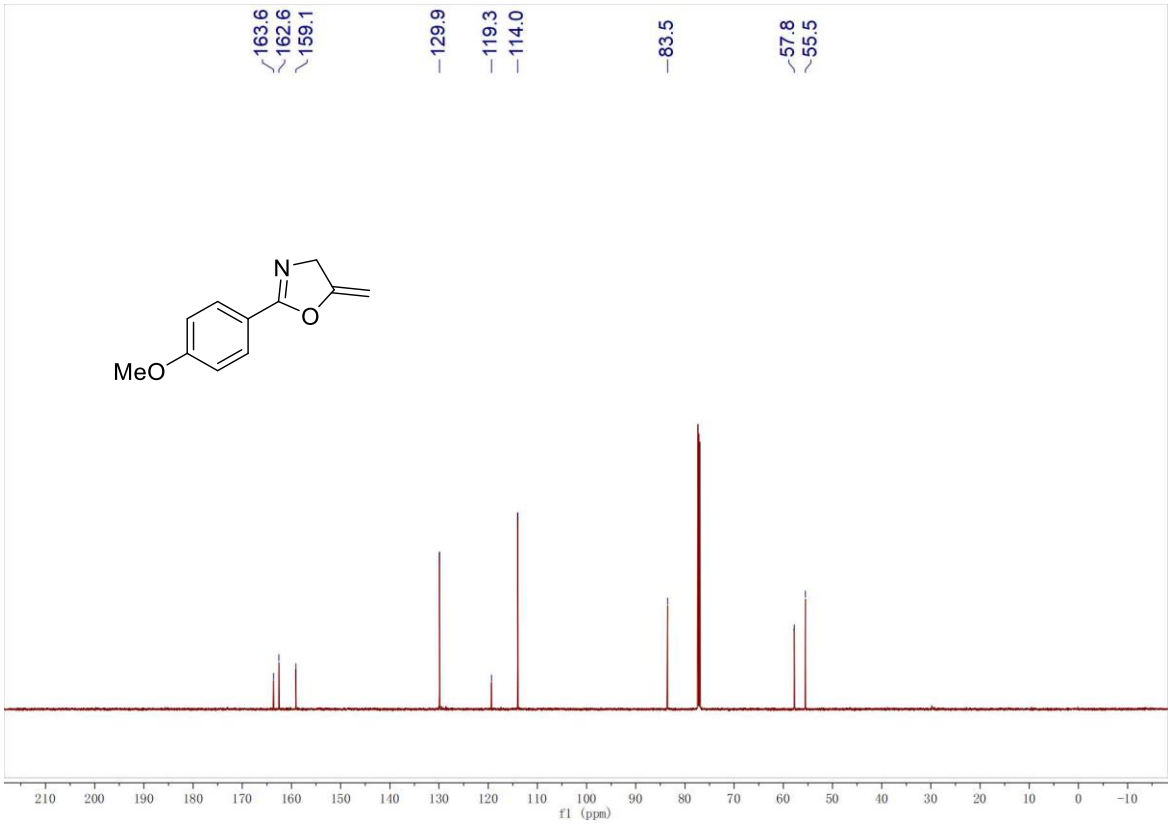

Figure S44. ^{13}C NMR (151 MHz, $CDCl_3$) Spectrum of Compound **9f**

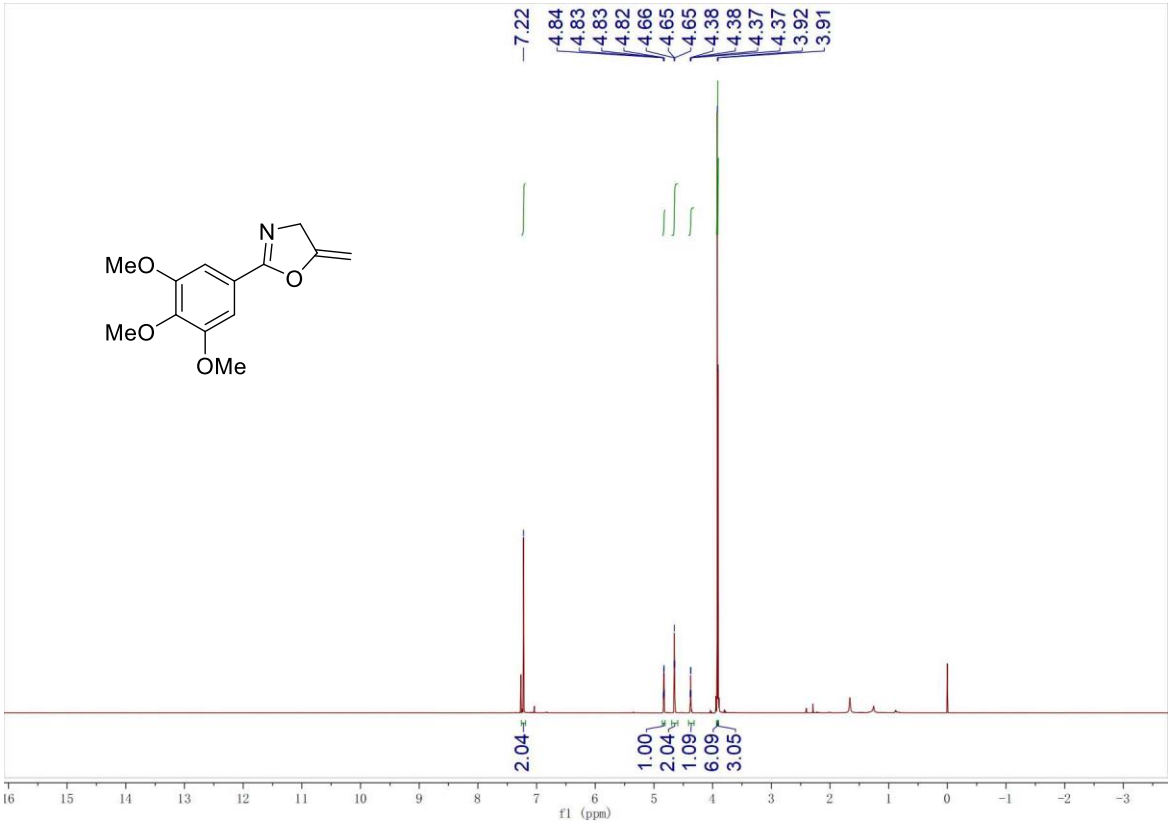

Figure S45. ^{1}H NMR (600 MHz, $CDCl_3$) Spectrum of Compound **9g**

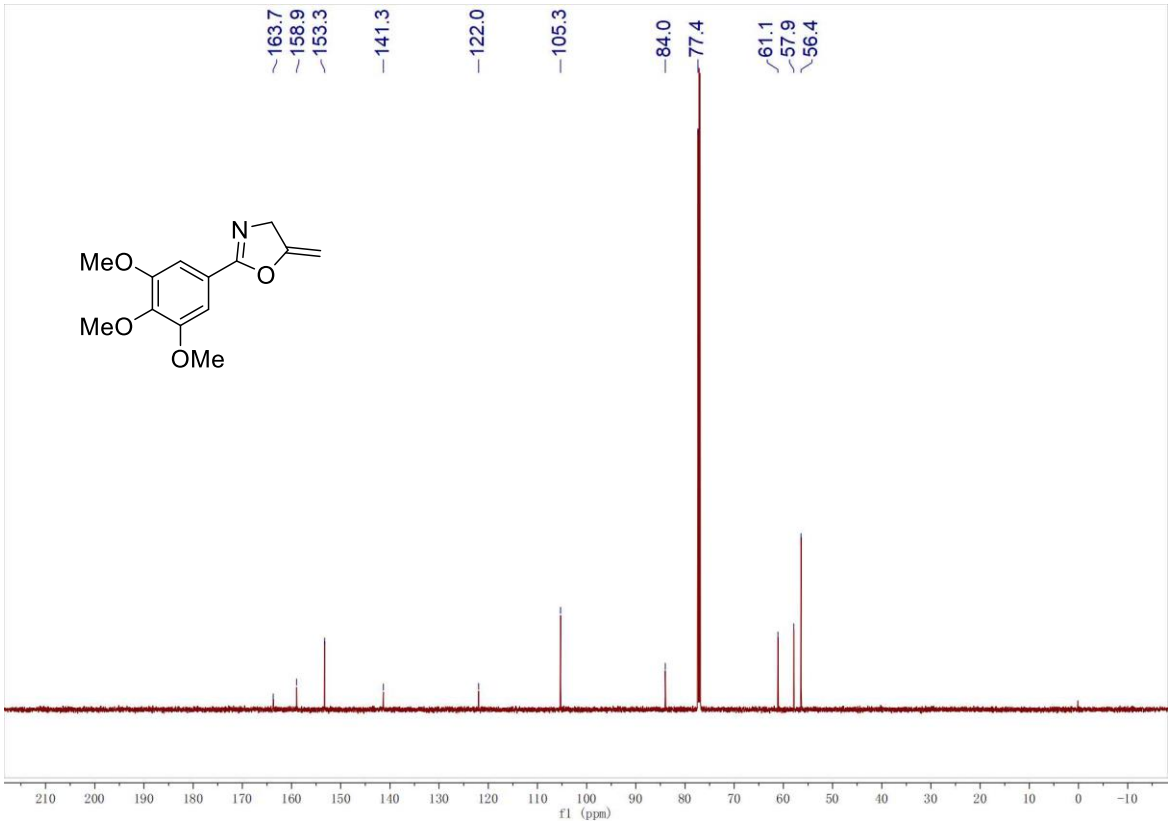

Figure S46. ^{13}C NMR (151 MHz, $CDCl_3$) Spectrum of Compound **9g**

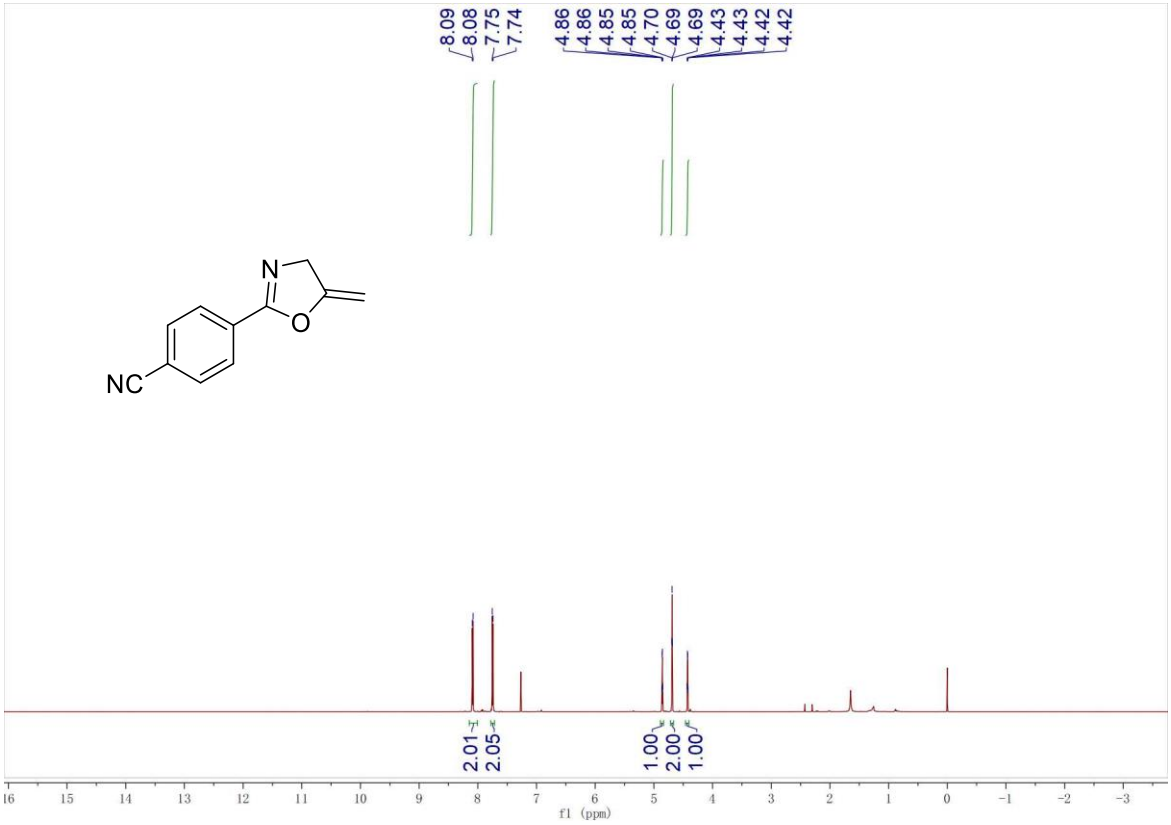

Figure S47. ^{1}H NMR (600 MHz, $CDCl_3$) Spectrum of Compound **9h**

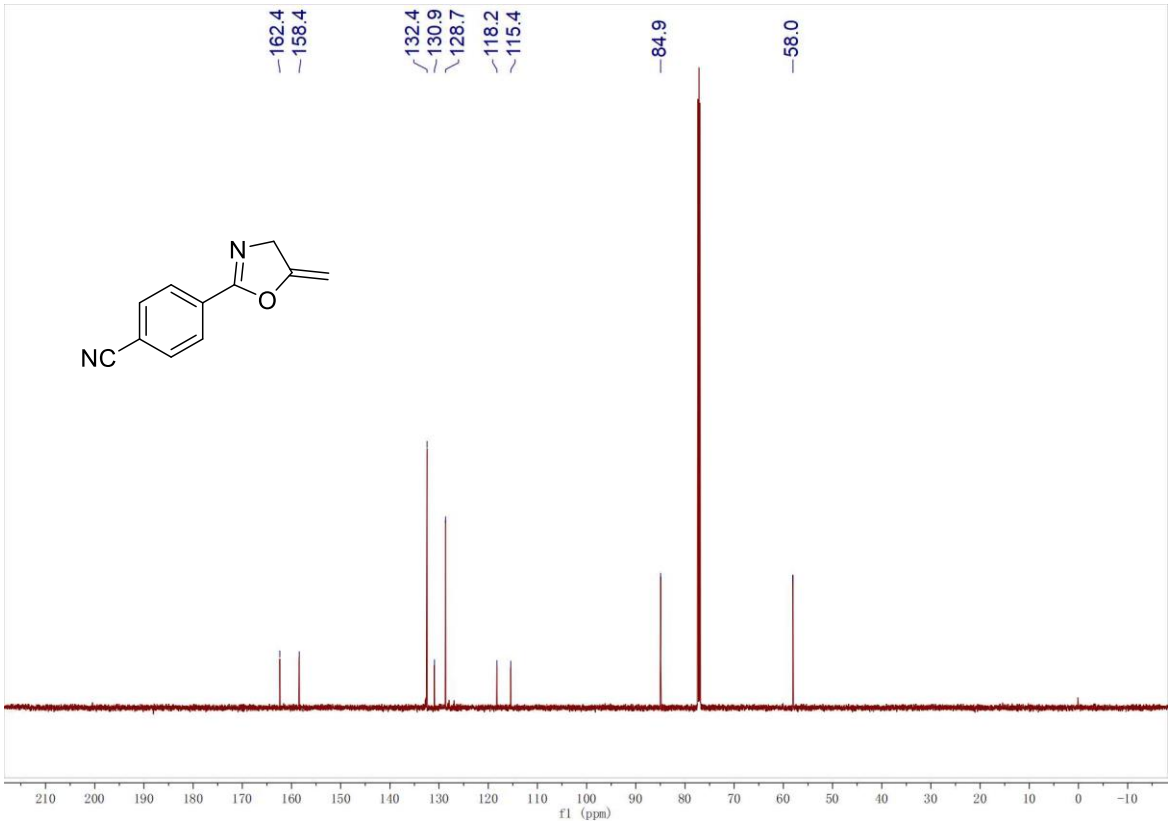

Figure S48. ^{13}C NMR (151 MHz, $CDCl_3$) Spectrum of Compound **9h**

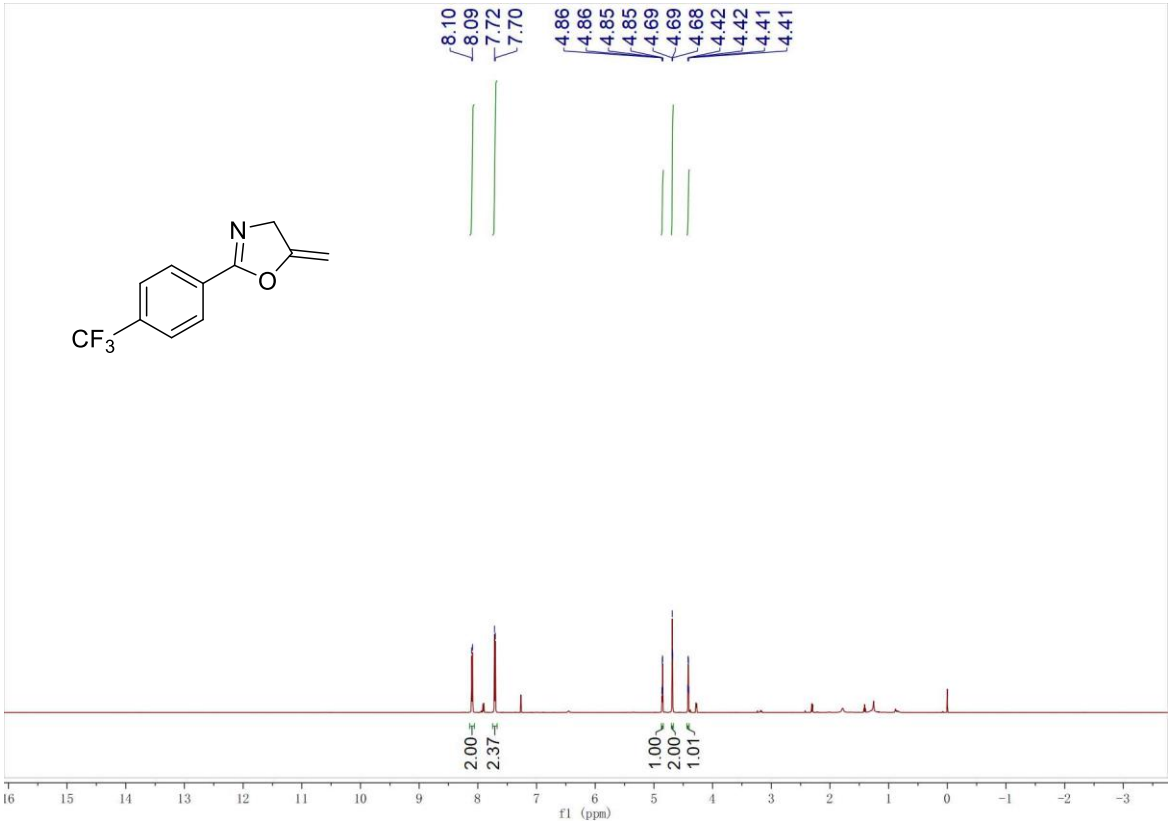

Figure S49. ^{1}H NMR (600 MHz, $CDCl_3$) Spectrum of Compound **9i**

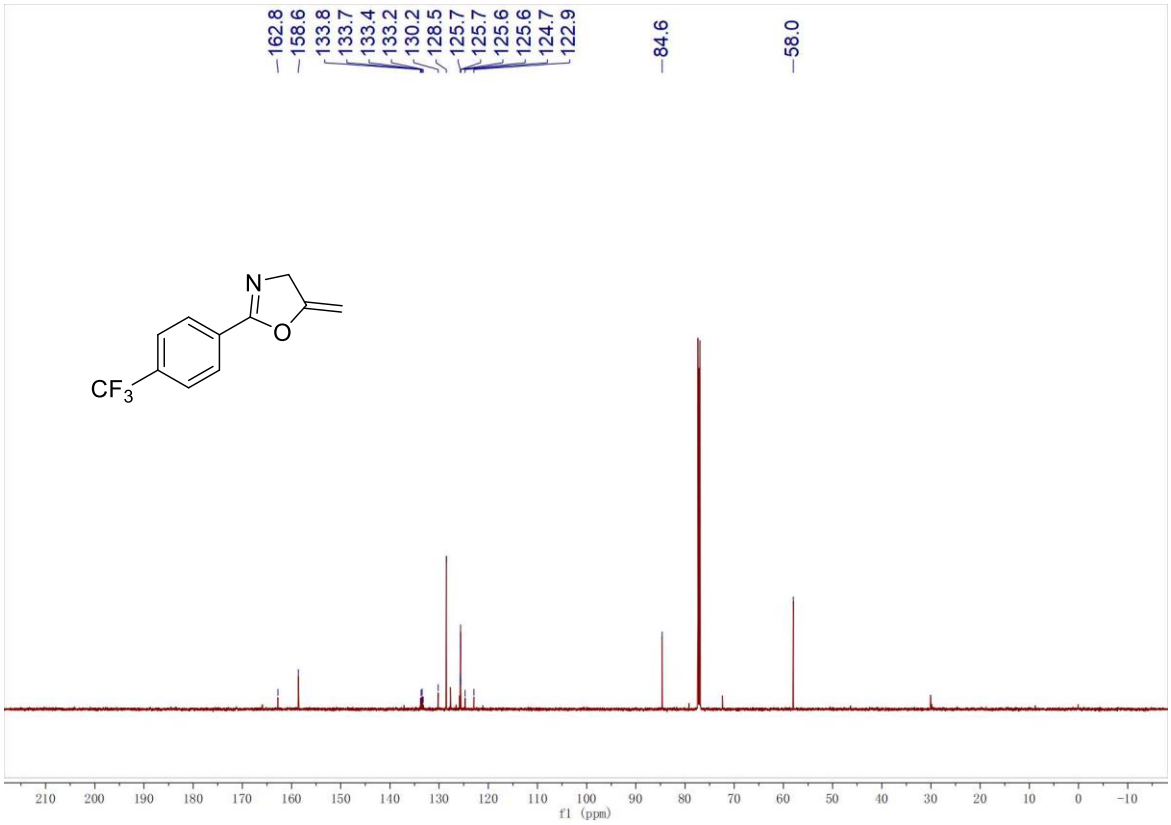

Figure S50. ^{13}C NMR (151 MHz, $CDCl_3$) Spectrum of Compound **9i**

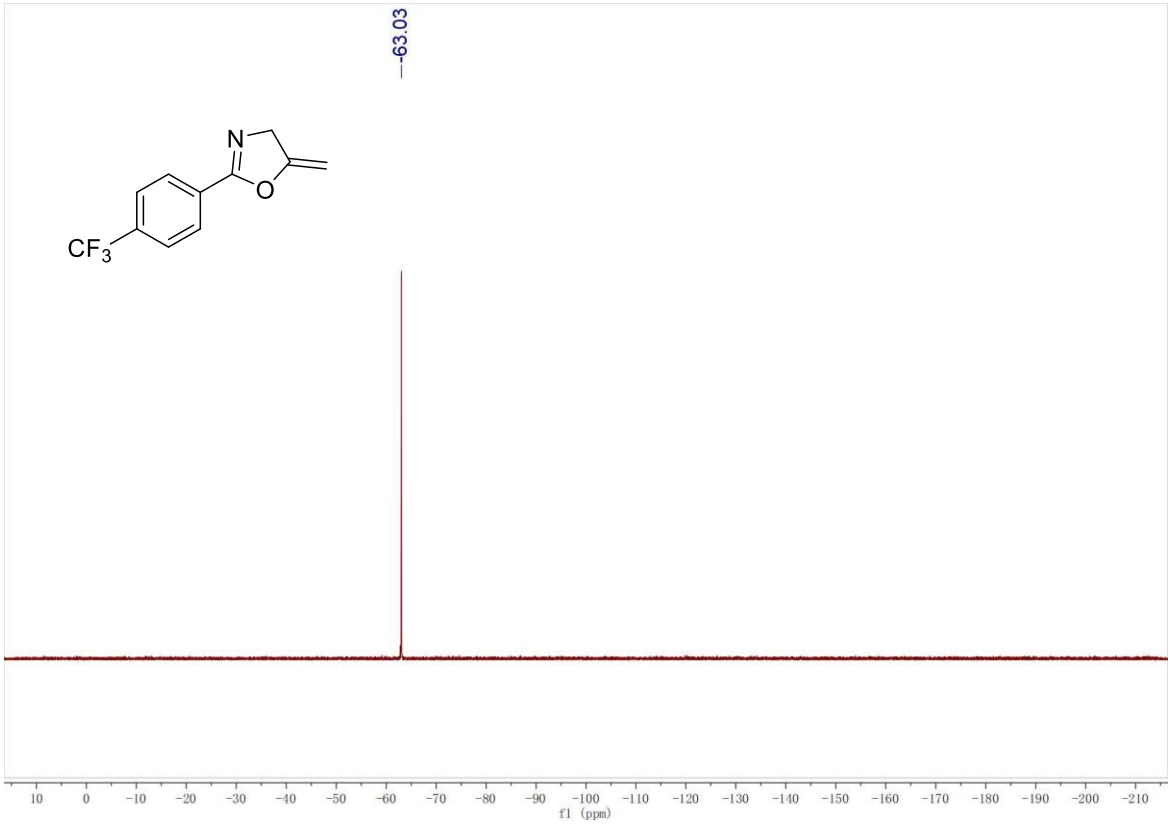

Figure S51. ^{19}F NMR (565 MHz, $CDCl_3$) Spectrum of Compound **9i**

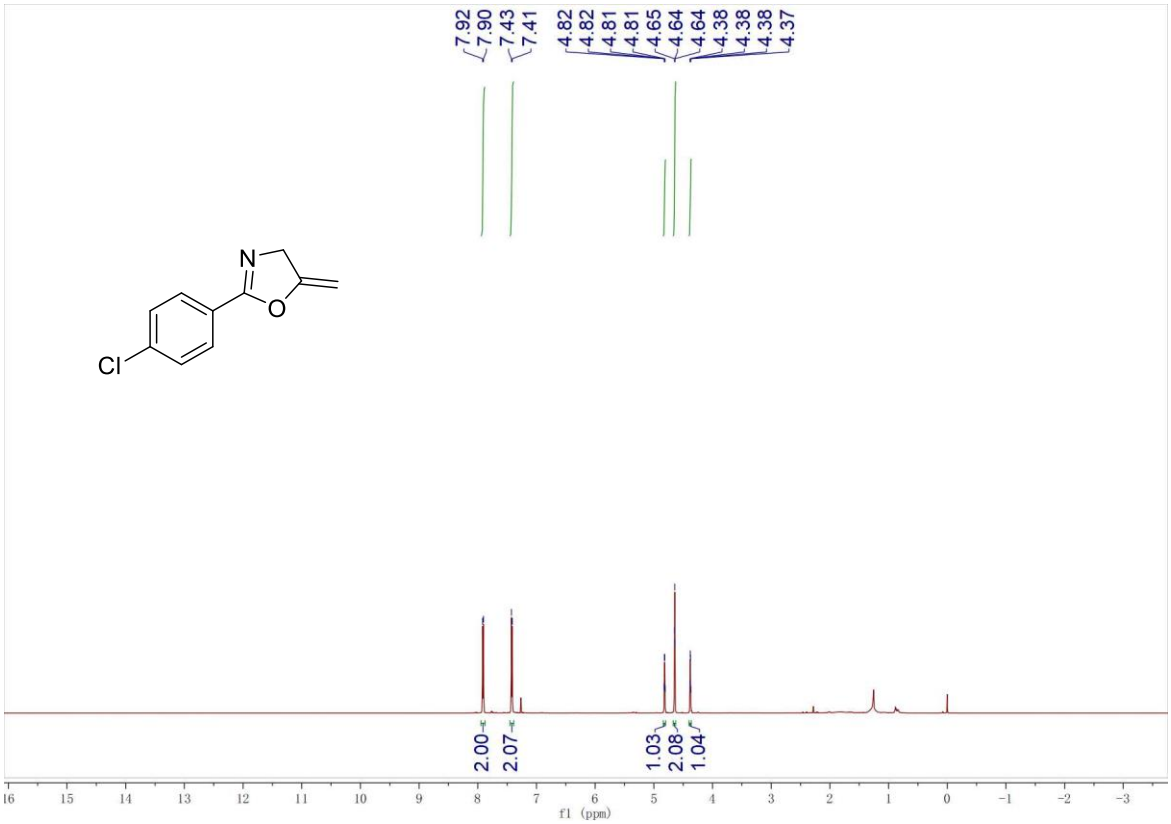

Figure S52. ^{1}H NMR (600 MHz, $CDCl_3$) Spectrum of Compound **9j**

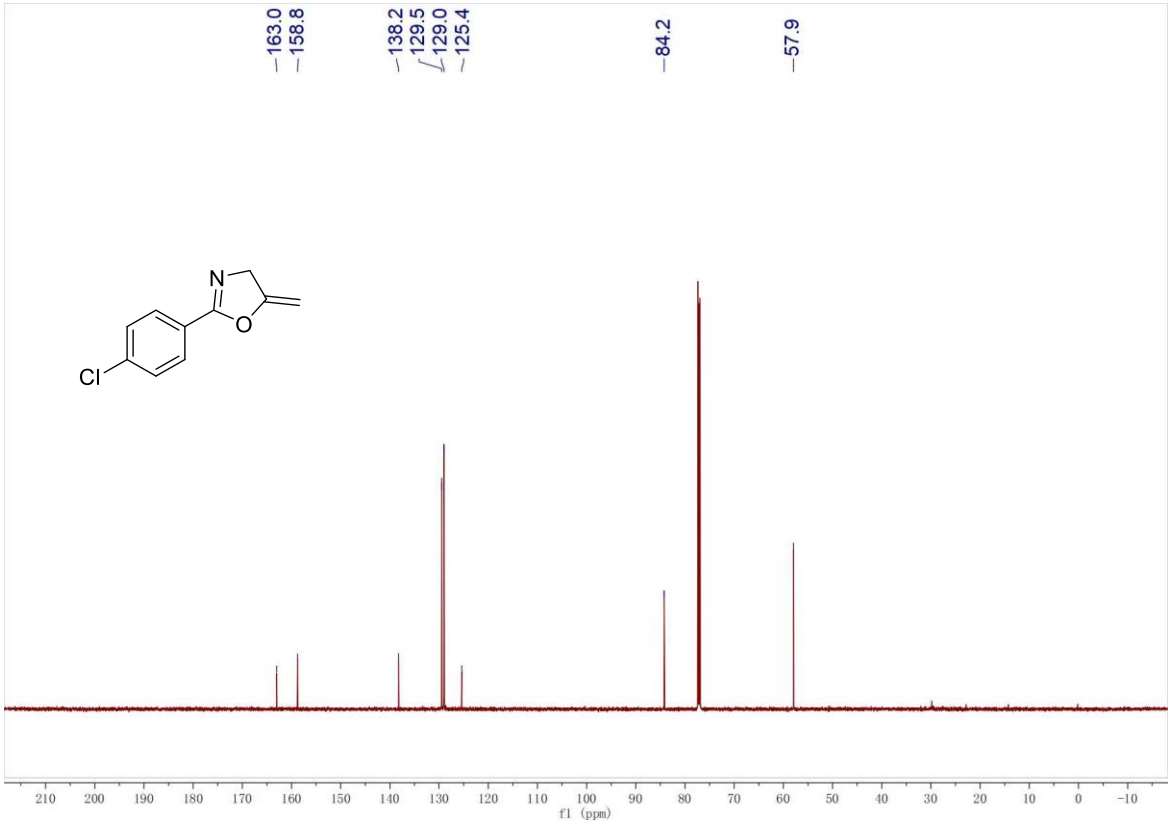

Figure S53. ^{13}C NMR (151 MHz, $CDCl_3$) Spectrum of Compound **9j**

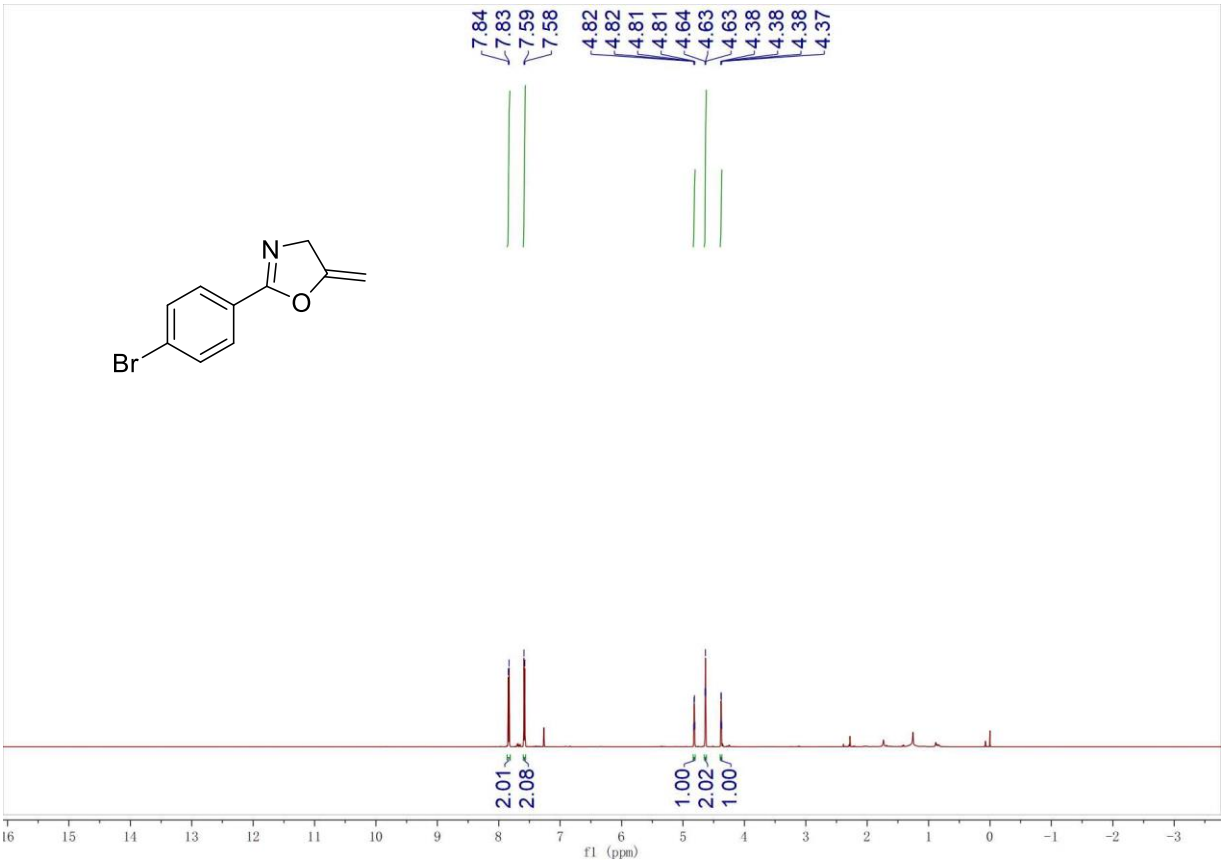

Figure S54. ^{1}H NMR (600 MHz, $CDCl_3$) Spectrum of Compound **9k**

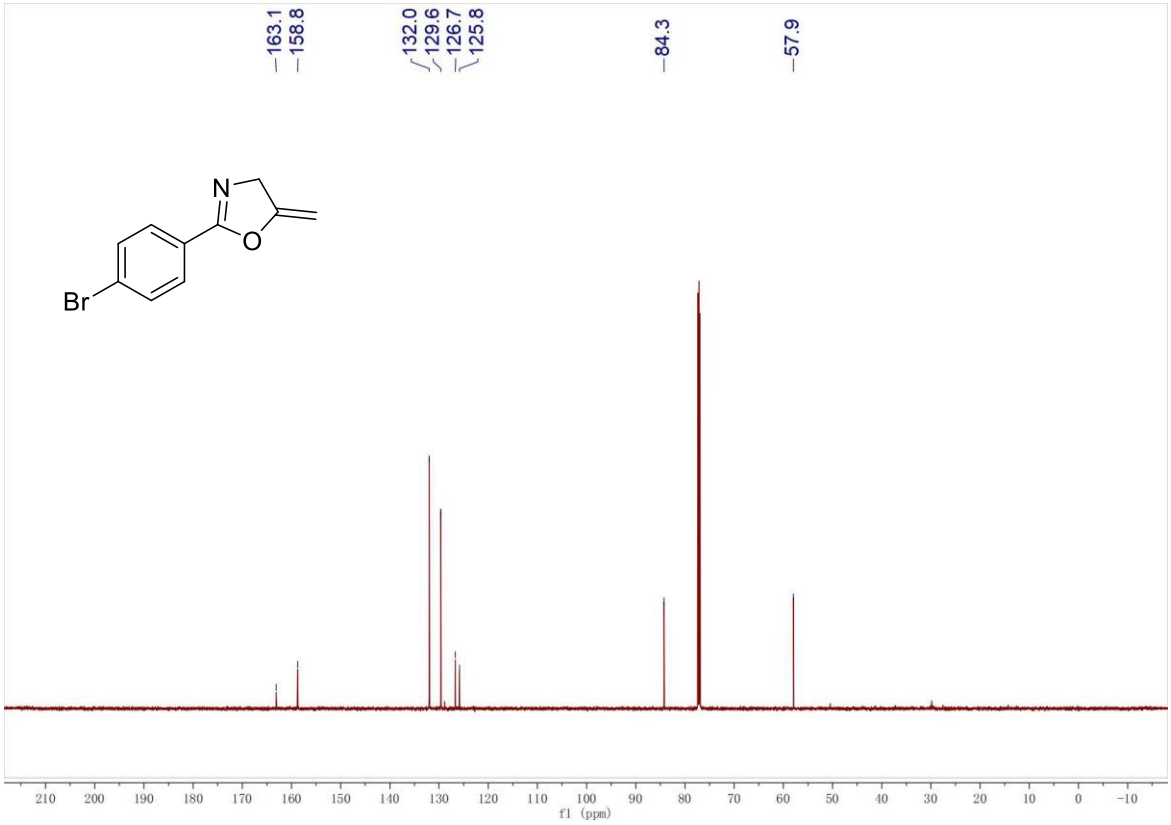

Figure S55. ^{13}C NMR (151 MHz, $CDCl_3$) Spectrum of Compound **9k**

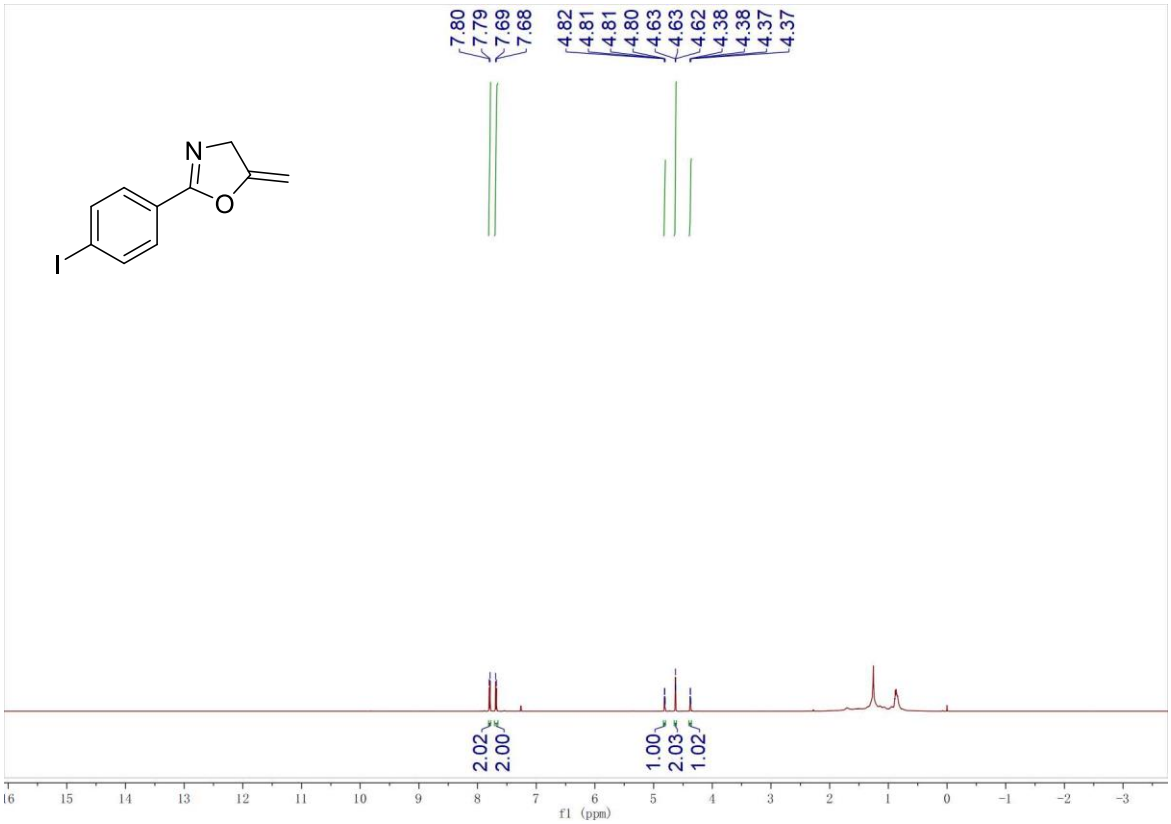

Figure S56. ^{1}H NMR (600 MHz, $CDCl_3$) Spectrum of Compound **9l**

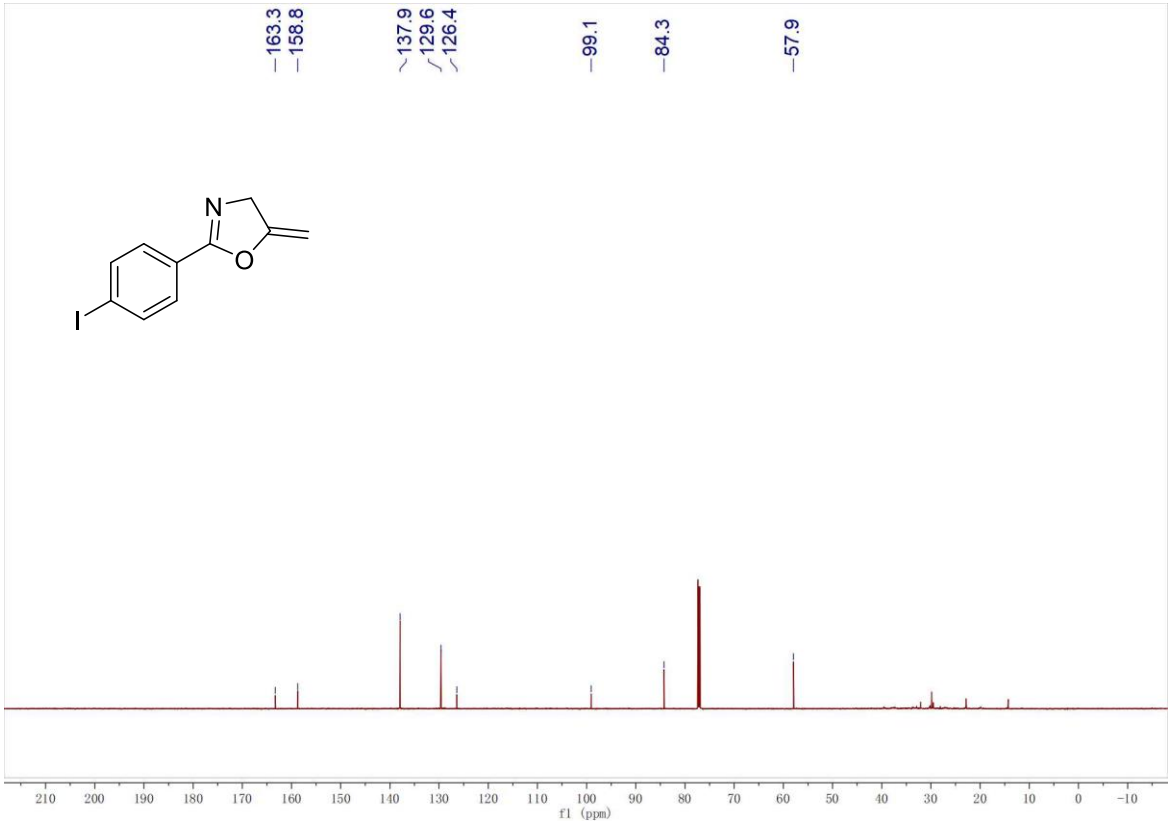

Figure S57. ^{13}C NMR (151 MHz, $CDCl_3$) Spectrum of Compound **9l**

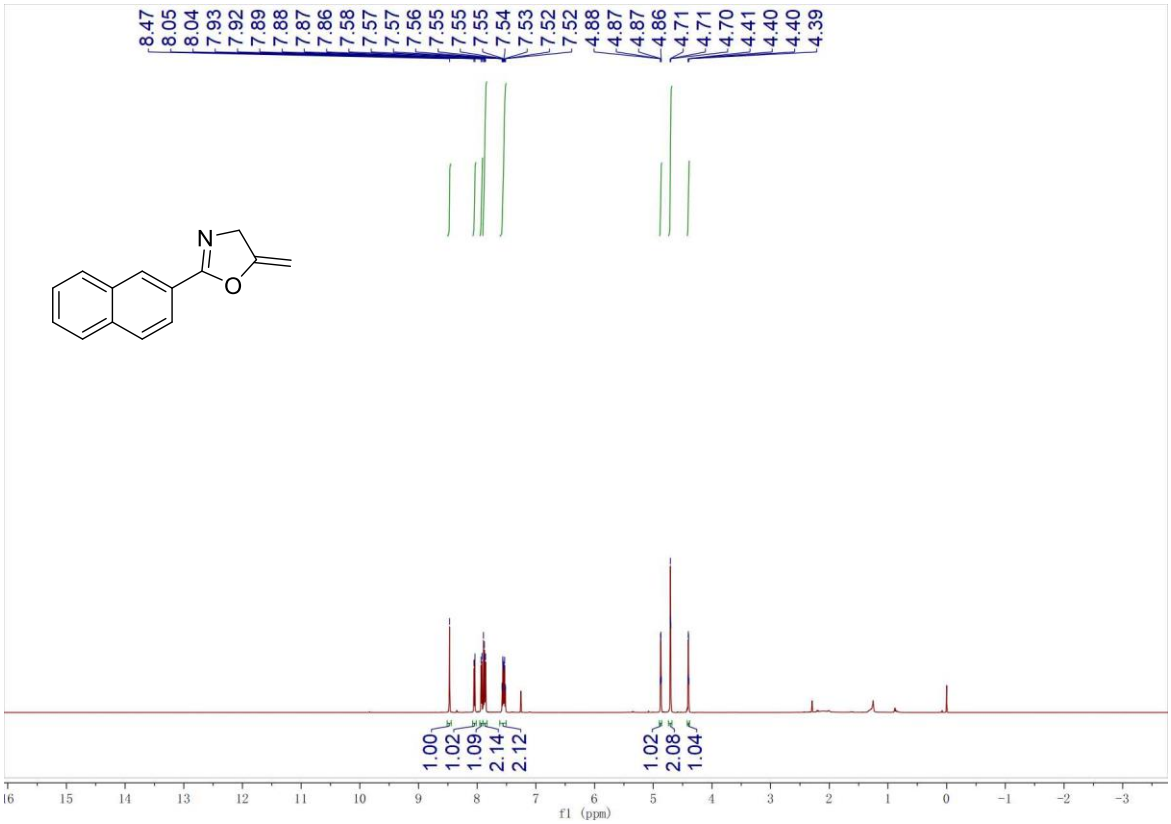

Figure S58. ^{1}H NMR (600 MHz, $CDCl_3$) Spectrum of Compound **9m**

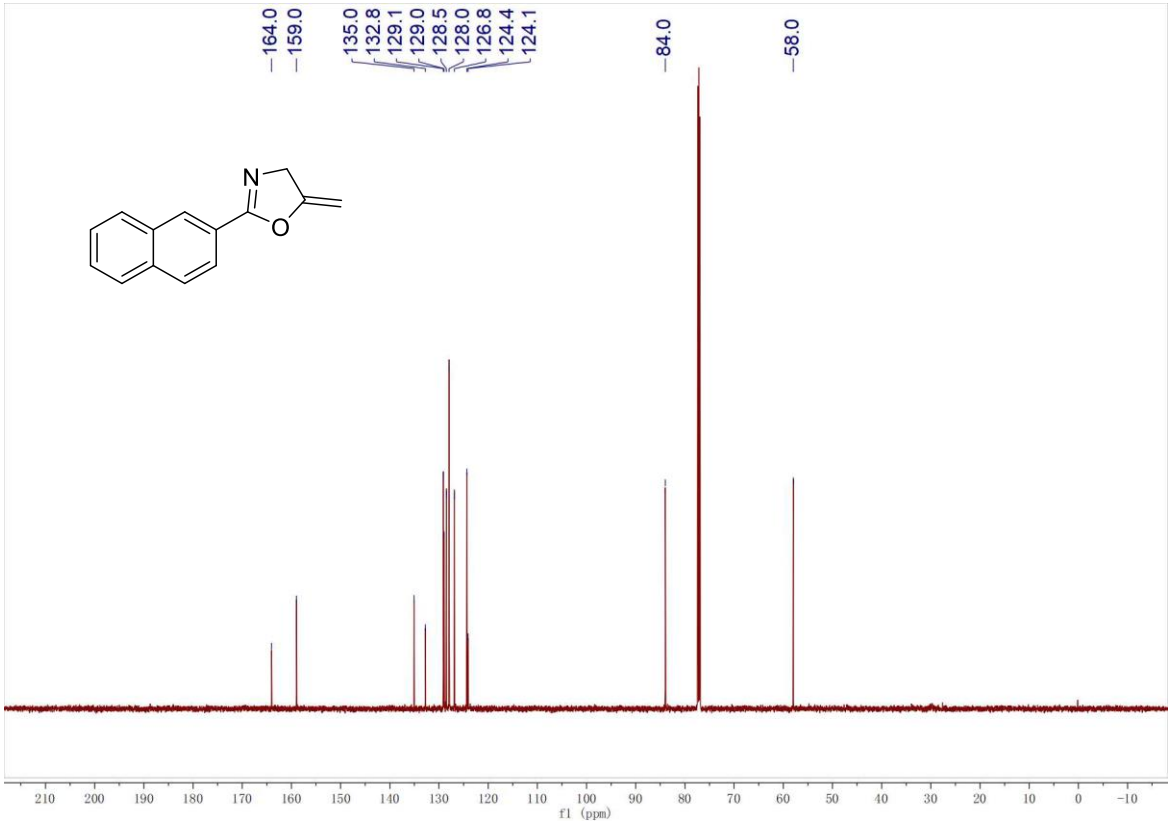

Figure S59. ^{13}C NMR (151 MHz, $CDCl_3$) Spectrum of Compound **9m**

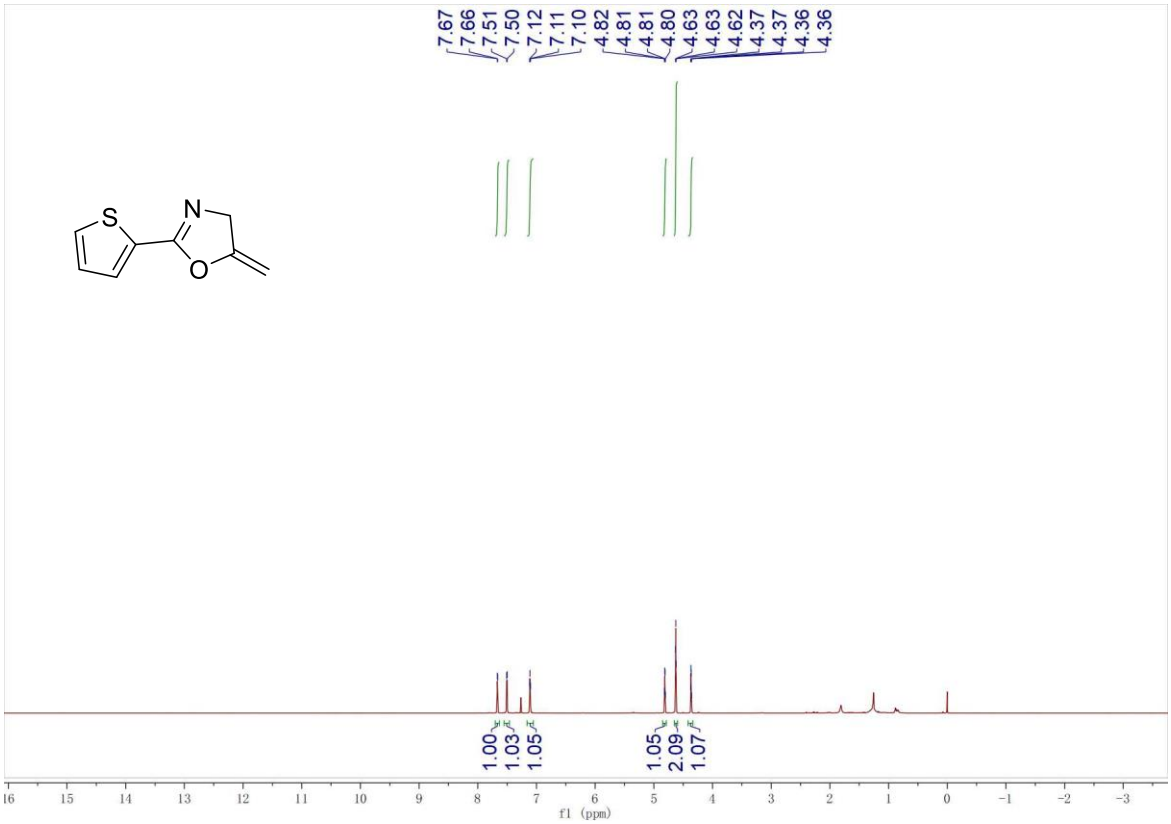

Figure S60. ^{1}H NMR (600 MHz, $CDCl_3$) Spectrum of Compound **9n**

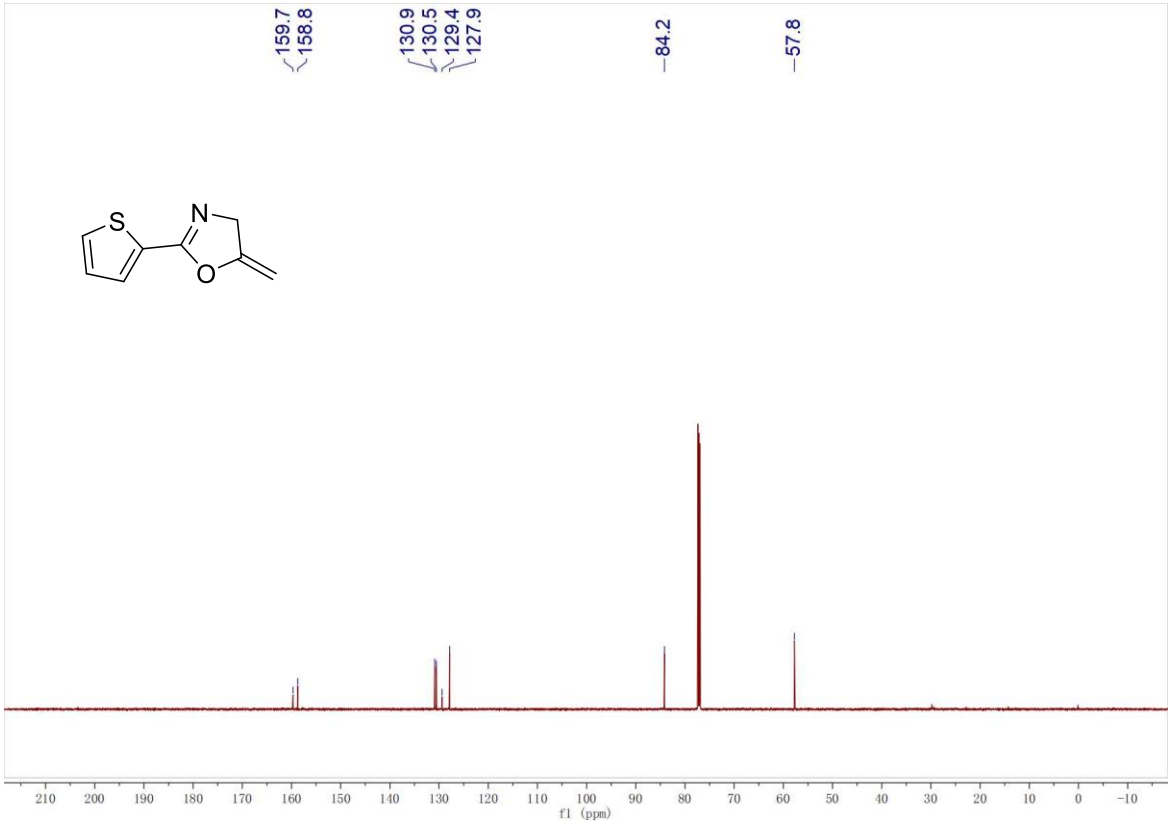

Figure S61. ^{13}C NMR (151 MHz, $CDCl_3$) Spectrum of Compound **9n**

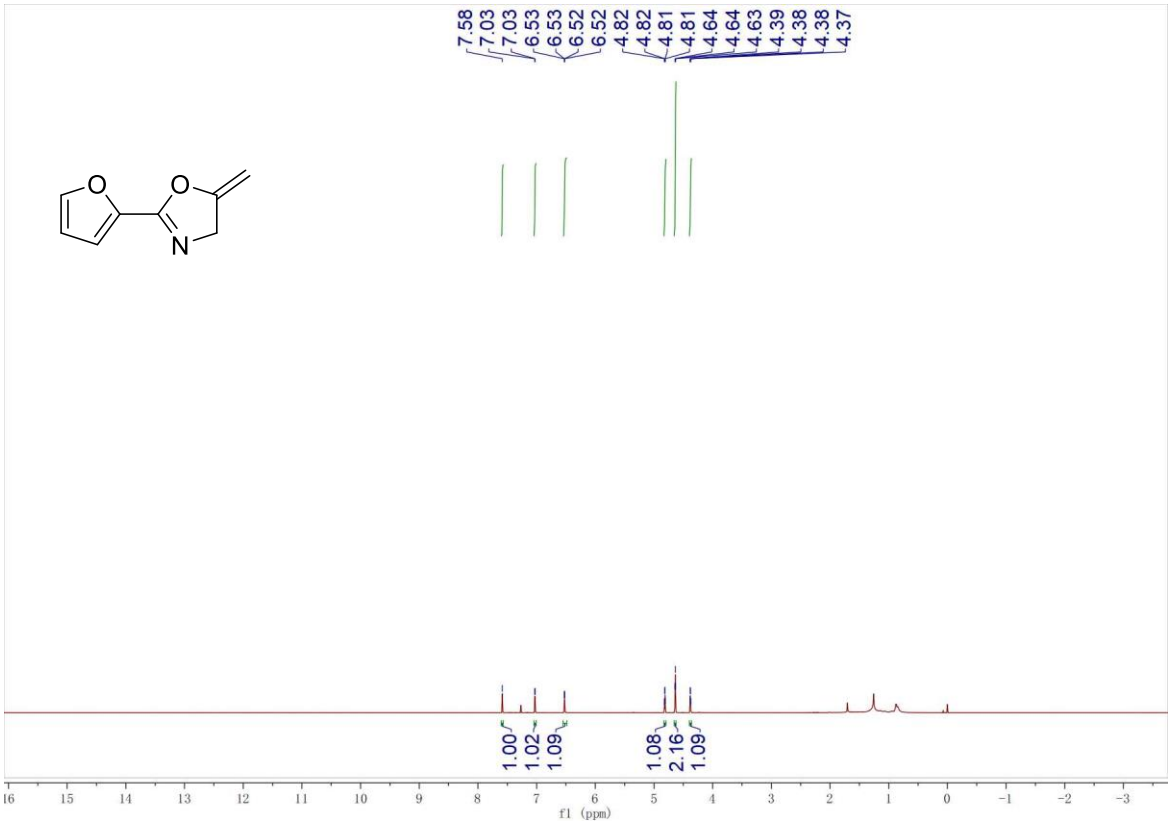

Figure S62. ^{1}H NMR (600 MHz, $CDCl_3$) Spectrum of Compound **9o**

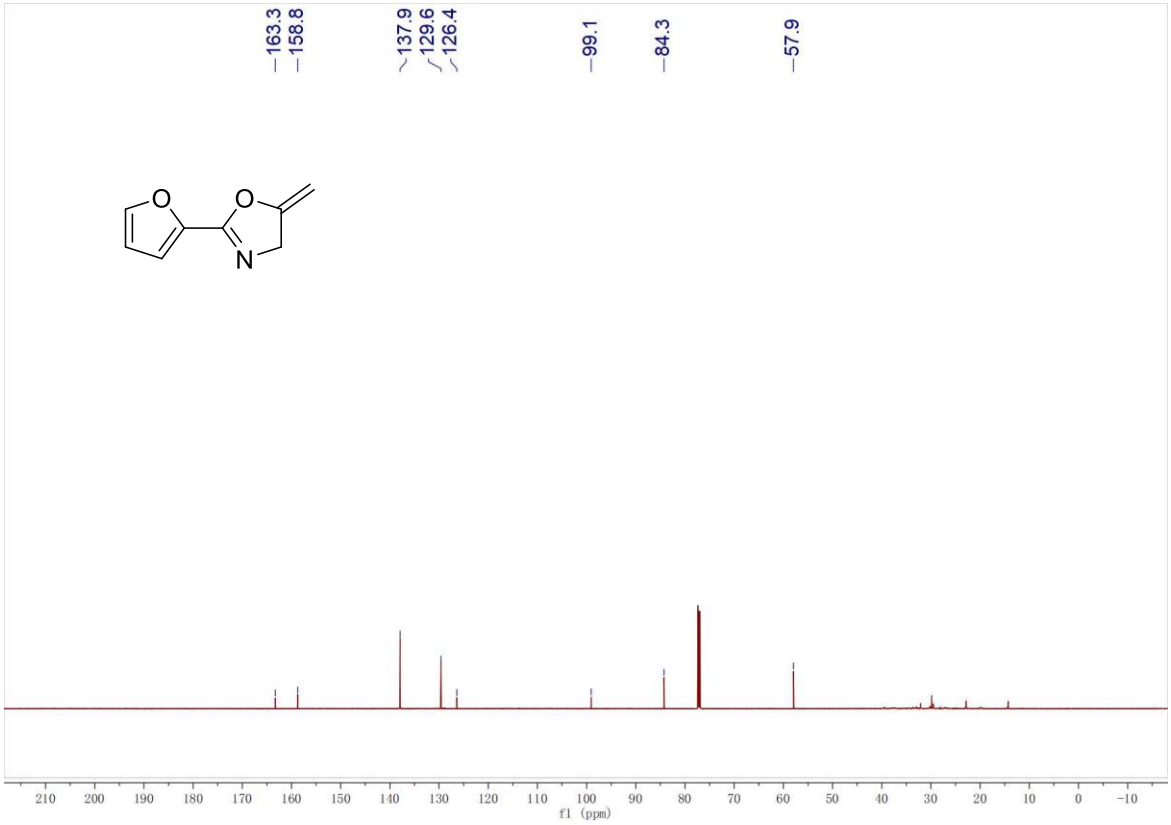

Figure S63. ^{13}C NMR (151 MHz, $CDCl_3$) Spectrum of Compound **9o**

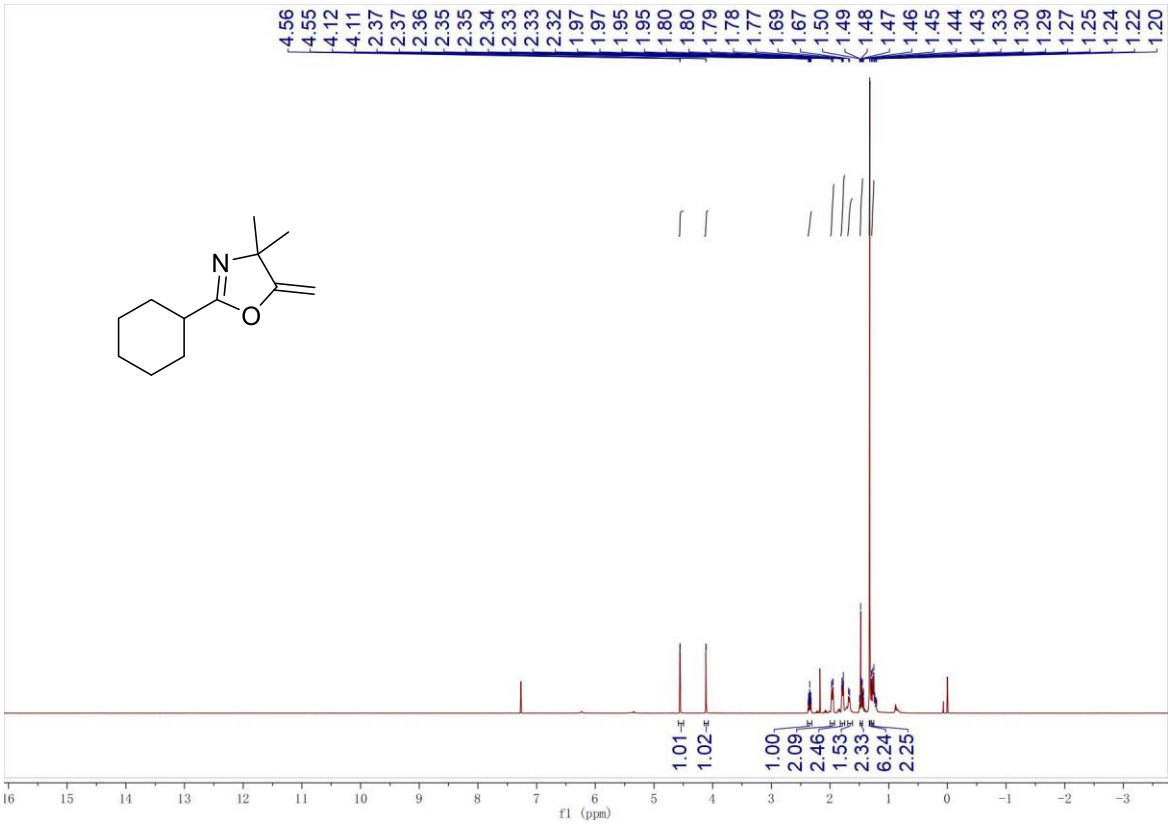

Figure S64. ^{1}H NMR (600 MHz, $CDCl_3$) Spectrum of Compound **9p**

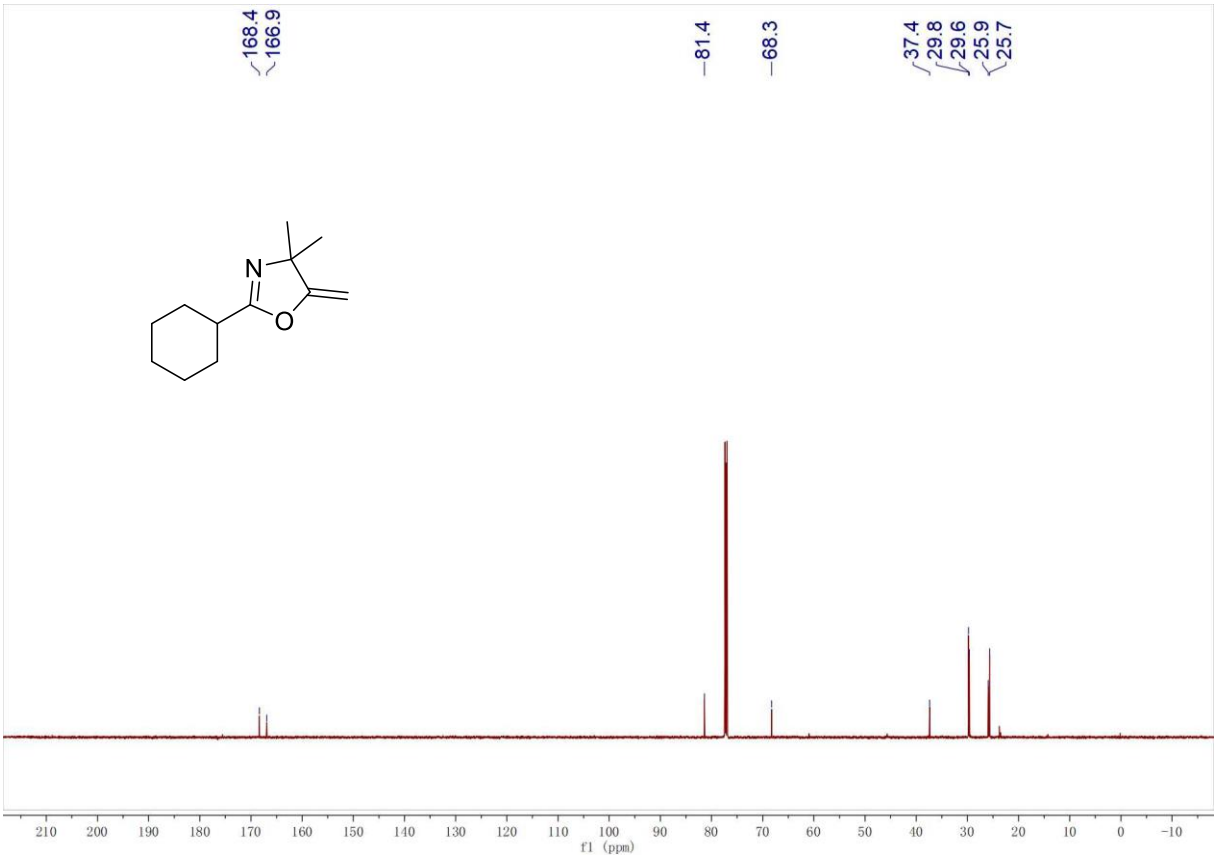

Figure S65. ^{13}C NMR (151 MHz, $CDCl_3$) Spectrum of Compound **9p**

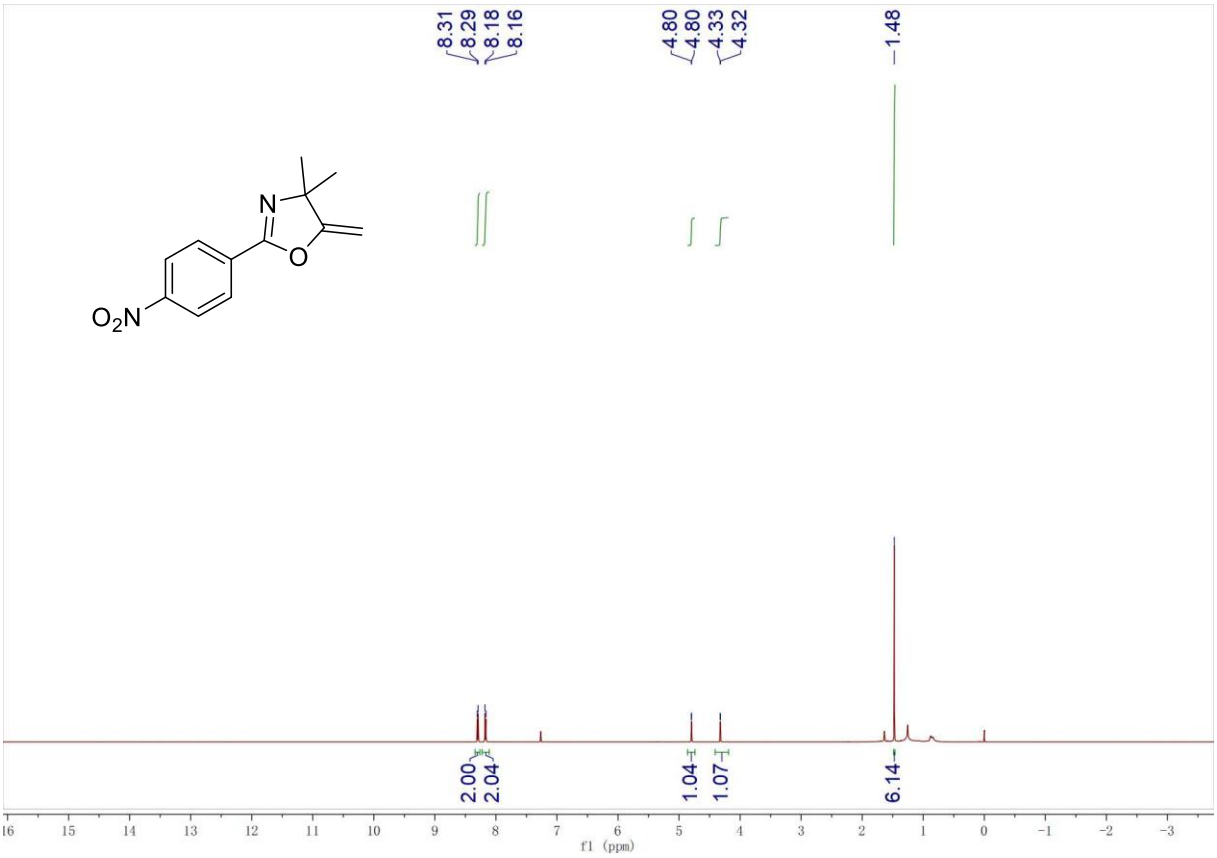

Figure S71. ^{1}H NMR (600 MHz, $CDCl_3$) Spectrum of Compound **9q**

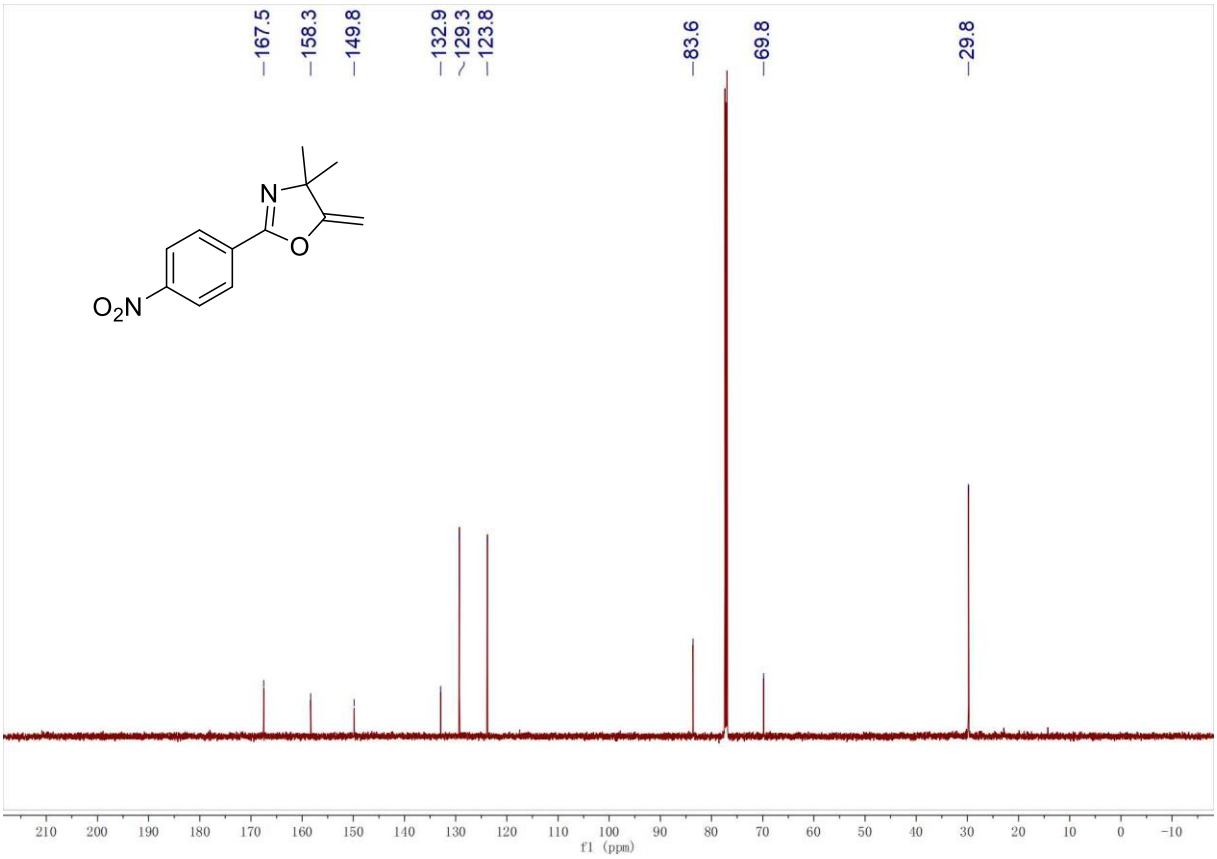

Figure S72. ^{13}C NMR (151 MHz, $CDCl_3$) Spectrum of Compound **9q**

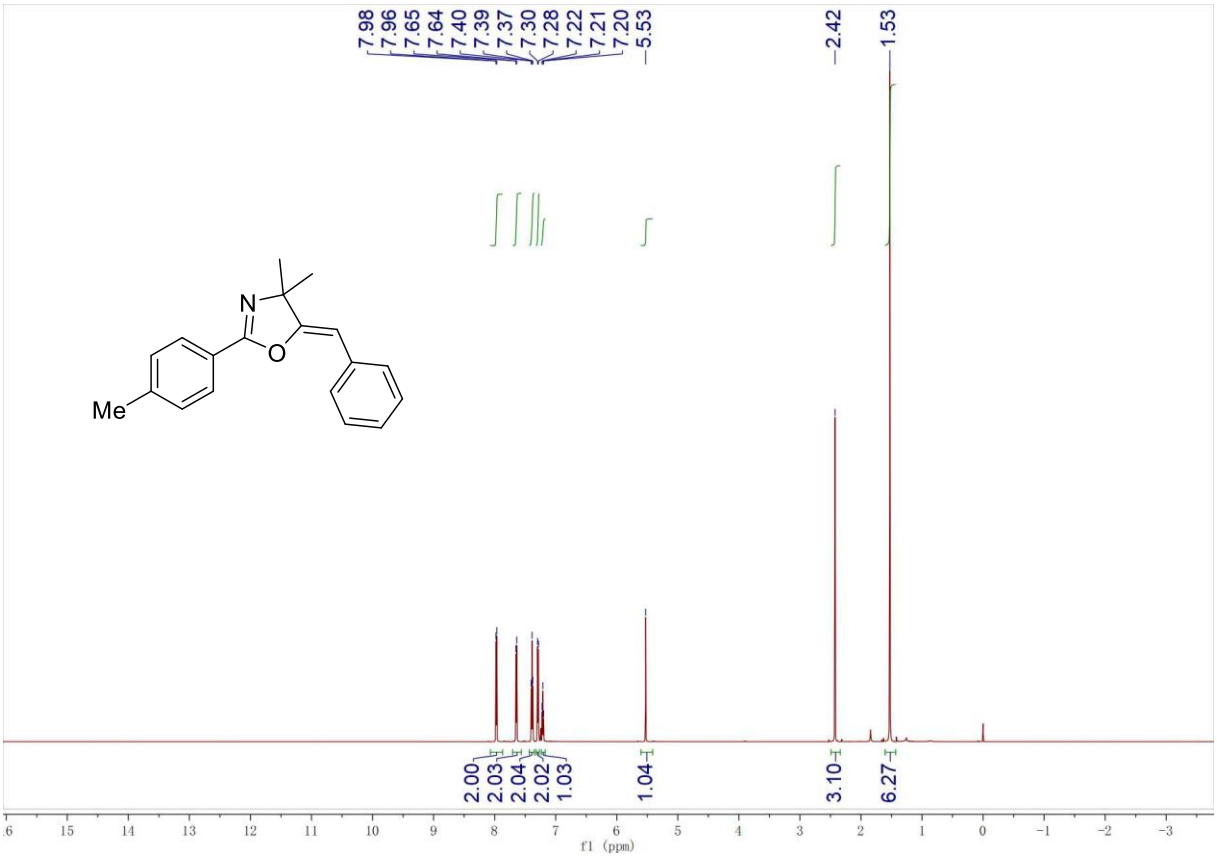

Figure S69. ^{1}H NMR (600 MHz, $CDCl_3$) Spectrum of Compound **9r**

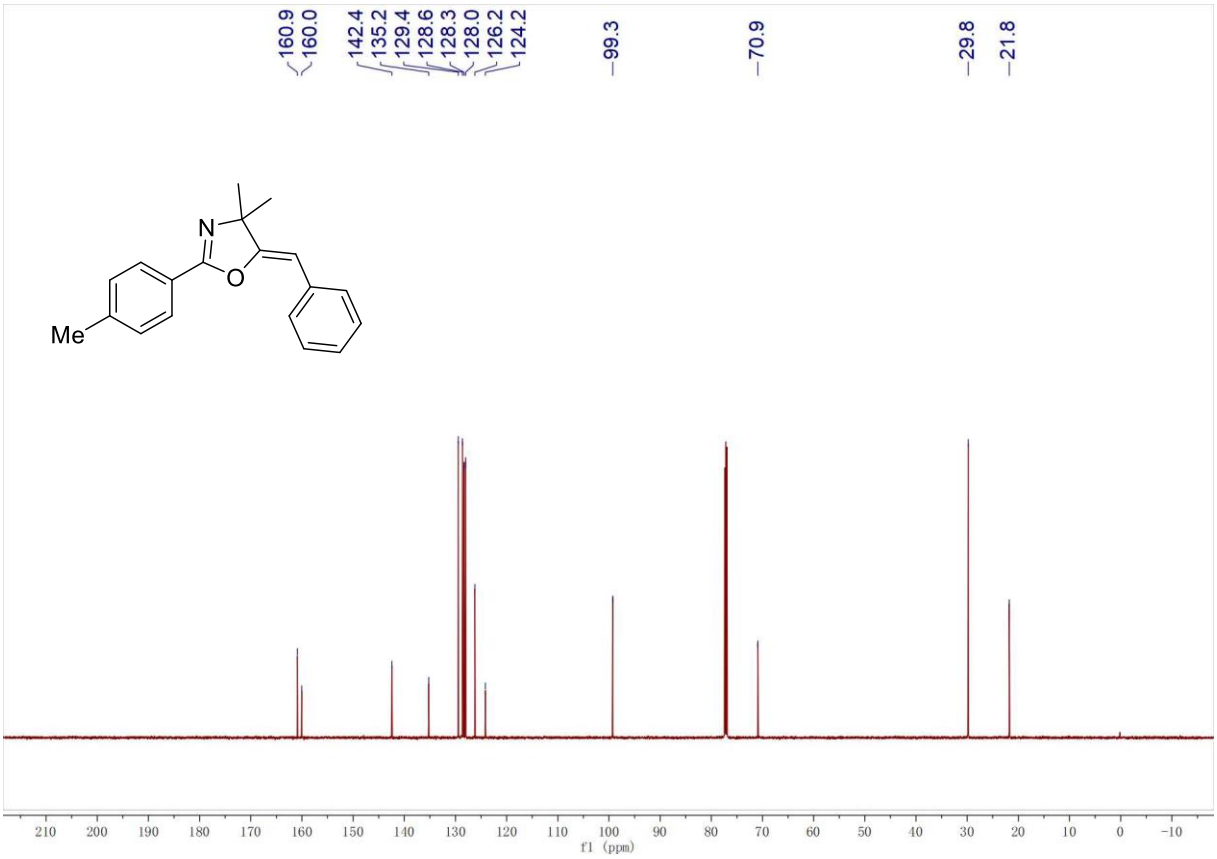

Figure S70. ^{13}C NMR (151 MHz, $CDCl_3$) Spectrum of Compound **9r**

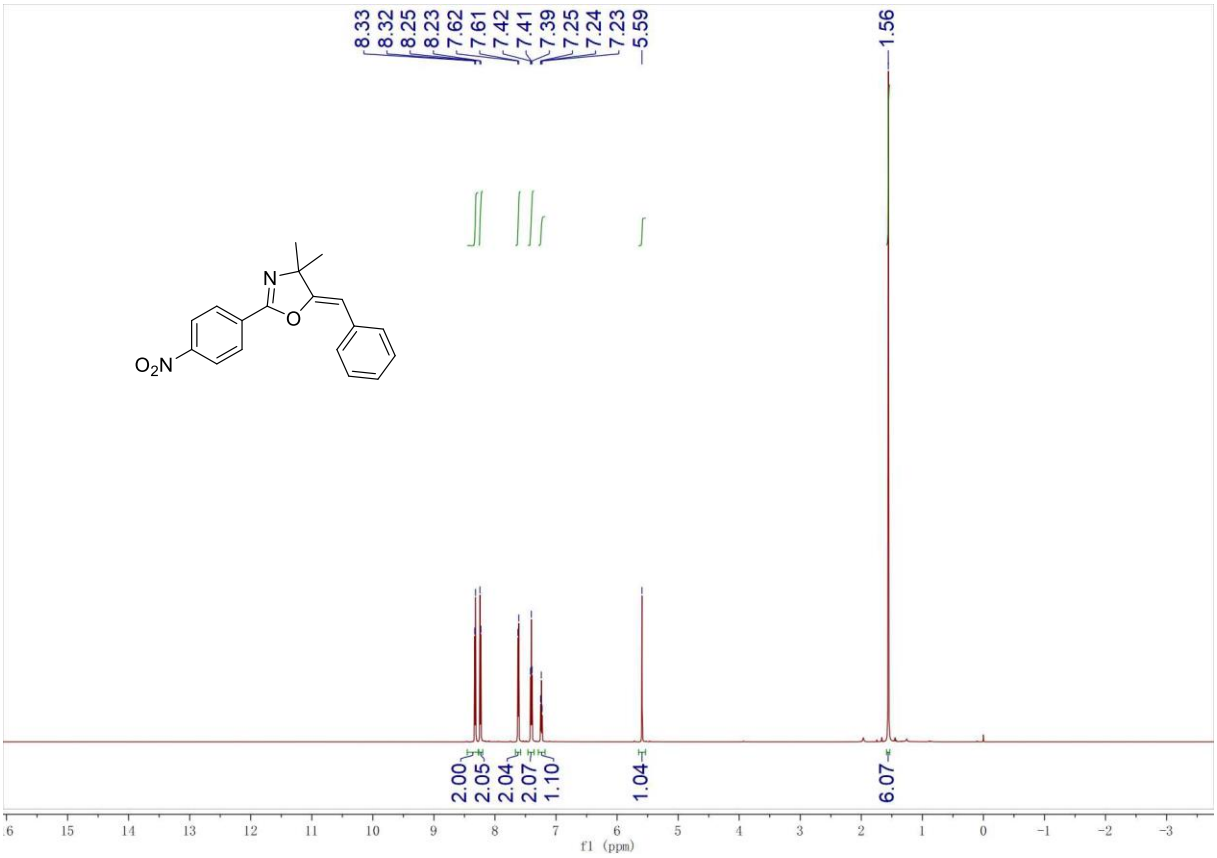

Figure S67. ^{1}H NMR (600 MHz, $CDCl_3$) Spectrum of Compound **9s**

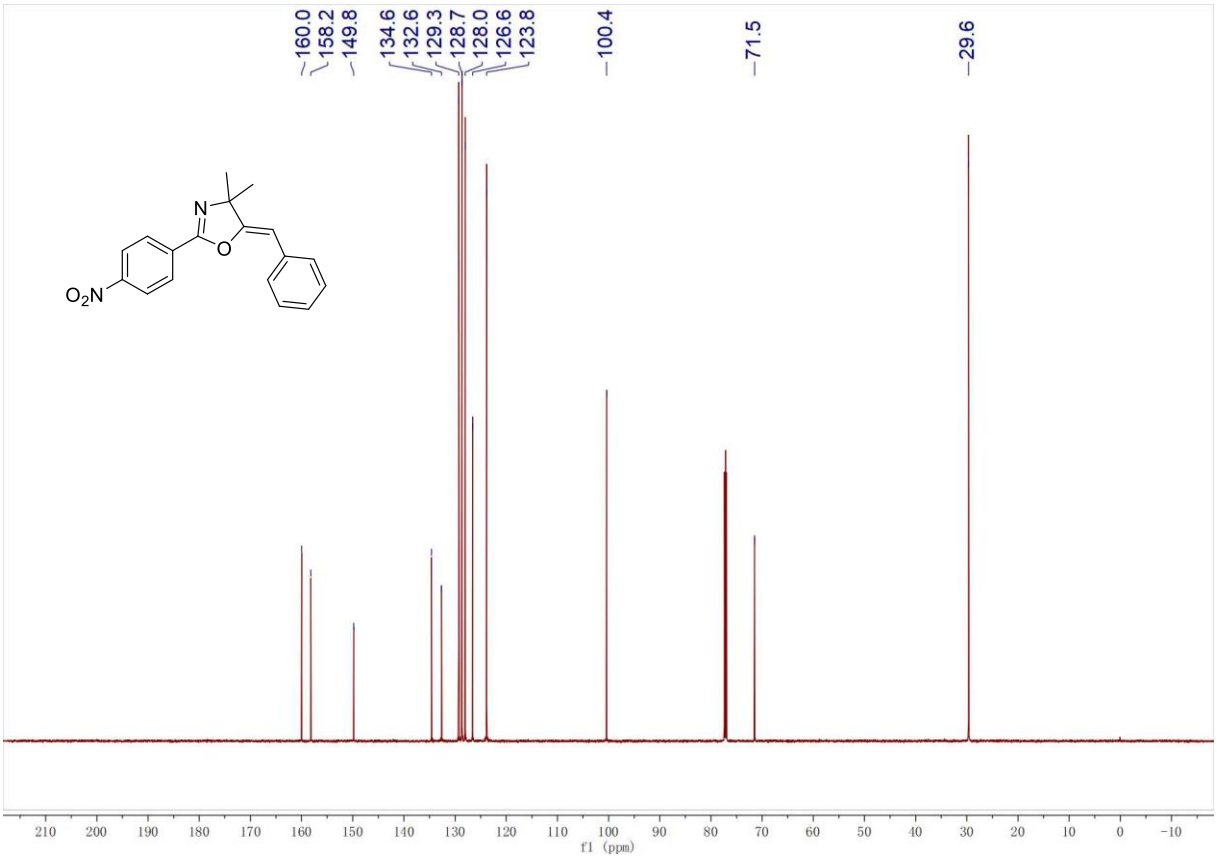

Figure S68. ^{13}C NMR (151 MHz, $CDCl_3$) Spectrum of Compound **9s**

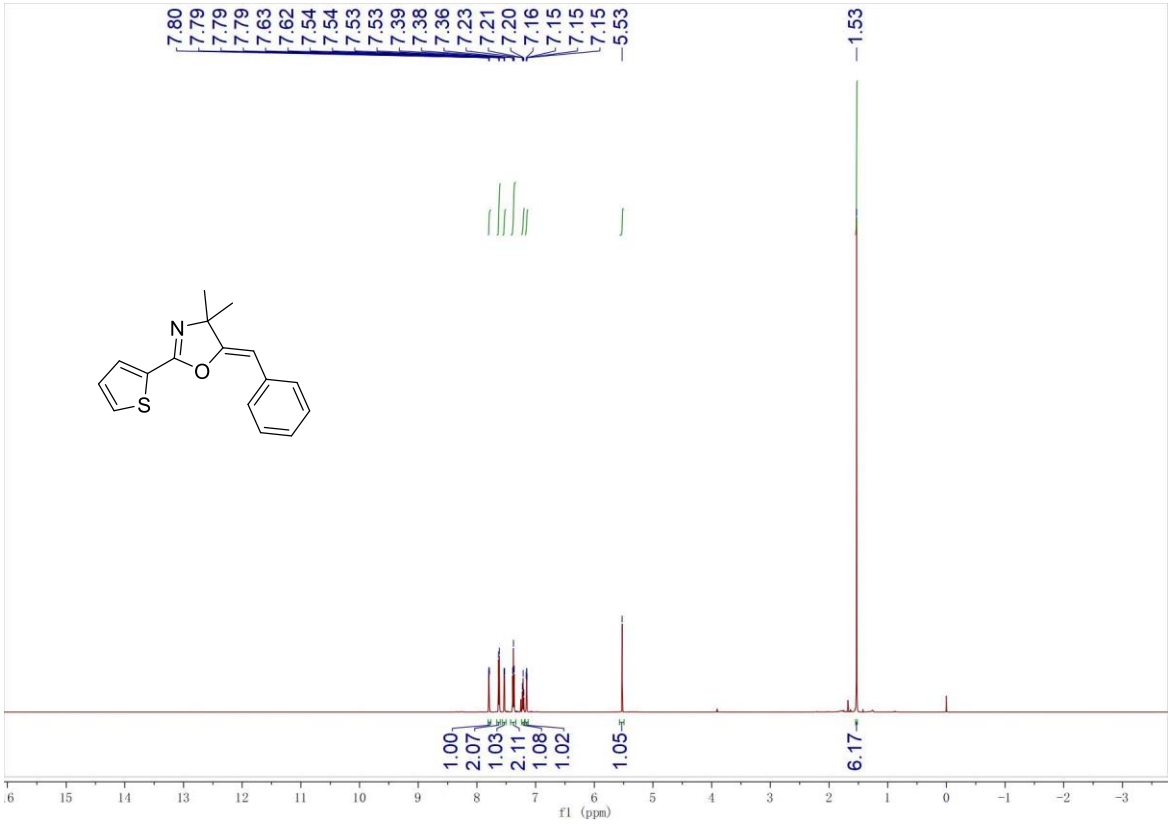

Figure S73. ^{1}H NMR (600 MHz, $CDCl_3$) Spectrum of Compound **9t**

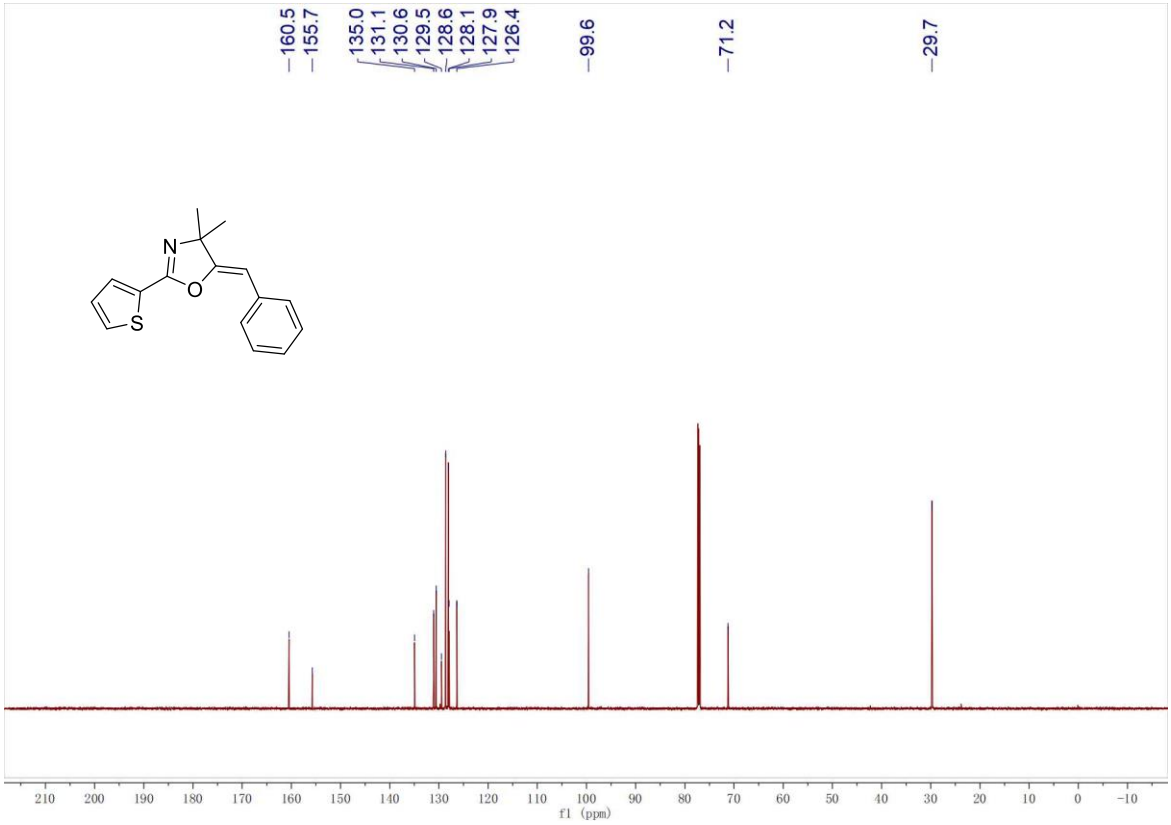

Figure S74. ^{13}C NMR (151 MHz, $CDCl_3$) Spectrum of Compound **9t**

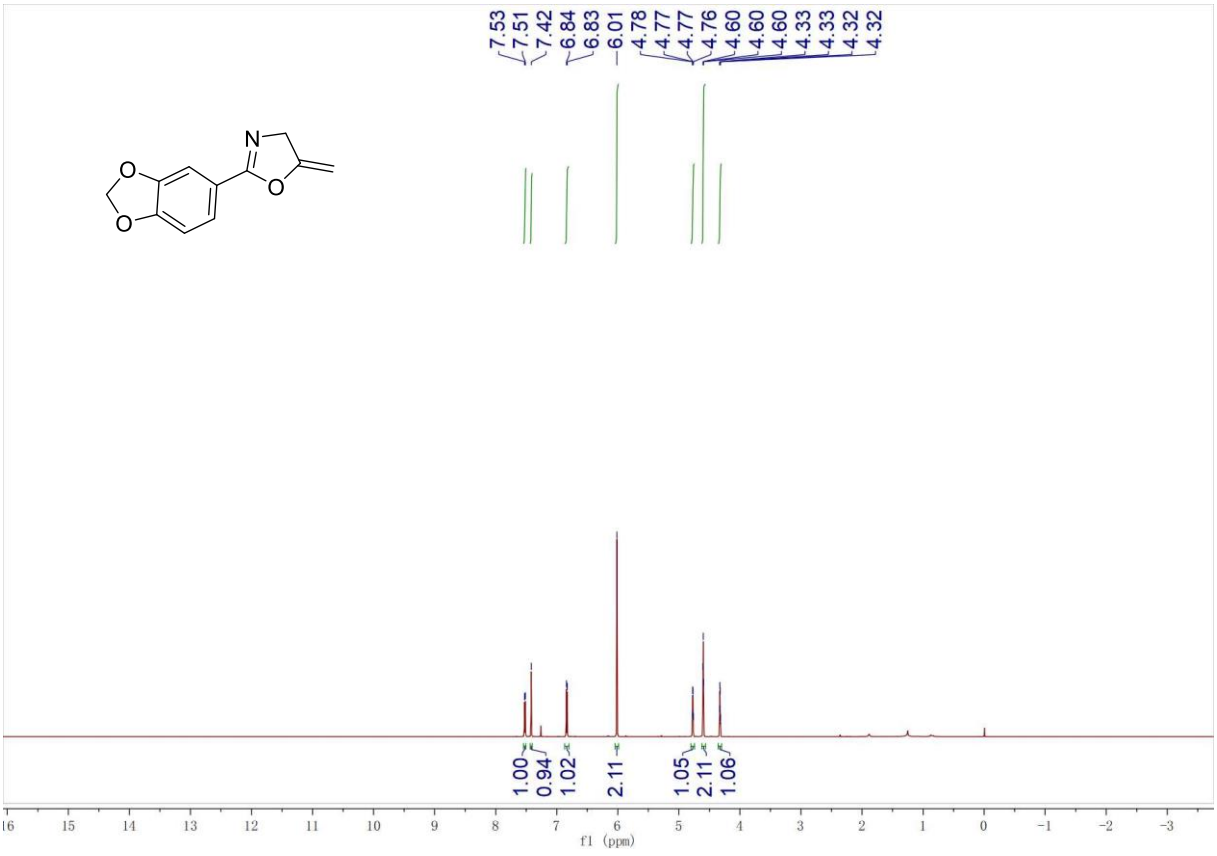

Figure S75. ^{1}H NMR (600 MHz, $CDCl_3$) Spectrum of Compound **9u**

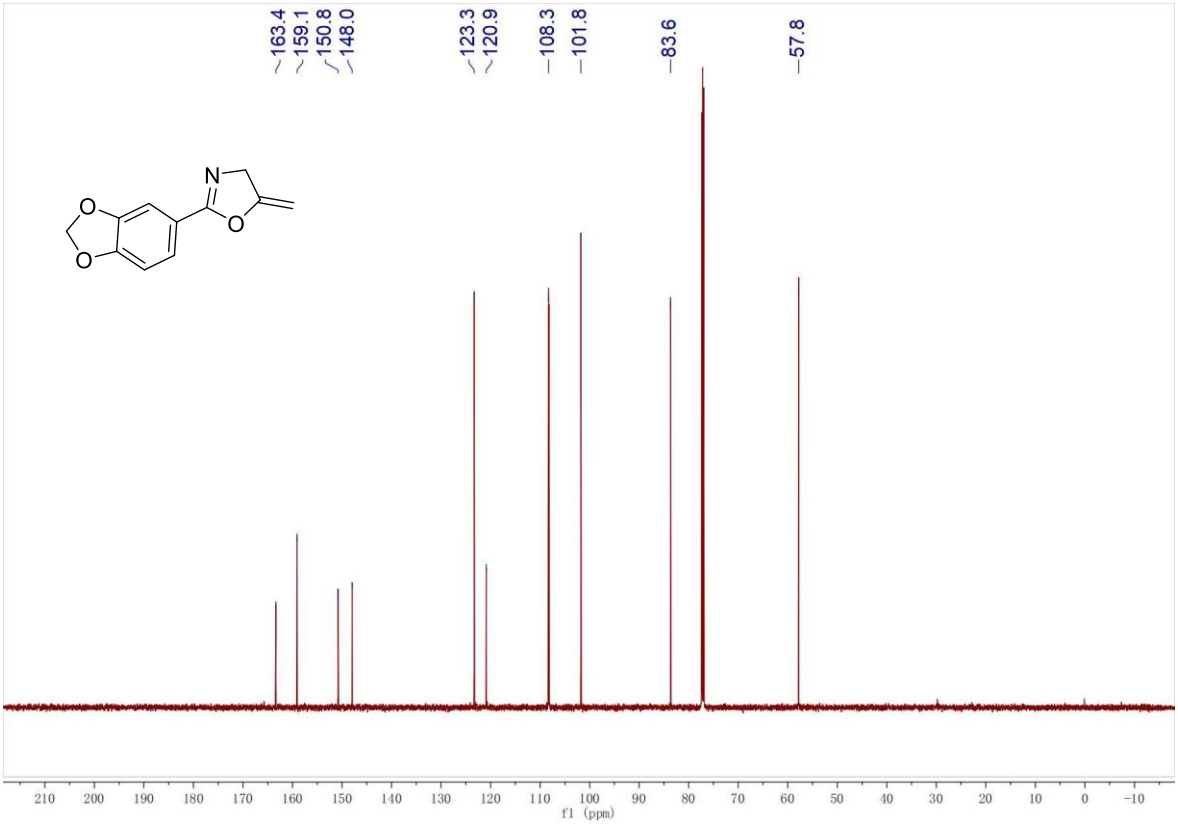

Figure S76. ^{13}C NMR (151 MHz, $CDCl_3$) Spectrum of Compound **9u**

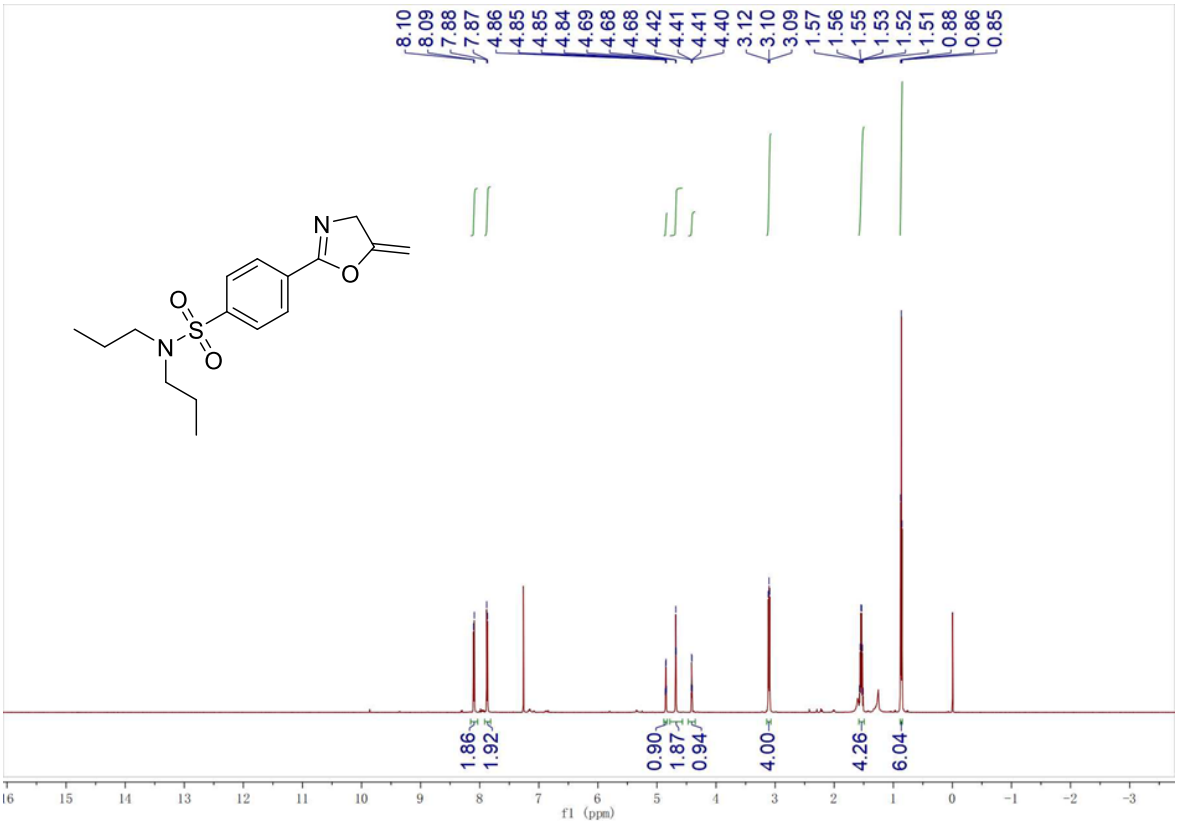

Figure S77. ^{1}H NMR (600 MHz, $CDCl_3$) Spectrum of Compound **9v**

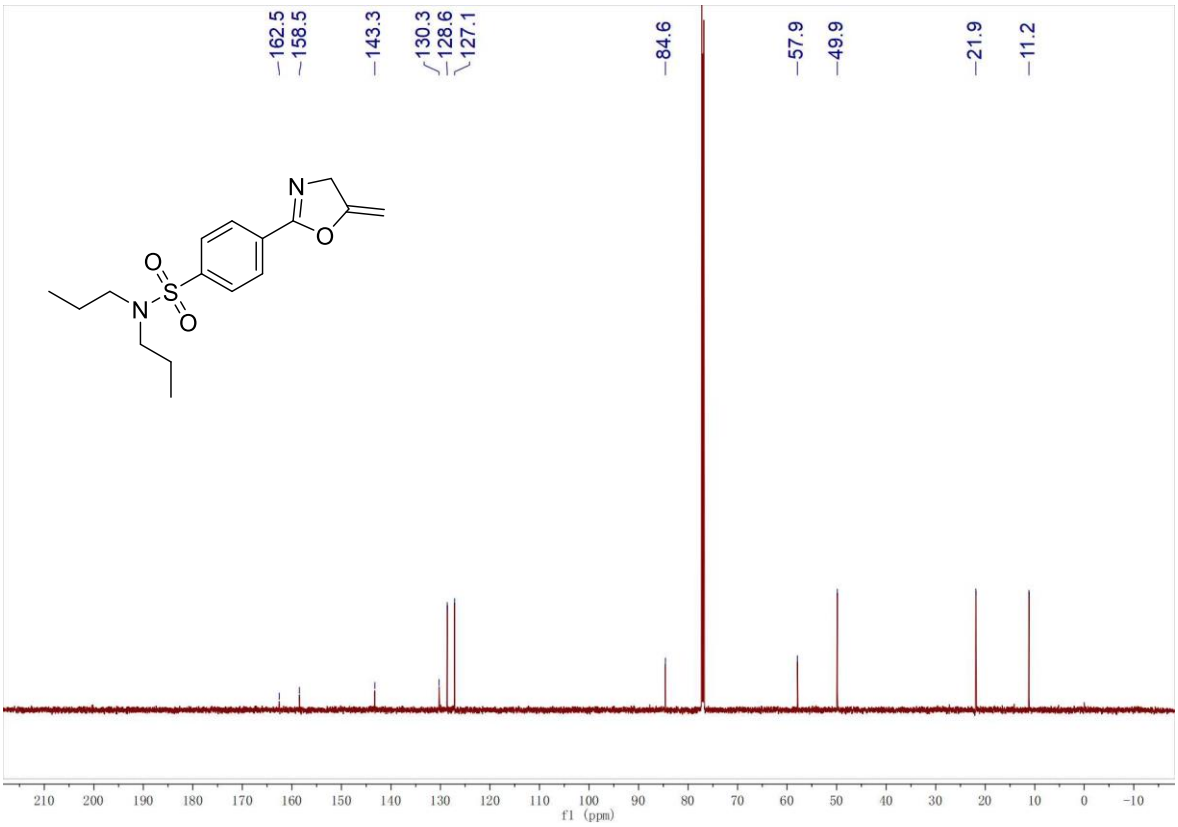

Figure S78. ^{13}C NMR (151 MHz, $CDCl_3$) Spectrum of Compound **9v**

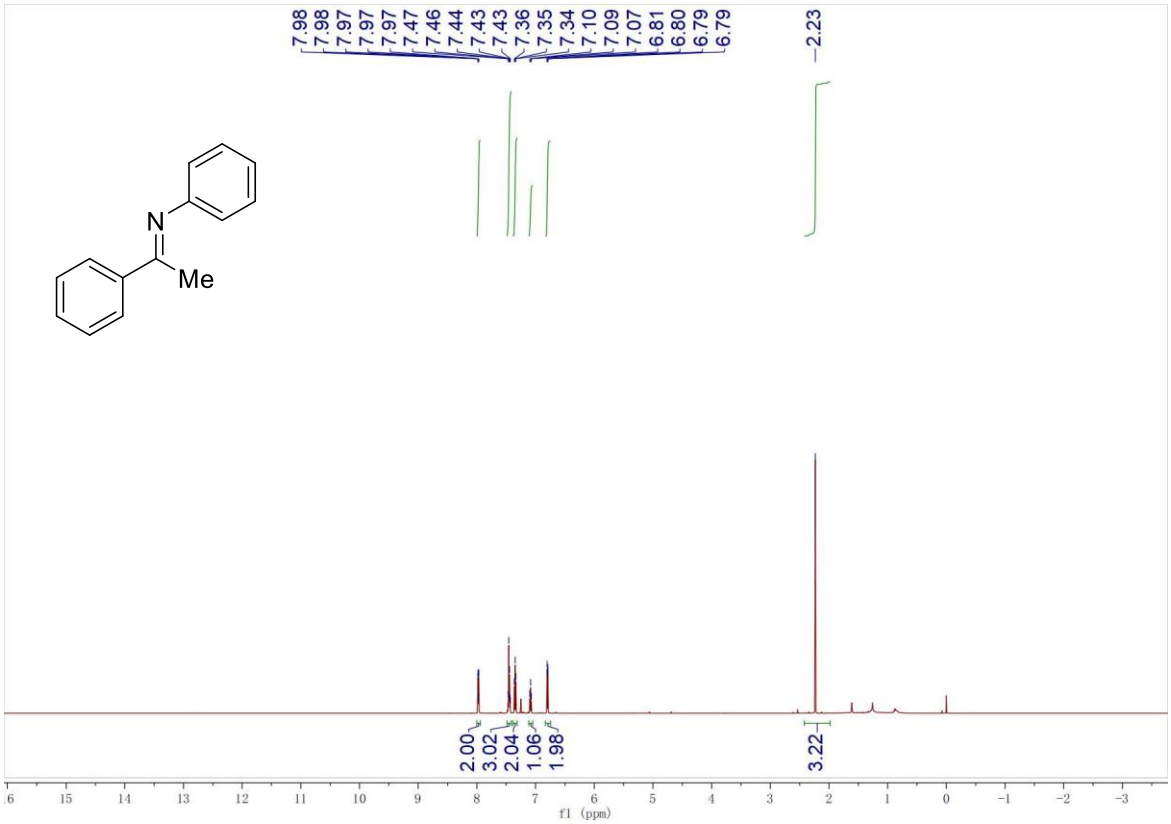

Figure S79. ^{1}H NMR (600 MHz, $CDCl_3$) Spectrum of Compound **10**

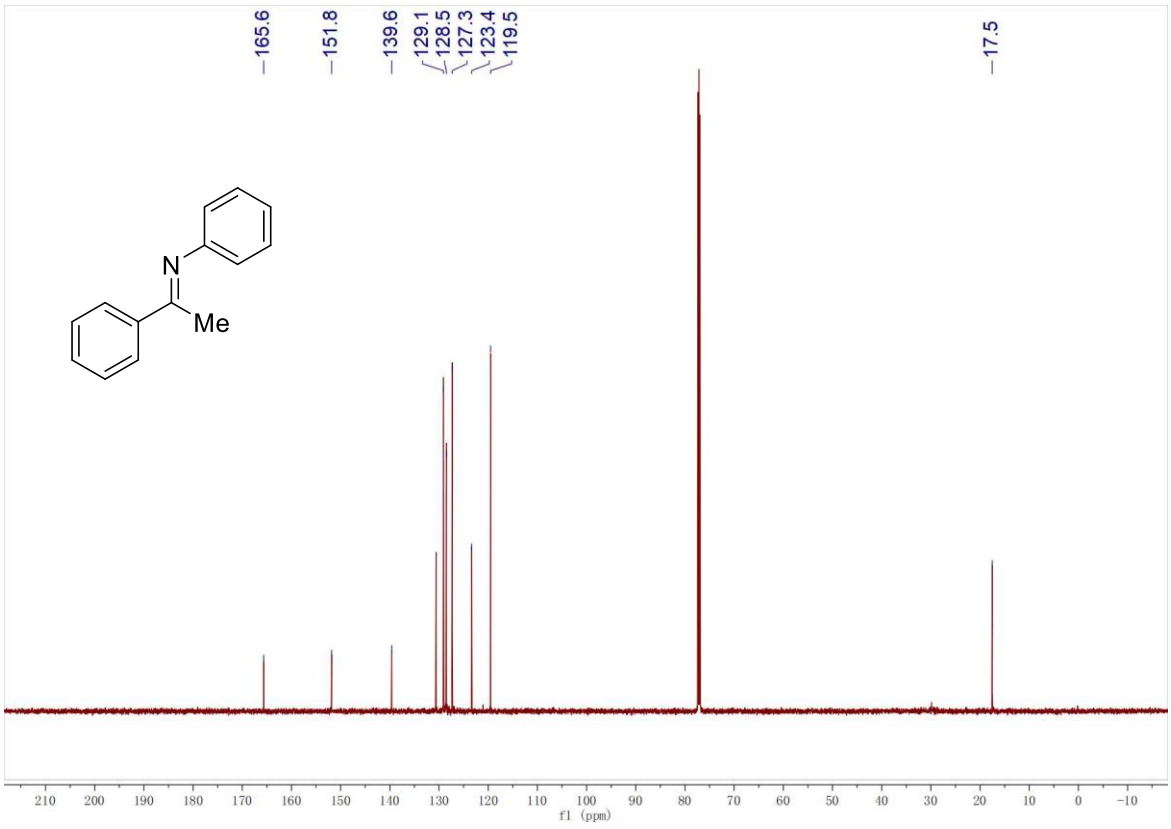

Figure S80. ^{13}C NMR (151 MHz, $CDCl_3$) Spectrum of Compound **10**

7. References

[1] Meiries, S.; Speck, K.; Cordes, D. B.; Slawin, A. M. Z.; Nolan, S. P., [Pd(IPr*OMe)(acac)Cl]: Tuning the N-Heterocyclic Carbene in Catalytic C-N Bond Formation. *Organometallics* **2013,** *32*, 330-339.

[2] Seppanen, O.; Aikonen, S.; Muuronen, M.; Alamillo-Ferrer, C.; Bures, J.; Helaja, J., Dual H-bond activation of NHC-Au(I)-Cl complexes with amide functionalized side-arms assisted by H-bond donor substrates or acid additives. *Chem. Commun. (Cambridge, U. K.)* **2020,** *56*, 14697-14700.

[3] Sen S , Gabbai F P .An ambiphilic phosphine/H-bond donor ligand and its application to the gold mediated cyclization of propargylamides[J].Chemical Communications, **2017**, *53(100)*, 13356-13358

[4] Hashmi, A. S. K.; Blanco Jaimes, M. C.; Schuster, A. M.; Rominger, F., From propargylic amides to functionalized oxazoles: Domino gold catalysis/oxidation by dioxygen. *J. Org. Chem.* **2012,** *77*, 6394-6408.

[5] Dong, S.; Hong, K.; Zhang, Z.; Huang, J.; Xie, X.; Yuan, H.; Hu, W.; Xu, X., Construction of Chiral Quaternary Carbon Centers via Asymmetric Metal Carbene gem-Dialkylation. Angewandte Chemie International Edition **2023**, *62(26)*, e202302371.

[6] Bárta, O.; Císařová, I.; Schulz, J.; Štěpnička, P., Assessing the influence of phosphine substituents on the catalytic properties of self-stabilised digold(i) complexes with supporting ferrocene phosphinonitrile ligands. *New Journal of Chemistry* **2019,** *43*, 11258-11262.

[7] Zhang, J.; Li, T.; Li, X.; Lv, A.; Li, X.; Wang, Z.; Wang, R.; Ma, Y.; Fang, R.; Szostak, R.; Szostak, M., Thiazol-2-ylidenes as N-Heterocyclic carbene ligands with enhanced electrophilicity for transition metal catalysis. *Commun. Chem.* **2022,** *5*, 60.

[8] Rendón-Nava, D.; Álvarez-Hernández, A.; Mendoza-Espinosa, D., Synthesis and Catalytic Applications of Multinuclear Gold(I)-1,2,3-Triazolylidene Complexes. *European Journal of Inorganic Chemistry* **2021,** *2021*, 840-847.

[9] Doherty, S.; Knight, J. G.; Perry, D. O.; Ward, N. A. B.; Bittner, D. M.; McFarlane, W.; Wills, C.; Probert, M. R., Triaryl-like MONO-, BIS-, and TRISKITPHOS phosphines: synthesis, solution NMR studies, and a comparison in gold-catalyzed carbon-heteroatom bond forming 5-exo-dig and 6-endo-dig cyclizations. *Organometallics* **2016,** *35*, 1265-1278.

[10] Patil, N. T.; Kavthe, R. D.; Shinde, V. S., Transition metal-catalyzed addition of C-, N- and O-nucleophiles to unactivated C–C multiple bonds. *Tetrahedron* **2012,** *68*, 8079-8146.

[11] Alhalib, A.; Moran, W. J., CuI-catalyzed cycloisomerization of propargyl amides. *Org. Biomol. Chem.* **2014,** *12*, 795-800.

[12] Wang, Y.; Jiang, M.; Liu, J.-T., Copper-catalyzed stereoselective oxytrifluoromethylation of propargyl amides for the construction of oxazolines. *Org. Chem. Front.* **2015,** *2*, 542-547.

[13] Kumar, A.; Singh, C.; Tinnermann, H.; Huynh, H. V., Gold(I) and Gold(III) Complexes of Expanded-Ring N-Heterocyclic Carbenes: Structure, Reactivity, and Catalytic Applications. *Organometallics* **2020**, *39*, 172-181.

8. Cartesian Coordinates with Zero-Point Energies and Thermal Corrections

Indy*

Energy: -1692.687986 au

Sum of electronic and thermal Energies: -1692.021386 au

Geometry:

N	0.38641700	2.00653700	0.13644500
N	-0.01481200	0.78793800	0.78673800
C	-1.36329800	-2.19670000	-0.97436200
H	-2.32409400	-2.65450000	-1.18211000
C	-4.80292000	-1.65681500	-0.14102200
H	-4.97153700	-1.18100800	-1.09990000
C	0.11770400	2.28006200	-1.26551300
H	0.30055300	1.38122200	-1.85053200
H	0.81737600	3.04609200	-1.60304700
H	-0.91066200	2.61743200	-1.42677000
C	0.14744500	2.27105100	2.36315200
C	-3.15994400	0.70452600	-0.86641800
C	-3.68332300	-1.31266400	0.61983400
C	3.38627800	-1.60773500	0.65986700
C	3.01782200	0.05998800	-2.37767500
H	2.37079000	-0.74302900	-2.70988500
C	-3.79374800	1.86585400	-0.40662500
H	-3.87671700	2.03794900	0.66164300

C	5.25122700	-3.15620500	0.54077100
H	6.09284000	-3.56137000	-0.01060300
C	0.42609900	2.93183400	1.13896800
C	3.99820000	1.37331100	-0.62311200
H	4.12104000	1.59216300	0.43263700
C	0.43850900	4.35898600	3.51685500
H	0.45377000	4.94232700	4.43008200
C	-5.53360600	-3.20698600	1.56576500
H	-6.24857600	-3.93571200	1.93117100
C	4.95532800	-3.63505900	1.81375700
H	5.56216100	-4.41534000	2.25942600
C	-5.72046100	-2.59972800	0.32735500
H	-6.58483900	-2.85235700	-0.27724600
C	-3.50826100	-1.92501900	1.86854200
H	-2.64627300	-1.65897300	2.47230300
C	-0.07633700	-0.42910600	0.02036400
C	-4.21476500	2.59107000	-2.67202400
H	-4.61922600	3.31773900	-3.36769000
C	-2.62958400	-0.29942800	0.15782800
H	-2.37649300	0.27812000	1.04840300
C	4.47376500	-2.14691800	-0.03099700
H	4.72740200	-1.77279700	-1.01591600

C	-0.26494500	-4.15820000	-2.12720600
H	-1.12488200	-4.75588900	-1.81609800
H	0.63753400	-4.75457200	-1.97709100
H	-0.36503200	-3.97772400	-3.20332100
C	0.16688800	3.00155900	3.56122200
H	-0.03614400	2.49669100	4.49893600
C	4.66961100	2.14500600	-1.56711100
H	5.30875800	2.95818500	-1.24085000
C	0.69129600	4.99950600	2.28522500
H	0.89446600	6.06504800	2.27793800
C	4.51888000	1.87543700	-2.92773300
H	5.03988800	2.47520600	-3.66559500
C	-1.33289400	-0.98475500	-0.28417200
C	-0.19679400	-2.85709300	-1.36464200
C	3.09978600	-2.09334900	1.94299600
H	2.25976100	-1.67976200	2.49253800
C	3.69015300	0.83088200	-3.32815000
H	3.56214200	0.61249800	-4.38289700
C	3.87574600	-3.09650400	2.51535200
H	3.64016000	-3.45606200	3.51104800
C	3.16332200	0.31737500	-1.01140100
C	2.48091800	-0.51299600	0.07875900

H	2.29200600	0.17510300	0.90482300
C	0.68835300	4.30891400	1.08282400
H	0.88478800	4.81855700	0.14697900
C	-3.58551800	1.44083700	-3.14317000
H	-3.49817300	1.26811700	-4.21046200
C	-4.42285900	-2.86284600	2.33763400
H	-4.27165400	-3.32242100	3.30831000
C	-3.06112100	0.50804600	-2.24763500
H	-2.56267200	-0.37463500	-2.63112200
C	1.11908500	-1.07984600	-0.33074500
C	-4.31590700	2.80116000	-1.29699500
H	-4.79885700	3.69464400	-0.91680600
C	-0.12263100	0.87383400	2.11237800
C	1.03010200	-2.29081500	-1.02141500
H	1.94354700	-2.82507700	-1.25851700

Indy*^{MeO}

Energy: -1767.917310 au

Sum of electronic and thermal Energies: -1767.244882 au

Geometry:

O	0.32649600	-4.05662000	1.60900700
N	-0.08334600	0.97378700	-0.76801900

N	-0.51937100	2.11524500	-0.00826800
C	1.32971600	-0.81763200	0.13060700
C	5.60588200	-2.66467200	-1.94274200
H	6.34973600	-3.32340100	-2.37691800
C	-4.75581400	1.91633700	1.76083300
H	-5.42295700	2.73614400	1.51778400
C	0.30544900	-2.81743400	1.04189000
C	0.04847700	-0.29835200	-0.11029400
C	-0.96178300	-2.29738200	0.77042300
H	-1.82546600	-2.91724200	0.97595800
C	-4.87573800	-3.57181800	-2.10635500
H	-5.45670800	-4.33736500	-2.60846500
C	1.44409400	-2.08530400	0.71008300
H	2.43090400	-2.50017300	0.85896300
C	3.08413400	0.90023600	0.84446100
C	-0.25459900	2.27353400	1.41148000
H	-0.98802500	2.97062500	1.81963400
H	0.75742200	2.64468800	1.59989100
H	-0.38905800	1.31755000	1.91295800
C	-1.11151800	-1.04149200	0.19452200
C	3.68140100	-0.94946100	-0.81943100
C	-0.40208700	3.41326800	-3.33411800

H	-0.19534500	3.00117500	-4.31539900
C	-3.37320100	-1.58434300	-0.80500600
C	-0.98577200	5.26819000	-1.88025700
H	-1.23249400	6.31944100	-1.77657800
C	-3.20017100	0.19778600	1.02358100
C	4.07798000	2.66871600	2.79799300
H	4.45881900	3.34991100	3.55065000
C	-0.00220600	1.18093800	-2.08273800
C	-4.58307200	1.52400000	3.08851600
H	-5.11489100	2.03440800	3.88368900
C	3.52074100	-1.45628200	-2.11646600
H	2.64086900	-1.17810800	-2.68806800
C	-3.84620700	-2.91437300	-2.78118400
H	-3.62398000	-3.16597400	-3.81245500
C	-0.61534600	3.12147300	-0.92395500
C	-5.15516900	-3.23132100	-0.78605200
H	-5.95768900	-3.73047800	-0.25388600
C	2.58696900	-0.03364200	-0.25962700
H	2.29286600	0.60708900	-1.09254200
C	-2.50469600	-0.50493300	-0.14523500
H	-2.35974700	0.25913200	-0.91106400
C	5.77870800	-2.16124000	-0.65658900

H	6.66123100	-2.42462600	-0.08356000
C	-4.41099200	-2.24165800	-0.14071500
H	-4.65174900	-1.97644700	0.88200400
C	4.47212500	-2.30536100	-2.67330500
H	4.33170000	-2.68330000	-3.68012900
C	2.99979800	0.58650200	2.20472300
H	2.53497800	-0.34210400	2.51480200
C	4.16359700	2.99580400	1.44488300
H	4.61046100	3.93541000	1.13908500
C	3.67149900	2.11881600	0.48120100
H	3.74148300	2.38222600	-0.56921900
C	-3.71910600	0.47241900	3.38206200
H	-3.57443800	0.15865200	4.41024100
C	-0.33180800	2.58218900	-2.20543900
C	-0.72820200	4.74891300	-3.16689400
H	-0.78344200	5.40855800	-4.02499500
C	3.49403100	1.46092100	3.17343800
H	3.41780600	1.19773900	4.22295600
C	-3.03299800	-0.18358800	2.35814500
H	-2.35930700	-0.99456100	2.60776900
C	4.82416900	-1.30700200	-0.09994700
H	4.98207000	-0.90866800	0.89545800

C	-4.07071800	1.25885600	0.74298300
H	-4.21107600	1.57242100	-0.28635100
C	-0.93358100	4.47613200	-0.74344900
H	-1.13455200	4.89320200	0.23625100
C	1.58424400	-4.67986300	1.84378300
H	1.35556000	-5.65254300	2.27595300
H	2.19078000	-4.10310200	2.55025500
H	2.14163600	-4.81742400	0.91177000
C	-3.10305400	-1.93094100	-2.13577300
H	-2.30142200	-1.42469400	-2.66472500